UNIVERSITY OF TWENTE.

INREDA

Master Thesis

Model optimization and parameter estimation in a bi-hormonal model of glucose dynamics in type 1 diabetes mellitus patients

M.J. Vosman

16 August, 2019

Graduation Committee:
Prof. dr. ir. P.H. Veltink
Prof. dr. ir. H.J. Zwart
Dr. ir. B.J.F. van Beijnum
A.J. Onvlee, MSc

Programme:
Biomedical Engineering

University of Twente
Faculty of Electrical Engineering, Mathematics and Computer Science
Department of Biomedical Signals and Systems

SUMMARY

Modelling of the glucose metabolism in people with type 1 diabetes mellitus (T1DM) is relevant for the in silico testing of artificial pancreas (AP) systems and can be applied to predictive control in such systems. Problems with existing models arise when these models need to be identified based on limited available data. In this thesis, simplification of existing model structures was applied to solve this problem. Models of subcutaneous insulin and glucagon kinetics were identified for simulating insulin and glucagon plasma concentrations in an average patient with T1DM. For modelling of the glucose concentration in response to these hormonal concentrations, model structures of varying complexity were proposed and identified. Performance of these models to predict glucose levels in patients with T1DM up to three hours forward was determined. Results showed that prediction performance was best for a simple nonlinear model structure with only two subject-specific parameters. 3 hours forward, the median absolute error was smaller than 1 mmol/L. This study shows that parameters in simplified model structures can be estimated with the applied methods. Main limitations were the estimation methods applied combined with the limited data availability and accuracy. Also, the effect of meal intake was not yet considered. In spite of these limitations, the study demonstrates the potential of a simple compartmental model to be applied for improvement of glucose control in T1DM patients.

SAMENVATTING

Het modelleren van het glucosemetabolisme in patiënten met type 1 diabetes mellitus (T1DM) is belangrijk voor het testen van kunstmatige alvleesklier (AP) systemen in silico. Deze modellen kunnen ook worden toegepast in een systeem dat glucoseniveaus controleert met behulp van modelvoorspellingen. Bij bestaande modellen ontstaan er problemen wanneer model parameters geïdentificeerd moeten worden op een beperkte hoeveelheid data. Om dit op te lossen zijn deze model structuren versimpeld. Modellen van de subcutane absorptie en kinetiek van insuline en glucagon zijn geïdentificeerd voor een gemiddelde T1DM patiënt. Voor het modelleren van de glucoseconcentratie in reactie op deze hormonale concentraties, werden model structuren van verschillende complexiteit voorgesteld en geïdentificeerd. Daarna is vastgesteld hoe goed deze modellen presteren in het voorspellen van de glucoseconcentraties in T1DM patiënten in drie uur durende simulaties. Uit de resultaten is gebleken dat de voorspellingen het beste waren voor een simpel non-lineair model met slechts twee patiënt-specifieke model parameters. De mediaan van de absolute error was kleiner dan 1 mmol/L na een voorspelling van drie uur. Deze studie laat zien dat de toegepaste methodes gebruikt kunnen worden om parameters in versimpelde glucose model structuren te schatten. De voornaamste beperkingen waren de methode die is gebruikt voor het schatten van de parameters en de beperke beschikbaarheid en nauwkeurigheid van data. Daarnaast is het effect van maaltijdinname nog niet meegenomen. Ondanks deze beperkingen, laat deze studie de potentie zien van een simpel compartimentenmodel voor toepassing op het verbeteren van glucose controle in T1DM patiënten

ACKNOWLEDGEMENT

I wish to thank various people for their support during my master thesis project. I would like to thank my first supervisor Peter Veltink for sharing his expertise and view, which was of great value for formulating of the research topic and applying the correct methodology. Furthermore, I would like to thank my daily supervisor Joannet Onvlee for her advice when I encountered problems and for the feedback on the research and writing. I would also like to thank committee members Bert-Jan van Beijnum and Hans Zwart for their feedback and insights into the research context of this thesis.

I am grateful to Robin Koops for giving me the opportunity to perform this research at Inreda Diabetic BV in collaboration with University of Twente. I would like to thank my colleagues at Inreda for the valuable conversations and positive working atmosphere. Finally, I want to express my gratitude to my family and friends for their support and encouragement.

Contents

List of abbreviations

Abbreviation	Meaning
2COM	Two-compartmental
AP	Artificial pancreas
BG	Blood glucose
BW	Body weight
CGM	Continuous glucose monitoring
CL	Closed loop
CV	Coefficient of variation
EGP	Endogenous glucose production
FDA	Food and Drug Administration
HbA1c	Haemoglobin A1c; type of haemoglobin bound to glucose; measure of mean glucose level over three months
H_{IR}	Glucagon infusion rate
I_{IR}	Insulin infusion rate
IR	Infusion rate
Inreda AP	Artificial pancreas as developed by Inreda Diabetic BV
IVGTT	Intravenous glucose tolerance test
MARD	Mean absolute relative difference
MM	Minimal model
OL	Open loop
OMM	Oral minimal model
OMM*	Labelled oral minimal modal
RMSe	Root mean squared error
SMBG	Self-monitoring of blood glucose
T1DM	Type 1 diabetes mellitus
T2DM	Type 2 diabetes mellitus
VAF	Variance accounted for

Chapter 1

Introduction

Over 1.1 million people suffer from diabetes in the Netherlands [1]. Diabetes is a chronic disease that affects the glucose metabolism in the body. For people with diabetes, managing their glucose levels can be a daily struggle. Not keeping glucose levels within safe limits often results in complications both on short- and long-term. These complications can affect various parts of the body, like the cardiovascular system, eyes, kidneys and nervous system [1]. Complications can be prevented by proper management of diabetes, which is focused on maintaining glucose levels stable and within safe ranges.

There has been a 50 percent increase in diabetes prevalence over the last two decades [1]. Diabetes results in elevated glucose levels in the blood, which is called hyperglycaemia. Most diabetic patients can be classified as having type 1 diabetes mellitus (T1DM) or type 2 diabetes mellitus (T2DM) [2]. 9% of Dutch patients diagnosed with diabetes suffer from type 1 diabetes [1]. In T1DM, hyperglycaemia is caused by a lack of insulin production. This is the result of destruction of the insulin producing beta cells in the pancreas [2]. In T2DM, glucose levels are high as a result of an insulin secretory defect on the background of insulin resistance [2]. Prevalence of T2DM is strongly related to age, weight and ethnicity [1].

In healthy people, glucose metabolism is regulated by complex physiological control mechanisms. Plasma glucose levels roughly depend on the balance between endogenous glucose production, glucose utilization by the various tissue types and the glucose rate of appearance resulting from intestinal absorption [3]. The endogenous glucose flux from the liver is mostly affected by the hormones insulin and glucagon [4]. Insulin is produced by the beta cells in the pancreas. This hormone stimulates the conversion of glucose into glycogen in the liver. Furthermore, it stimulates the uptake of glucose by adipose tissues. Glucagon is the counter-regulating hormone that is produced by the alpha cells in the pancreas. This hormone stimulates the release of glucose from the liver into the blood by conversion of stored glycogen into glucose.

In people with T1DM, glucose metabolism cannot be controlled without administration of insulin [2]. Episodes of hypoglycaemia and hyperglycaemia will occur if glucose control is not managed properly. Euglycaemia is the normal range of blood glucose concentrations that is defined in this study as being in between 3.9 and 10.0 mmol/L [5]. Hyperglycaemia occurs when blood glucose levels are elevated above the euglycaemic range and hypoglycaemia occurs when blood glucose levels drop below the euglycaemic range. Repeated periods of hypoglycaemia can result in hypoglycaemia unawareness, impaired glucose counter-regulation and severe hypoglycaemia episodes [6, 7]. Hypoglycaemia causes many neurogenic symptoms and eventually results in brain dysfunction [7]. Prolonged, severe hypoglycaemia episodes can lead to cognitive impairment and recurrent seizure activity [7]. On short-term, hyperglycaemia results in less severe symptoms, although it can lead to diabetic ketoacidosis (accumulation of ketones) when left untreated. Long-term complications include cardiovascular disease, nerve damage, kidney damage, eye problems, etc. [8].

It is known that risk of complications that are associated with diabetes can be reduced by early treatment and glucose control [9]. The HbA1c is applied as a measure for the mean glucose level over three months. According to guidelines, its value needs to be kept below 7%, reflecting that glucose levels were well within the euglycaemic range on average in this period [2]. Current treatment of a diabetes patient starts with an individualized treatment plan in order to reduce the short- and long-term effects [2].

This involves glucose monitoring in combination with insulin therapy by insulin injections, continuous subcutaneous insulin infusion or insulin pump therapy. Meal intake and physical exercise need to be considered to establish proper glycaemic control. In case of hypoglycaemia, glucagon can be applied to raise glucose levels [2]. Glucose levels are measured either by self-monitoring of blood gluocse (SMBG) or by continuous glucose monitoring (CGM). SMBG requires the patient to apply a blood drop to a SMBG device. CGM uses a sensor that measures the glucose level in the interstitial fluid continuously.

Current treatment methods cannot prevent regular episodes of hypoglycaemia or hyperglycaemia in people with T1DM. Research has been performed to improve current treatment methods. Transplantation of islets has shown to be a promising technique in T1DM treatment. Islets contain the endocrine cells in the pancreas. Studies are ongoing to find techniques suitable for islet transplantation. Islet cell death and poor perfusion of transplanted islet areas are the issues that are currently encountered. Another problem is the limited availability of islets. Application of stem cells may help to accomplish successful islet transplantations. [9]

Next to research into the treatment of diabetes on cellular level, studies have also been performed in order to improve treatment by exogenous intervention. Artificial pancreas (AP) systems have been developed that are either insulin delivery systems [10, 11] or bi-hormonal systems [12, 13] that apply infusions of both insulin and glucagon to stabilize glucose levels. These devices are closed loop systems, meaning that these systems receive feedback and adjust the output, i.e. hormonal infusions, based on this feedback. CGM is applied to provide feedback to the system. An advantage of "closing the loop" is that no human decisions are required to regulate glucose levels, which could diminish patient burden.

Insulin-delivery AP systems have shown to get closer to optimal insulin administration compared to normal insulin pumps, but due to variable pharmacokinetics and absorption rates of insulin analogues it is still a challenge to prevent hypoglycaemic events. One such system has been approved by the FDA [14]. This system has the disadvantage that it still requires meal announcement by the patient. Bi-hormonal AP systems use the counter-regulating effect of glucagon to prevent hypoglycaemia. It has been shown that bi-hormonal AP systems can reduce hypoglycaemia after exercise and improve nocturnal glycaemic control [9]. A small clinical study on the bi-hormonal AP system as developed by Inreda Diabetic BV has indicated that this AP system performs better at maintaining euglycaemia than regular insulin pump therapy [13].

Many mathematical models of glucose metabolism in the body have been developed over the years. The aim of these models was initially to provide insight into parameters related to glucose metabolism, such as insulin sensitivity [4]. Later on, models have been developed with the goal of performing simulations. These models can be applied for in silico testing of diabetic treatments. Mathematical models of glucose metabolism are either data-driven (black box) or they are based on the processes that occur physiologically [4]. This last type of model can be very complex, which has the advantage that complex dynamics can be represented by such a model. Problems occur when parameter values for these systems need to be determined [5]. Direct measurement of the model variables either requires extensive tracer experiments or is not possible at all. Estimation of all model parameters based on limited available data is often not possible.

A proprietary model of glucose metabolism has been developed. This model is suitable for in silico testing of the AP system developed by Inreda Diabetic BV [5] on T1DM patients. Although a working model was provided, it has not been possible to set up an in silico population based on the limited available data. Thereby, the model is yet to be identified and validated [5]. The current study is aimed at performing parameter estimations for this model based on data acquired in a study on the Inreda AP [13]. Model structure of the various submodels of the Inreda model is reviewed and structural simplifications are applied when this is required to find unique parameter estimations. Consequently, the research question for this thesis is defined as: how can critical model parameters be identified and what is glucose prediction performance for identified models of varying structures and complexity?

An overview of existing models of glucose metabolism is given in the next chapter and their limitations are discussed. Some physiological background on the processes involved in glucose metabolism is also provided. Chapter 3 will then explain the methods that were applied for answering the research question. The last two chapters of this report contain the results and a discussion of these results respectively.

Chapter 2

Literature Study

In this chapter, the state of the art in glucose modelling methods is discussed. Most of these models are built up from differential equations, with each variable describing the mass or concentration of a certain molecule or hormone in a compartment. Such a compartment often has a physiological meaning, for example the blood plasma or peripheral tissues in the body. Parameters describe the rates at which masses flow in and out of the compartments. [4]

This literature study starts with some background information on the kinetics and existing model descriptions of the hormones insulin and glucagon. Such models are required to establish a valid model of the glucose system when these hormones are applied to regulate blood glucose concentrations. In the second part of this literature study, the glucose dynamics and kinetics including the effects of insulin and glucagon on glucose levels are discussed. A conclusion is formulated at the end of this chapter.

2.1 Insulin and glucagon systems

As mentioned in the introduction, insulin and glucagon are hormones that influence blood glucose (BG) levels in the body. The dynamics of insulin and glucagon determine how these hormones affect the glucose system [15], which is called insulin and glucagon action throughout this report. Before insulin and glucagon action can be described, kinetics of insulin and glucagon need to be identified. These kinetics determine the hormonal concentrations at the site(s) of action. In healthy people, insulin and glucagon kinetics involve the entry of secreted hormone into the blood stream, distribution through other body pools, and elimination [15]. When applying bi-hormonal control of BG levels, insulin and glucagon kinetics also involve the pharmacokinetics in case of subcutaneous delivery of insulin and glucagon [16, 13, 17].

2.1.1 Insulin kinetics

Early models of glucose metabolism were identified for healthy people. In order to describe insulin action on glucose kinetics for these people, it was necessary to first describe the insulin production by the pancreatic beta cells and the insulin kinetics after release. A well known model of insulin kinetics in healthy people was developed by Hovorka et al. [18]. The model structure consisted of five compartments reflecting the insulin distribution over the systemic plasma, hepatic plasma, interstitial fluid, and the binding of insulin to either liver or peripheral receptors that mediate insulin degradation. This physiological approach was implemented with even more detail by Koschorreck et al. [19] and Ohashi et al. [20]. Although these models can provide insight into the processing of insulin by the body, the complexity may not be required for the modelling of insulin kinetics solely to determine insulin action on glucose metabolism.

A more simple model was described by Ferrannini et al. [21]. Insulin was modelled to be transferred between the blood plasma compartment and either highly or poorly perfused tissue compartments in which insulin degradation takes place. This model was implemented into the glucose model that was developed by Dalla Man et al. [3], in which the plasma compartment was merged with the highly perfused tissue compartment. The result was a two-compartmental model of insulin kinetics, representing the flows of insulin between the blood plasma and the liver including the insulin degradation that occurs in both of

these compartments [3]. This model was updated for modelling in a T1DM patient by removal of insulin secretion by the beta cells from the equation and addition of a submodel of the rate of appearance of injected insulin in the plasma [22]. Parameters were estimated based on measurements of the plasma insulin concentration in healthy subjects after meal intake. The Inreda model [5] uses the same model structure to model insulin kinetics, which is shown in Figure 2.1.

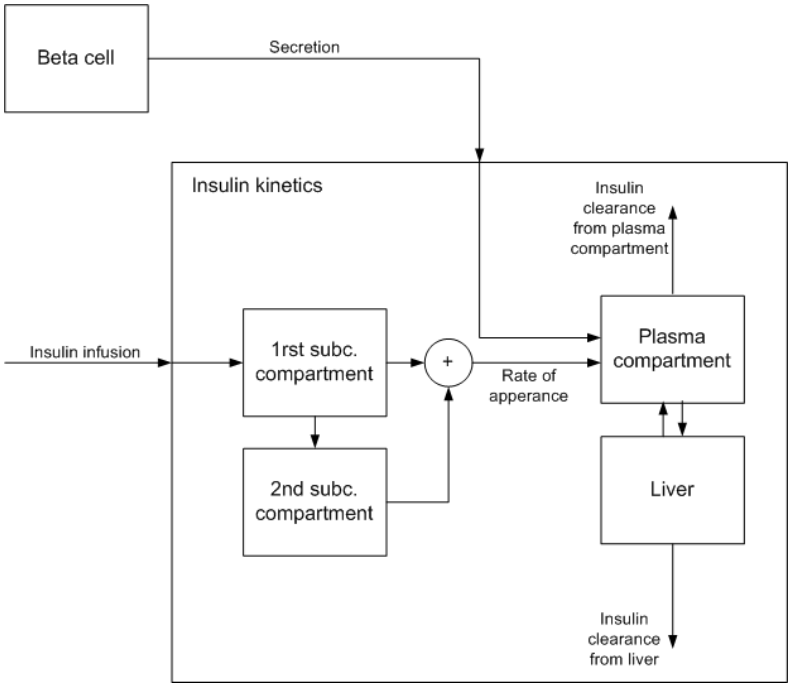

Figure 2.1: Box scheme of insulin kinetics as applied in the Inreda model [5]. Beta cell insulin secretion is set to zero for modelling in a T1DM patient. Rate of appearance of subcutaneously injected insulin into the blood plasma results from insulin transfer through one or two subcutaneous (subc.) compartments. Insulin is cleared from the liver and blood plasma.

Much research has been performed on the development of a model describing the appearance of subcutaneously administered insulin in the blood plasma [23, 24]. Most of these studies applied subcutaneous bolus injection of insulin, after which blood samples were taken multiple times from which insulin concentrations could be determined. An example of such a dataset is shown in Figure 2.2. A study performed by Kraegen et al. [25] showed that a three-compartmental model is capable of reasonably describing experimental data. The model assumed that insulin was injected into a first subcutaneous compartment and could be transferred towards the blood plasma compartment through a second subcutaneous compartment. Another assumption determined that insulin could be cleared from both subcutaneous compartments and from the blood plasma.

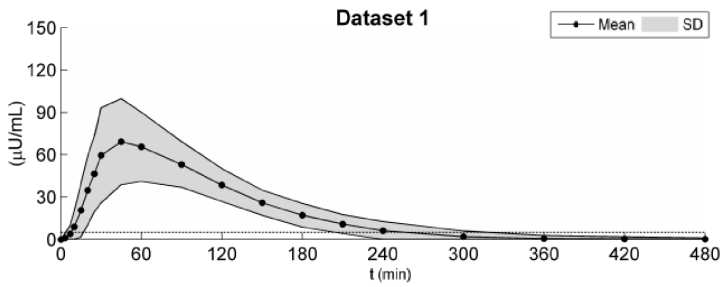

Figure 2.2: Example of a dataset with plasma insulin concentrations measured in venous blood samples after insulin bolus injection in T1DM patients. The dotted line represents the mean of the measured plasma insulin concentrations and the area between the mean ± standard deviation is marked grey. [26]

The model developed by Shimoda et al. [27] was similar, with the difference that it assumed that insulin could only be cleared from the second subcutaneous compartment and the blood plasma. More recently, the models implemented by Herrero et al. [28] and Dalla Man et al. [29] assumed that insulin injected into the first subcutaneous compartment could enter the plasma both directly and through a second compartment [29], and was only cleared once it reached the blood plasma [29, 28]. This is the approach that is shown on the left side of Figure 2.1.

The review published by Schiavon et al. [26] validated these models for a short-acting insulin (lispro). It was shown that the subcutaneous insulin model implemented in the Dalla Man model [29] resulted in the best fit for the data, with a delay added to the administration of insulin for several subjects [26]. A study performed by Lv et al. [30] agreed with this result and also showed that intradermal delivery of insulin could be modelled with a similar model structure.

Except from Dalla Man, none of these studies of subcutaneous insulin absorption applied an additional mathematical description of insulin kinetics once it had reached the blood plasma. It was indicated that plasma insulin kinetics could be described by assuming a constant clearance rate of insulin from the plasma, without including an additional liver compartment [26]. A study by Li et al. [31] also indicated that the complex model that was implemented in the Dalla Man model that combines a compartmental model of insulin kinetics in healthy people [3] with a model of subcutaneous insulin absorption [29], is not required for simulation of insulin concentrations in T1DM patients. The study [31] showed that Padé approximants can be applied to develop a model of even lower order and with less parameters that is still able to accurately simulate of insulin concentrations [31].

2.1.2 Glucagon kinetics

In order to determine the glucagon action on the glucose system, the glucagon concentration in the blood plasma needs to be modelled. A study by Dobbins et al. [32] has shown that glucagon rapidly reaches an equilibrium state in the blood plasma after venous infusion, which can be modelled by a one-compartmental model. Compartmental analysis was applied to identify important parameters of glucagon kinetics and was based on measurements on conscious dogs. Studies investigating the subcutaneous absorption of glucagon [33, 16] have indicated that glucagon kinetics are quick in humans as well.

A study performed by Lv et al. [34] structurally identified the absorption of subcutaneously administered glucagon to the blood plasma. In this study, various models were fit to a data set provided by a bi-hormonal closed loop clinical trial study [12]. Best model fit was found for a two-compartmental model of subcutaneous glucagon absorption and an additional plasma compartment. Other studies applied two-compartmental models with the second compartment already representing the blood plasma [33, 35]. These were also successful in describing measurements with sufficient accuracy. A limitation of these studies are that glucagon secretion may not have been completely absent during the experiments. Furthermore, due to different study designs in terms of participants and types of insulin and glucagon perturbations, it is hard to determine whether presence of insulin and frequency of glucagon injections have an effect on model fit and parameter estimations.

The one-compartmental model of glucagon kinetics and the two-compartmental model of subcutaneous glucagon absorption as found by Dobbins et al. [32] and Lv et al. [34] were implemented into the update of the Dalla Man model in 2014 [36]. Next to subcutaneous injection of glucagon, glucagon can also appear in the blood plasma after secretion by the pancreatic alpha cells. A model describing this secretion was also included in the Dalla Man model [36]. The same model structure was adopted for the Inreda model [5], which is shown in Figure 2.3.

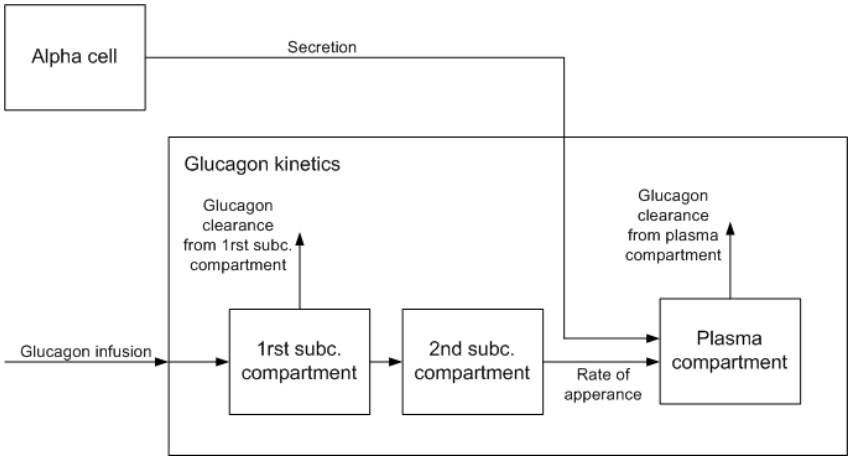

Figure 2.3: Box scheme of glucagon kinetics as applied in the Inreda model [5]. Rate of appearance of subcutaneously injected glucagon into the blood plasma results from glucagon transfer through two subcutaneous (subc.) compartments. Glucagon that is secreted by the alpha cells also enters the blood plasma. Glucagon is cleared from the first subc. compartment and from the plasma compartment.

2.1.3 Alpha cell glucagon secretion

Although the response of alpha cells to hypoglycaemia can be impaired in T1DM patients, the cells do not lose the ability to produce glucagon [37]. The response to hypoglycaemia decreases progressively with diabetes duration. Studies have conflicting results about the period of time in which this occurs [37, 6]. More recent studies have shown that in T1DM patients, in contrast to healthy alpha cell function, glucagon secretion suppression during hyperglycaemia can be dysfunctional [38, 39]. Also, glucagon secretion stimulation during hypoglycaemia is impaired [40, 41, 42]. A study performed by Hinshaw et al. [43] showed that glucagon secretion is not negligible in T1DM patients. Detailed models have been developed to get more information about the dynamics underlying glucagon secretion in healthy people and T1DM patients [44, 45, 46].

Another glucagon secretion model [47] was implemented into the update of the Dalla Man glucose model [36]. In this model, based on the physiological situation, glucagon secretion is assumed to consist of a static component and a dynamic component. The dynamic component is dependent on the glucose rate of change, meaning that dynamic secretion increases when glucose levels start to drop. The static component is dependent on glucose concentrations. Static secretion would be inhibited for high glucose levels. Stimulation of static secretion occurs when glucose levels are lower. As soon as glucose levels drop even further, stimulation of static secretion becomes dependent on the insulin level as well: the stimulation is stronger for lower insulin levels. Glucagon secretion parameters were adjusted to diabetes disease duration in order to account for the loss of alpha cell responsivity [36]. Parameter estimations were not performed for data acquired in T1DM patients.

The Inreda model [5] applies a similar model of alpha cell secretion, with the difference that switching between different states of inhibition and stimulation of alpha cell secretion is slightly simplified, as is presented by Carson and Cobelli [4]. Secreted glucagon is transferred from the alpha cells to the blood plasma, as shown in Figure 2.3. A study performed by C. Braem [48] attempted to perform parameter estimations for a linearisation of the alpha cell secretion model of Inreda. This proved to be difficult both due to the limited availability of suitable data and due to the complexity of the model structure. Results indicated that secretion dynamics change dependent on glucose concentrations. Dependency on insulin concentrations was not studied.

2.2 Glucose system

Two main types of glucose models have been developed over the years: models to measure and models to simulate [4]. Typically, models to measure are so-called minimal models that are structurally simple and have the goal to describe system functions and quantify metabolic relationships in the system. Models to simulate are typically maximal in the sense that these models are higher-order models that contain

nonlinearities and many model parameters. Next, the first minimal models are described (subsection 2.2.1). Then, modelling developments in various parts of the glucose metabolism chain are discussed (subsections 2.2.2-2.2.5). Lastly, an overview of the state of the art glucose models is provided (subsection 2.2.6).

2.2.1 Glucose minimal models

The glucose minimal model (MM) was originally described by Bergman et al. [49] and is shown in Figure 2.4. In this minimal model, one compartment is used to describe glucose kinetics after a venous glucose injection D. The description consists of insulin-independent (G_b, k_1 and k_5) and insulin-dependent (k_4 and k_6) components. G_b is the basal net glucose production at zero glucose. There is balance between hepatic glucose production and utilization (k_5) and extra-hepatic glucose utilization (k_1). Insulin action is both on the hepatic glucose balance (k_6) and extra-hepatic glucose utilization (k_4). The model description is shown in Equation 2.1. The input variable is the plasma insulin concentration C_{ip} and the output variables are the delayed insulin signal C_{id} and the glucose mass q_{gp} in the blood plasma. Plasma glucose concentration C_{gp} is related to the glucose mass q_{gp} through the volume of distribution V_g. Equation 2.2 shows an equivalent description of the model with the insulin action $X(t)$ that is proportional to C_{id}. Insulin action is a first order transfer of the insulin concentration C_{ip} relative to the basal insulin concentration $C_{ip,b}$.

Glucose minimal model:

$$\begin{cases} \dot{q}_{gp}(t) &= -(k_1 + k_5) \cdot q_{gp}(t) - (k_4 + k_6) \cdot C_{id}(t) \cdot q_{gp}(t) + G_b \\ \dot{C}_{id}(t) &= k_2 \cdot (C_{ip}(t) - C_{ip,b}) - k_3 \cdot C_{id}(t) \\ C_{gp}(t) &= \frac{q_{gp}(t)}{V_g} \end{cases} \tag{2.1}$$

Substitute $(k_4 + k_6) \cdot C_{id}(t) = X(t)$:

$$\begin{cases} \dot{q}_{gp}(t) &= -(k_1 + k_5) \cdot q_{gp}(t) - X(t) \cdot q_{gp}(t) + G_b \\ \dot{X}(t) &= k_2 \cdot (k_4 + k_6) \cdot (C_{ip}(t) - C_{ip,b}) - k_3 \cdot X(t) \\ C_{gp}(t) &= \frac{q_{gp}(t)}{V_g} \end{cases} \tag{2.2}$$

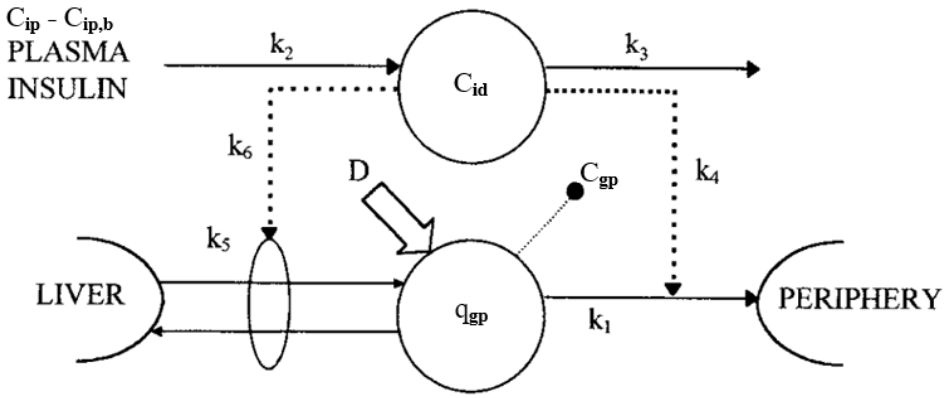

Figure 2.4: One-compartmental Bergman minimal model [49, 50] describing the glucose mass in the blood plasma q_{gp} after venous infusion of glucose (D). The model considers flow of glucose and insulin (solid lines), as well as insulin action (dotted lines) affecting the glucose flows.

Data that was applied to identify the Bergman MM [49] was obtained in cold intravenous glucose tolerance test (IVGTT) experiments, in which peripheral plasma was frequently sampled after an intravenous glucose injection. Although this cold IVGTT data could not be used to determine the hepatic glucose production and utilization separately, it did allow for a description of the hepatic glucose balance. After re-parametrization, model parameters as shown in Equation 2.3 were uniquely a priori identifiable from cold IVGTT data. This model has been used to estimate the insulin sensitivity S_I (Equation 2.4),

that measures the rate at which insulin stimulates the glucose-dependent glucose disappearance. It also has been used to estimate the glucose effectiveness S_G (Equation 2.5), i.e. the enhancement of glucose disappearance as glucose concentration increases.

Re-parameterize equation 2.2 by applying $k_g = k_1 + k_5, m = k_2 \cdot (k_4 + k_6), n = k_3$:

$$\begin{cases} \dot{q}_{gp}(t) & = -k_g \cdot q_{gp}(t) - X(t) \cdot q_{gp}(t) + G_b \\ \dot{X}(t) & = m \cdot (C_{ip}(t) - C_{ip,b}) - n \cdot X(t) \\ C_{gp}(t) & = \frac{q_{gp}(t)}{V_g} \end{cases} \tag{2.3}$$

$$S_I = -\frac{m}{n} \tag{2.4}$$

$$S_G = k_g \tag{2.5}$$

Later on, it was shown that simultaneous injection of cold and labelled (hot) glucose could provide more information about glucose kinetics than injection of cold glucose alone [51]. The same one-compartmental model was applied, with the difference that parameters were considered to only contribute to the hot glucose levels. As a consequence, these system parameters were a reflection of the glucose utilization only, instead of the balance between utilization and production. By comparison of cold and hot glucose parameter estimates, the rate of liver glucose production could also be obtained.

More recent studies [52, 53] showed that the one-compartmental glucose minimal model was not able to model glucose kinetics in non-steady-state. The minimal model was adjusted by considering two glucose compartments [53], one with slowly-equilibrating glucose kinetics (q_{gt}) and the other with quickly-equilibrating glucose kinetics (q_{gp}), as shown in Figure 2.5. Insulin action was assumed to take place on the slowly-equilibrating glucose compartment. The model was identifiable from hot IVGTT data.

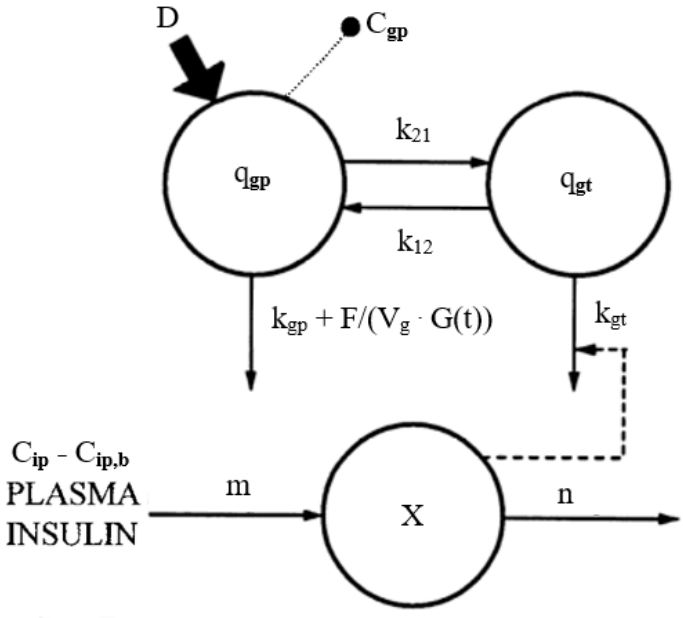

Figure 2.5: Two-compartmental minimal model [54, 50] describing the glucose masses in the slowly equilibrating tissues (q_{gt}) and in the quickly equilibrating tissues and blood plasma (q_{gp}) after venous glucose infusion. The model considers flow of glucose and insulin (solid lines), as well as insulin action (dotted lines) affecting glucose levels.

The system of differential equations of the compartmental hot glucose masses are shown in Equation 2.6. Plasma glucose concentration C_{gp} is related to the glucose mass in the slowly-equilibrating compartment q_{gp} through the volume of distribution V_g. Rate of glucose disappearance is constant (k_{gt}) for the slowly-equilibrating compartment and is time-variant for the quickly-equilibrating compartment ($k_{gp} + F/(V_g \cdot G(t))$). Here, $G(t)$ is the measured cold glucose concentration. k_{21} and k_{12} represent the rates of glucose transfer between the compartments. Glucose action X is again a first order transfer of the plasma

insulin concentration. This model was also applied to estimate the indexes of glucose effectiveness and insulin sensitivity [54]. These two-compartmental models have the disadvantage that unique parameter estimation was now only possible by using a tracer glucose bolus and physiological constraints [53, 54] or by Bayesian estimation [50].

$$\begin{cases} \dot{q}_{gp}(t) & = -k_{21} \cdot q_{gp}(t) + k_{12} \cdot q_{gt}(t) - k_{gp} \cdot q_{gp}(t) - F/(V_g \cdot G(t)) \cdot q_{gp}(t) \\ \dot{q}_{gt}(t) & = k_{21} \cdot q_{gp}(t) - k_{12} \cdot q_{gt}(t) - k_{gt} \cdot q_{gt}(t) - X(t) \cdot q_{gt} \\ \dot{X}(t) & = m \cdot (C_{ip}(t) - C_{ip,b}) - n \cdot X(t) \\ C_{gp}(t) & = \frac{q_{gp}(t)}{V_g} \end{cases} \tag{2.6}$$

2.2.2 Insulin action

Separating between the effect of insulin on glucose transport and disposal was first attempted by Ferrannini et al. [55]. Shortly after, tracer experiments were applied to develop labelled minimal models that could separate between the effect of insulin and glucose on glucose disposal and endogenous glucose production (EGP) by the liver [51, 56]. Another model that was developed by Hovorka et al. [57] was made to separate between the effects of insulin not only on glucose disposal and endogenous glucose production, but also on glucose transfer. Application of dual tracer technology in combination with a (minimal) model allowed for measurement of the suppression of the EGP after insulin bolus administration. It was indicated that the main effect of insulin after meal intake is to suppress the EGP and that stimulation of glucose disposal is less strong.

Availability of data acquired in model-independent triple-tracer methods [58] (Figure 2.6) allowed for the development of models that could not only describe EGP and glucose utilization after meal intake, but also the glucose rate of appearance after carbohydrate ingestion. A model describing the endogenous glucose production (EGP) during a meal in the liver was developed by Dalla Man et al. [59]. In contrast to the original glucose minimal model [49], the insulin action on the EGP was assumed to be independent of the glucose concentration and dependent on the insulin concentration through an additional compartment, adding an extra delay to the effect of insulin. The value of this EGP model for modelling of glucose concentrations in people with T1DM is limited due to the data being acquired on healthy people after meal intake.

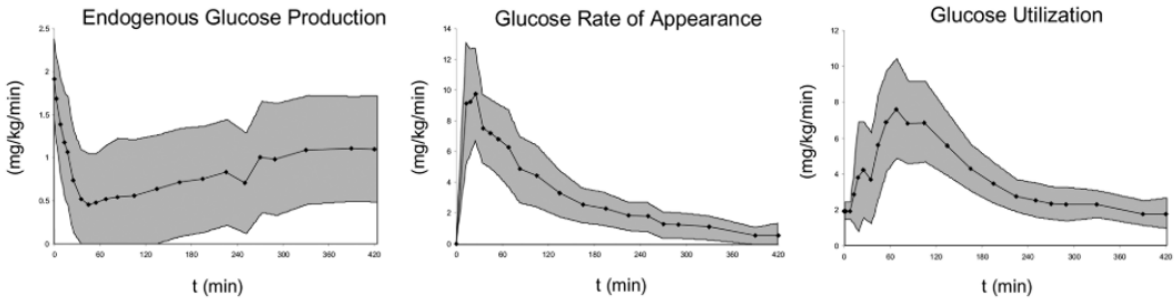

Figure 2.6: Data acquired in a triple-tracer experiment [58, 3] in healthy subjects with on the left the EGP, in the middle the glucose rate of apperance (Ra) and on the right the glucose utilization. These were measured during the first 480 minutes after ingestion of a mixed meal. As meal glucose appeared in the blood, EGP was suppressed and glucose utilization increased.

2.2.3 Glucose intestinal absorption

The oral minimal model (OMM) was developed as an extension of the glucose minimal model by Dalla Man et al. [60]. A model was assumed for the rate of intestinal glucose absorption after meal intake, such that the insulin sensitivity during meal perturbation could be estimated. Triple-tracer experiments [58] allowed for application of a labeled oral minimal model (OMM*) for the estimation of the glucose disposal's insulin sensitivity individually (S_I^*) next to the net insulin sensitivity (S_I) that also included glucose production [61]. A physiologically detailed model meant for simulation of glucose absorption in the gastrointestinal tract was firstly developed in another study performed by Dalla Man et al. [62].

Model validation was based on data gathered in mixed-meal (Figure 2.6) [58] and oral glucose [61] multiple tracer experiments. The model consisted of three compartments and was nonlinear.

2.2.4 Glucose utilization

Glucose disposal (U) has been characterized as being dependent on the glucose concentration C_{gp} through a Michaelis-Menten relationship [63]: $U(t) = (V_{max} \cdot C_{gp}(t))/(K_m + C_{gp}(t))$. This relationship originates from modelling enzyme kinetics. The parameter V_{max} in the numerator of the equation represents the maximum utilization rate possible. The Michaelis-Menten constant K_m in the denominator of the equations is the glucose concentration at which the utilization rate is half of the maximum utilization rate. The effect of the equation is that utilization rate becomes saturated as the glucose concentration increases, which can be seen in Figure 2.7.

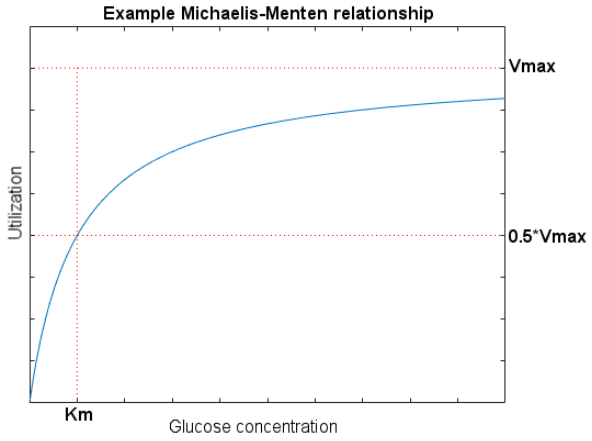

Figure 2.7: Example of Michaelis-Menten relationship for modelling of glucose utilization.

Implementation of this relationship in the glucose model of Dalla Man suggested that the parameter V_{max} in this relationship is not constant, but dependent on the insulin concentration in a remote insulin compartment [3]. This means that the maximum utilization rate increases when the insulin concentration rises. Fitting the model to the available data (Figure 2.6 [58]) also indicated that a basal rate of glucose utilization was always present independent of the insulin concentration [3].

A study that also applied the Michaelis-Menten relationship in a glucose model was performed by Wong et al. [64]. In contrast, glucose utilization was now characterized as being dependent on the remote insulin concentration through a Michaelis-Menten relationship with the saturation parameter dependent on the glucose concentration [64]. The effect of this equation is that utilization rate becomes saturated as the insulin concentration increases. The maximum utilization rate is proportional to the glucose concentration. The model showed to be successful in glucose level prediction in people receiving critical care. It has not been validated on healthy people or people suffering from diabetes.

Dynamics of glucose utilization differ between people with T1DM and healthy people. It has been shown that glucose utilization in long-standing T1DM subjects is reduced compared to healthy subjects in euglycemia and hyperglycaemia, even when insulin levels are elevated excessively [65, 66]. This is not the case in newly diagnosed cases [67]. Other studies indicated in hyperinsulemic clamp experiments that insulin action increases for low glucose values in people with T1DM [68, 69]. Therefore, counter-regulation of both hypoglycaemia and hyperglycaemia through the decrease and increase of glucose utilization respectively is impaired in people with T1DM.

The utilization submodel of Dalla Man was adjusted to a T1DM subject by addition of a risk function to the insulin parameter in the Michaelis-Menten relationship [36]. This risk function represents the impaired hypoglycaemia counter-regulation by assuming that glucose utilization increases when glucose decreases below a certain threshold. In the Inreda model [5] the same model of glucose utilization is applied, but the risk function is not included.

2.2.5 Glucagon action

A clinical trial that was performed by Hinshaw et al. [70] showed that in people with T1DM, there is glucagon action on the EGP both in euglycaemia and hypoglycaemia. Sensitivity of the liver to glucagon did not change between euglycaemic and hypoglycaemic glucose levels. Clearance rate of glucagon from the plasma did not change for increasing glucagon concentrations. A later study by Emami et al. [71] attempted to model insulin action and glucagon action on the EGP. Results suggested that EGP always has a basal rate independent of insulin and glucagon as a result of gluconeogenesis. EGP was modelled to depend linearly on the delayed insulin signal similar to what was done earlier by the EGP model of Dalla Man [59]. Best model fit was found for EGP depending linearly on the glucagon concentration as well as on a delayed glucagon signal proportional to the glucagon rate of change [71]. The update of Dalla Man [36] applied a different model for which EGP depended linearly on a delayed glucagon signal that stimulates EGP as soon as glucagon concentration is above basal.

2.2.6 Complete glucose simulation models

Many glucose simulation models have been developed over the years. In this subsection, an overview of some existing models is presented. This overview is summarized in Table 2.1. The considered models have been applied as basic structures in research into T1DM treatment and control [4]. Many variations to these models exist and are currently mainly applied to study closed loop glucose control systems. These systems can be either insulin delivery systems or bi-hormonal control systems that apply infusions of both insulin and glucagon.

Table 2.1: Overview of glucose models found in literature

	Parameter values	Purpose	Glucagon model	Intrasubject variability	Intersubject variability	Notes
Sorensen [72]	Based on literature	Simulation for average T1DM subject	Included in detail	Not considered	None	Contains errors [73]
Hovorka [74]	Based on literature or estimated from data acquired in T1DM subjects	In silico testing of nonlinear preditive controller of glucose levels	Excluded	Oscillatory variability for part of parameters (Bayesian estimation)	10 virtual patients (based on clinical data)	Physical activity model is included. Model is validated on data 12 young T1DM patients [75].
Fabietti [76]	Estimated based on clinical data or taken from literature.	Simulation model simple enough for real time parameter estimation	Excluded	Sinusoidal representation of carcadian variability of insulin sensitivity that are estimated off-line	None	Extension of Bergman
Medtronic [77]	Estimated based on clinical data	Simulation environment for in silico testing of closed loop delivery systems in T1DM subjects	Excluded	Parameter values adjusted in real-time based on RMS	10 virtual patients based on 10 T1DM subjects	Extension of Bergman
Herrero [28]	Parameters were fixed based on literature or estimated from clinical data in 3 T1DM subjects (closed loop study)	Simulation environment for in silico testing of closed loop delivery systems, build cohort of virtual T1DM subjects	Glucagon action through remote compartment. Subc. kinetics similar to insulin	Parameter estimations performed separately for three time windows during day	Identification performed for three subjects	Extension of Bergman
Dalla Man [3, 36, 78, 79]	Based on triple-tracer experiment in healthy people and additional databases for T1DM pateints	In silico testing of closed loop control	Model of absorption and kinetics included	Diurnal variability is added for several parameters	300 virtual patients	

One of the first complex models of glucose metabolism was developed by Sorensen et al. [72]. This model consists of six compartments that are based on body physiology. Glucose uptake was assumed to take place in the (1) brain, (2) heart and lungs, (3) periphery, (4) gut, and (5) liver. Glucose is excreted from the kidney compartment (6). The liver was considered the only source of glucose. In addition, insulin kinetics and action were considered. Parker et al. [80] altered the Sorensen model to include absorption of glucose in the gut [81]. The main disadvantage of this model is that parameter estimations were taken from literature such that the model can only be applied to simulate glucose levels in an average subject with T1DM.

Hovorka et al. [74] combined two-compartmental models of subcutaneous insulin and glucose kinetics with the Hovorka model of insulin action [57]. Intestinal glucose absorption was included by a simple two-compartmental transfer. Model parameters were either estimated from measurements on T1DM subjects or taken from probability distribution databases. Oscillatory intra-subject variability was implemented for a selection of the parameters by Bayesian parameter estimation. The disadvantage of this model is that intestinal glucose absorption and intra-subject variability may not be implemented with enough refinement. Advantages are that the in silico patients are validated with a clinical study and that a submodel of physical exercise is included. The model has been applied for design of a nonlinear predictive controller for juveniles. Only the averages of the parameter values have been made public.

A study by Fabietti et al. [76] altered the Bergman minimal model [49] to represent a T1DM patient: a compartment was added to describe subcutaneous absorption of insulin. The insulin secretion submodel was removed and renal clearance was added. Also, an additional glucose compartment and intestinal glucose absorption were included. Part of the parameters were estimated based on the acquired clinical data and the remaining parameters were adopted from literature. Clinical data was also applied to estimate the circadian variation of the insulin sensitivity. The disadvantage of this model as well, is that it only represents an average subject with T1DM.

Medtronic [77] also adapted the Bergman minimal model [49]: two-compartmental models of subcutaneous insulin absorption and intestinal glucose absorption were added. Intra-subject variations of insulin sensitivity, glucose effectiveness and endogenous glucose production were introduced based on ten glucose profiles and a virtual population was created. Model structure and parameter estimations have not been published. The model results in overestimation of the glucose effectiveness and underestimation of the duration of insulin action [82]. Despite this result, a first validation study on 10 T1DM subjects during routine insulin treatment showed that simulated glucose values did not differ significantly from clinical measurements. Therefore, the model could be suitable for in silico studies of insulin delivery systems [83].

A model that did include glucagon dynamics into a glucose simulation model was composed by Herrero et al. [28]. The Bergman minimal model [49] (Figure 2.4, Equation 2.3) was extended with a compartment that incorporates glucagon action on the endogenous glucose production, which is shown in Figure 2.8 and Equation 2.7. Insulin action X acts on liver glucose uptake (k_6) and extrahepatic glucose utilization (k_4). Glucagon action Y acts on the endogenous glucose production (k_9). Both X and Y are first order transfers of the insulin and glucagon concentrations relative to the basal levels respectively. Submodels of subcutaneous insulin kinetics and intestinal glucose absorption were taken from the Hovorka model [74]. Subcutaneous glucagon kinetics were modelled with the same model structure as subcutaneous insulin kinetics. The model was identified based on a closed loop bi-hormonal control study with three subjects of 26-hour duration (Figure 2.9). Parameters were estimated in three different time windows during the day in order to account for diurnal variations of the parameters.

$$\begin{cases} \dot{q}_{gp}(t) & = -k_g \cdot q_{gp}(t) - X(t) \cdot q_{gp}(t) + Y(t) \cdot q_{gp}(t) + G_b \\ \dot{X}(t) & = m_i \cdot (C_{ip}(t) - C_{ip,b}) - n_i \cdot X(t) \\ \dot{Y}(t) & = m_h \cdot (C_{hp}(t) - C_{hp,b}) - n_h \cdot Y(t) \\ C_{gp}(t) & = \frac{q_{gp}(t)}{V_g} \end{cases} \tag{2.7}$$

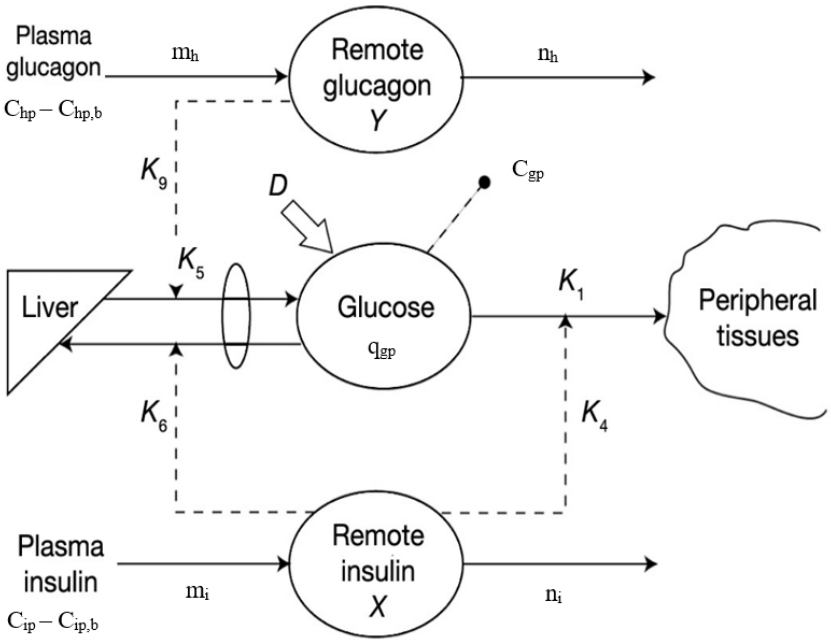

Figure 2.8: Model structure of extended minimal model [49] (Figure 2.4) as applied by Herrero et al. [28] that incorporates both insulin and glucagon action on glucose metabolism (dotted lines). Solid lines represent transfer of glucose/insulin/glucagon.

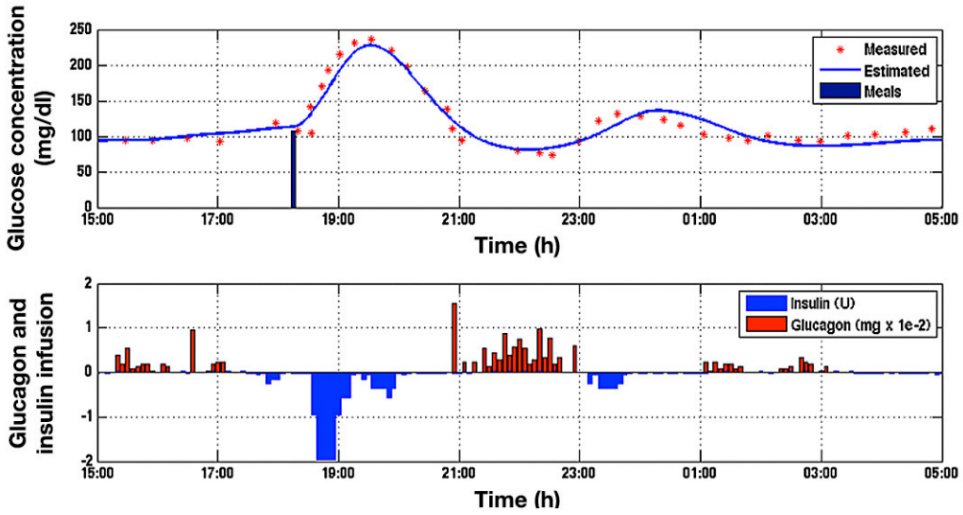

Figure 2.9: Model fit of simulation to data acquired in bi-hormonal closed loop control study is shown in upper graph. Data was applied to perform parameter identification for the glucose model of Herrero et al. [28]. Lower graph shows applied infusions of glucagon and insulin.

A model that is approved by the FDA for in silico testing of glucose control systems was developed by Dalla Man et al. [3, 36, 78]. Complex submodels of insulin and glucose fluxes were identified based on clinical data acquired on 204 healthy subjects in a triple-tracer experiment after meal intake [58]. A database of virtual T1DM patients was computed [22] and submodels of (subcutaneous) glucagon kinetics and action have been added [36].

The Dalla Man model was validated based on 24-hour duration measurements on people with T1DM during controlled conditions: three predetermined mixed meals were consumed, no physical activity was undertaken and no subcutaneous infusion of glucagon was applied [79]. The limitation of the model to account for diurnal variations of glucose dynamics becomes clear from the fact that different virtual subject parameter sets were matched to fit the measurements after breakfast and dinner in the same real subject. Diurnal parameter variations were added in a later model update [78], but this has not been

validated on data yet. The effect of these variations is shown in Figure 2.10. Other studies [84, 85] have shown that submodels of this simulation model can be simplified to lower order systems with similar simulation accuracy by application of methods like Padé approximants.

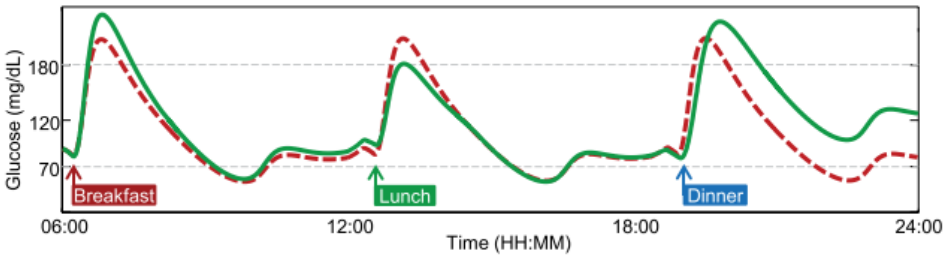

Figure 2.10: Simulation performed with Dalla Man model. Three identical meals were used as input. The lines represent simulations without (red dashed line) and with (green line) diurnal parameter variations. [78]

2.3 Conclusion

It can be concluded that many simulation models have been developed for which research has indicated that these models are feasible for in silico testing of glucose control systems. Limitations of all models are that the change of glucose kinetics diurnally and over a longer period of time have not been fully identified. Both oscillatory patterns and stepwise adjustments have been applied to parameter values. Only recently, glucagon kinetics have become relevant in these simulation models, so a limited amount of studies into glucagon kinetics and action has been performed. Part of the available glucose models has not considered the effect of glucagon at all. Moreover, the influence of external factors like varying meals, physical activity and stress is largely unknown and has not been incorporated into the simulation models. Due to the complexity of the discussed models, it may not be possible to determine the effects of these external factors on all model parameters.

From the literature overview, it can be seen that in most models a large part of the model parameters are fixed and only several parameters are estimated to fit the data. The disadvantage of this strategy is that assumptions need to be made about the origin of inter- and intra-subject variations. Estimation of the complete set of parameters in a model enables researchers to identify the effect of inter- and intra-subject variations on all parts of the model. This can be accomplished either by doing extensive tracer experiments for identification of variations in the physiological processes or by application of less complex model structures. The current study applies the second option. Model structure of the Inreda model [5] that is largely based on the Dalla Man model [36] was adapted. Several model structures were proposed and identified based on clinical data for the insulin, glucagon and glucose subsystems. For each model, precision of the parameters and performance of the models to predict glucose levels in a T1DM patient were determined.

Chapter 3

Methods

From the literature study, it has become clear that complete identification of the parameters of a complex model of glucose metabolism is not possible when the only data available are measurements of glucose, insulin and glucagon concentrations in the blood plasma. For that reason, the available data was applied for the identification of newly proposed model structures. The studies from which data is available and criteria of inclusion and exclusion of sections of data are discussed in section 3.1. Then, in section 3.2, explanation on calculations to acquire model inputs is provided. In section 3.3, models of varying complexity are proposed to describe the glucose metabolism, which includes models of insulin and glucagon kinetics. This is followed by section 3.4 on the methods that were applied for parameter identification. The chapter is concluded with section 3.5 in which it is explained how results of the identification of proposed models were quantified and validated.

3.1 Available data

For parameter estimations in the three subsystems, different data was applied. The insulin subsystem was identified on data taken from the study performed by Schiavon et al. [26]. In this study, three different datasets were applied for parameter estimations in various proposed models of subcutaneous insulin absorption. Each dataset contains measurements of the plasma insulin concentration in subjects with T1DM after a subcutaneous bolus injection of insulin lispro. Measurement sampling times and insulin dosages varied slightly between the three datasets. Experimental procedures were similar. The average response of the plasma insulin concentration was published [26] for each of these datasets. Data was not available to the current study, so the published averaged responses were applied here for the parameter estimations in the insulin subsystem.

Data acquired in two different experiments was available to the current study. For identification of the glucagon subsystem, data acquired in the first experiment was applied. This experiment was part of the study performed by Blauw et al. (2015) [16]. The aim was to determine the influence of glucagon on blood glucose (BG) levels. The experiments were performed twelve times for each of the six T1DM patients. Three different glucagon dose sizes were given at each of the four different initial BG levels. These initial BG levels were established before the glucagon bolus injection by variable manual venous infusion of either glucose or insulin. Insulin levels were as low as possible before the start of the glucagon injections. Blood samples were taken before the glucagon injections and every 10 minutes after until 60-160 minutes. Glucagon and glucose concentrations were measured for each sample. In Figure 3.1, measurement data of glucagon concentrations after a bolus injection is shown [16]. Seven experiments with unrealistic progress of glucagon concentrations over time were excluded, leaving 65 measurement periods for the identification of glucagon kinetics. The measurements of glucose concentrations were not applied in the current study, since the time window of sampling was shortly after the bolus injection and therefore not valuable for model identification.

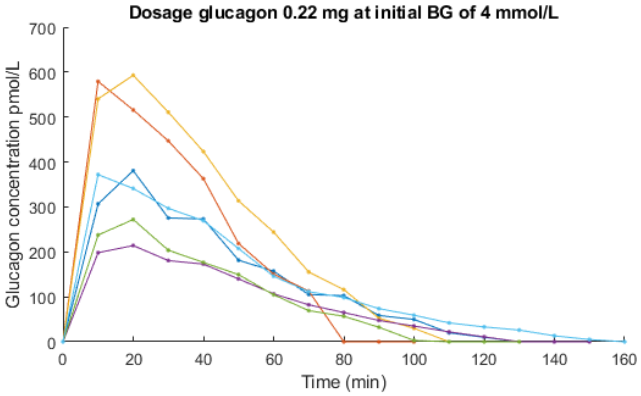

Figure 3.1: Example of measured glucagon concentrations [16]. Glucagon concentrations are shown for six subjects to which a subcutaneous bolus injection of 0.22 mg glucagon was applied at an initial BG of 4 mmol/L.

For the identification and validation of the glucose subsystem the data acquired in the second experiment was applied. This experiment was part of the study performed by Blauw et al. (2016) [13]. Ten patients completed the study. The aim was to determine the performance and safety of an artificial pancreas system. The influence of subcutaneous insulin and glucagon infusions combined with normal meal intake on the BG levels was determined over a four-day period. The crossover experiment consisted of a closed loop (CL) and open loop (OL) part. In the CL part, bolus insulin and glucagon infusions were controlled by an artificial pancreas system that was developed by Inreda Diabetic BV. In the OL control period, no glucagon was infused and insulin infusion was controlled by the patients themselves using their own insulin pump. Such pumps apply continuous insulin infusion at various rates during the day and additional bolus injections before meal intake. Continuous glucose monitoring (CGM) was applied in order to measure the glucose concentrations subcutaneously, with a frequency of 6 min^{-1}. Regular self monitoring of blood glucose (SMBG) measurements are available without a predetermined frequency.

Periods in which glucose levels were influenced by glucagon and meals were identified from the OL and CL CGM data. For glucagon, this was defined as a period of 80 minutes after infusion was applied, since glucagon concentrations were mostly levelled off after this period (Figure 3.1) [16]. For meal intake, this was defined as a period of 180 minutes after meal intake, since studies have shown that most ingested glucose is absorbed after this period [86, 3]. The regular anti-occlusion shots of glucagon in the CL data were neglected. An example of available CGM data in the CL part is shown in Figure 3.2. Periods in which glucose levels were influenced by meal intake are marked red and periods in which glucose levels were influenced by glucagon infusions are marked green. OL data looks similar to CL data, but without any infusion of glucagon. To begin with, the sections of data that were only perturbed by insulin were applied for model identification of glucose dynamics and insulin action on glucose dynamics only. These are the white areas in the figure. Then, data sections of closed loop data that were influenced by glucagon and insulin infusions, but not by meal intake, were selected to identify the influence of glucagon on glucose dynamics. These are the white and green areas in the figure.

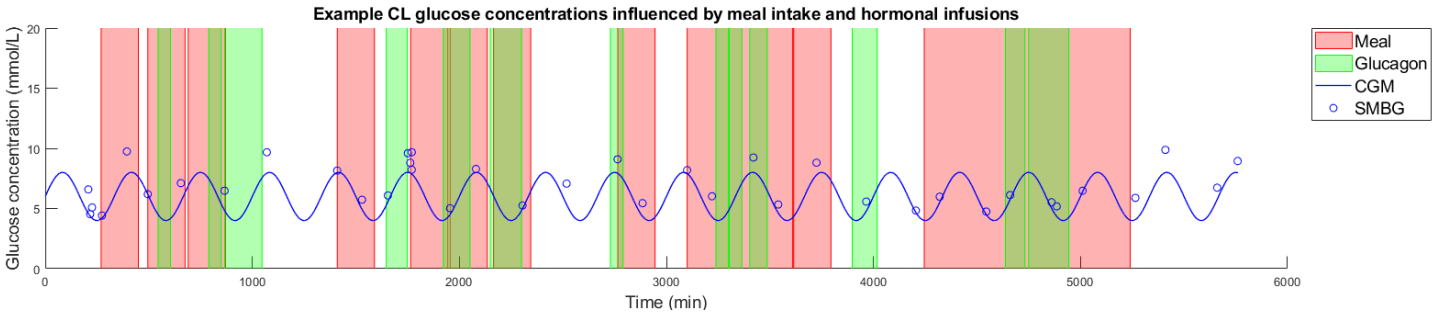

Figure 3.2: Example of closed loop glucose data [13]. Meal ingestion and digestion in the 180 minutes after meal intake is represented by the areas that are marked red. Subcutaneous glucagon infusion and processing in the 80 minutes after infusion is represented by the areas that are marked green. Subcutaneous insulin infusions affect glucose levels during the entire measurement period, including the unmarked (white) areas in the plot.

Not all available data sections that were selected based on the above criteria could be applied for model identification or validation. The first exclusion criterion was that data inspection showed a positive slope in the measured glucose concentrations, while the insulin concentration was above the average that was simulated for the considered subject and no glucagon infusions were applied. This criterion was included, because its occurrence suggests that this increase is related to meal intake and the effect of meal ingestion is currently not considered in the model. Data sections were also excluded when deviations of over 2 mmol/L were found between the SMBG and CGM measurements or when physical activity was performed during the period.

Furthermore, when during a data section the glucose levels showed a stepwise increase or decrease of over 2 mmol/L, this period was shortened until after this step in the measured BG. The data section was excluded when the remaining period was shorter than 60 minutes. Such steps in CGM measurements can occur when adjustments to the calibration factor between the electric current and measured glucose concentration are made. The same procedure of shortening or exclusion of the data section was also followed when data was missing for prolonged periods of time (> 30 minutes) during the interval. Lastly, data sections were excluded when showing instability of the CGM measurements, meaning that there were fluctuations related to sensor variability rather than physiological change. This event occurred in two situations. The first situation was characterized by periods with sudden increases/decreases in glucose concentrations that were reversed within the next three hours and that occupied less than a quarter of the duration of the entire interval. The second situation was characterized by an increase or decrease in the measured SMBG in a certain period of time, while the measured CGM showed a decrease or increase of the glucose concentration respectively.

A number of 57 data sections with insulin input only were included, of which 36 were taken from the CL study period and 21 from the OL study period. One to nine data sections were included for each of the ten subjects. Length of these varied from 75 minutes to 11 hours, with a mean of about 6 hours. 49 out of 54 data sections were taken from the night, starting between 21 pm and 6 am. A number of 24 data sections with insulin and glucagon input only were included. Length of these varied from 97 minutes to almost 13 hours, with a mean of about 7.5 hours. For these sections, 16 out of 24 data sections were taken from the night.

3.2 Model inputs

The model inputs that were considered in the current study are insulin infusion rate (I_{IR}) and glucagon infusion rate (H_{IR}). It was assumed that the amounts of insulin and glucagon infused during the study period were known without error. Dosed quantities of insulin and glucagon were measured in units (U) as defined in column three of Table 3.1. Insulin was infused in steps of 0.25 units per second. Maximum insulin infusion was 15 units (60 s). Glucagon was infused in steps of 0.5 units per second with a maximum infusion of 10 units (20 s). Meal input was neglected in the current study, since only data uninfluenced by meal glucose absorption were considered (section 3.1)

The remaining time-dependent model inputs, I_{IR} and H_{IR}, were set to be equal to zero when no dosages were given. By performing all simulations at a sampling frequency of 60 min^{-1}, bolus infusions were modelled by setting a number of samples (seconds) corresponding to the applied dosage equal to the infusion rate of either insulin or glucagon. The infusion rates of insulin and glucagon each had a fixed size. Calculations of these infusion rates for both hormones is shown in Table 3.1. Since the amounts of insulin and glucagon in the compartments were measured in pmol/kg, the infusion rates (IR) of insulin and glucagon should be expressed in pmol/kg/min. M_i and M_h are the molar masses of insulin and glucagon respectively. Values used were $M_i = 5813.677$ g/mol and $M_h = 3482.75$ g/mol [5]. Since dosages were distributed over the entire body, these were divided by the body weight (BW) in kg of the subject considered.

Table 3.1: Conversion of insulin and glucagon dosages to infusion rates (IR) of both hormones

Hormone	Maximum dosage (U)	mg in 1 U	pmol in 1 U	IR (U/s)	IR (pmol/kg/min)
Insulin	15	0.0347	$\frac{0.0347 \cdot 10^9}{M_i}$	0.25	$0.25 \cdot 60 \cdot \frac{0.0347 \cdot 10^9}{M_i \cdot BW}$
Glucagon	10	0.01	$\frac{0.01 \cdot 10^9}{M_h}$	0.5	$0.5 \cdot 60 \cdot \frac{0.01 \cdot 10^9}{M_h \cdot BW}$

3.3 Models

The general model structure is shown in Figure 3.3. The system consists of three subsystems. The insulin subsystem has as input the insulin infusion rate (I_{IR}) and as output the amount of insulin per kg of body weight (q_{ip}) or insulin concentration (C_{ip}) in the blood plasma. Likewise, the glucagon subsystem has as input the glucagon infusion rate (H_{IR}) and as output the amount of glucagon per kg of body weight (q_{hp}) or glucagon concentration (C_{hp}). The glucose subsystem in turn has these glucagon/insulin subsystem outputs as input and the output is the glucose mass (q_{gp}) or glucose concentration (C_{gp}). Intestinal glucose absorption was assumed to be absent for the data sections selected for glucose subsystem identification. Since the hormonal subsystems could not be identified based on the same data [13] as the glucose subsystem, the insulin and glucagon subsystems were identified with the aim of obtaining parameter estimates for a patient with T1DM. Model structure of the insulin and glucagon subsystems was proposed based on the literature study. Linear and nonlinear model structures with varying complexity were proposed for the glucose subsystem.

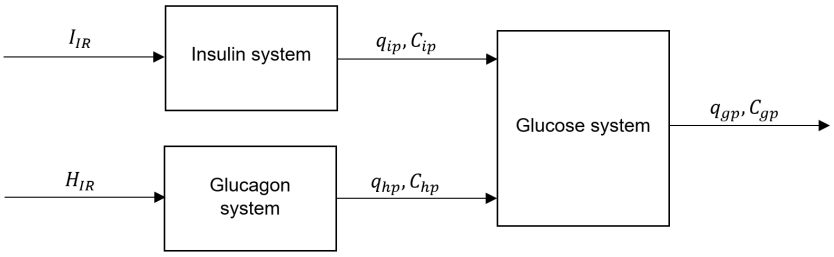

Figure 3.3: Box scheme of general model structure of the glucose model in this study. Insulin and glucagon subsystems are aimed at modelling insulin and glucagon concentrations in the blood plasma in response to infusion of insulin (I_{IR}) and glucagon (H_{IR}). The glucose subsystem is aimed at modelling plasma glucose concentrations depending on levels of insulin and glucagon in the blood.

3.3.1 Insulin subsystem

The insulin that was administered during the crossover experiment [13] was fact-acting insulin lispro. The insulin model as applied originally by Inreda Diabetic BV [5] was not used as a basis for the new insulin submodel, since parameter estimations [22] were based on unknown data, possibly applicable to another type of insulin. Schiavon et al. [26] has developed a model of subcutaneous insulin absorption for insulin lispro. Attempts at simulating plasma insulin concentrations after an insulin bolus injection with the Inreda model applying the same input as in the study by Schiavon et al. [26], resulted in much weaker output insulin concentrations than in the averaged measured insulin responses that were found by Schiavon et al. This was an additional reason for dropping the insulin submodel in the Inreda model. An assumption made in the Inreda model that was also applied in the current study, was that beta cell secretion of insulin is absent in people with T1DM [5].

A study performed by Schiavon et al. [26] assessed three different models of subcutaneous insulin lispro absorption and insulin kinetics on the ability to describe the insulin concentration in T1DM subjects after single bolus injections. In the results, precision of parameter estimations and their physiological interpretation were considered. The model best capable of describing the subcutaneous insulin absorption with a meaningful physiological interpretation of the parameters was a three-compartment model that is shown in Equation 3.1 and Figure 3.4. Parameters and variables with their meaning and unit are presented in Table 3.2.

As mentioned in Section 3.1, the insulin subsystem parameters were identified based on three different average plasma insulin concentration responses. Starting from the model in Figure 3.4, attempts were made to simplify the model structure that was found to be required for modelling the response in individual patients [26]. Four different versions of the model with increasing complexity were applied to find a description of the plasma insulin concentration for an average T1DM patient. No estimation of the delay τ_{Isc} on the model input was performed for any of these versions, since this parameter could not be estimated reliably with the applied estimation method. Although this is less than ideal, it was expected that this delay was not critical in obtaining a good fit for the data.

Four versions of the model in Equation 3.1 were estimated. Version 1 was of 2nd order with estimation of m and a_{p1}. Version 2 was similar to version 1, but with additional clearance from q_{Isc1} represented by parameter m_{sc}. This parameter reflects the degradation of insulin at the injection site [87]. Version 3 was of 3rd order without the direct flow from q_{Isc1} to q_{ip} and with estimation of m, d_i and a_{p2}. Version 4 differed from version 3 by including the parameter a_{p1} representing this direct flow. Resulting parameter values were the mean value of the estimations found for the averaged responses. These parameter values were applied to simulate plasma insulin concentrations for the identification and validation of the glucose subsystem. Parameter V_i was assumed to be constant and was fixed to the average of 0.126 L/kg found by Schiavon et al. [26].

$$\begin{cases} \dot{q}_{Isc1}(t) &= -(a_{p1} + d_i) \cdot q_{Isc1}(t) + I_{IR}(t - \tau_{Isc}) \\ \dot{q}_{Isc2}(t) &= -a_{p2} \cdot q_{Isc2}(t) + d_i \cdot q_{Isc1}(t) \\ \dot{q}_{ip}(t) &= -m \cdot q_{ip}(t) + a_{p1} \cdot q_{Isc1}(t) + a_{p2} \cdot q_{Isc2}(t) \\ C_{ip}(t) &= \frac{q_{ip}(t)}{V_i} \end{cases} \tag{3.1}$$

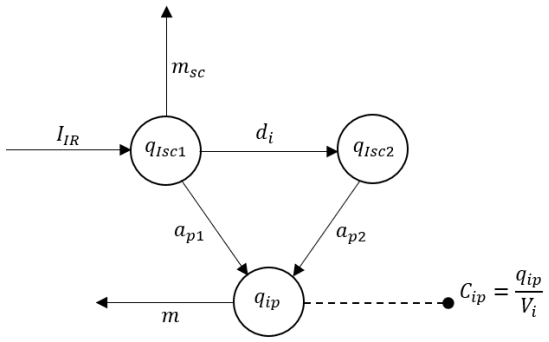

Figure 3.4: Model structure of insulin model as found by Schiavon et al. [26]. Flow of subcutaneously infused insulin to the blood plasma is either directly through the first subcutaneous compartment (a_{p1}) or indirectly through both the first and second subcutaneous compartment (d_i and a_{p2}).

Table 3.2: Overview of variables and parameters in insulin subsystem model

Parameter	Description	Unit
Insulin subsystem variables		
I_{IR}	Rate of insulin infusion	pmol/kg/min
q_{Isc1}	Amount of insulin in first subcutaneous insulin compartment	pmol/kg
q_{Isc2}	Amount of insulin in second subcutaneous insulin compartment	pmol/kg
q_{ip}	Amount of insulin in blood plasma	pmol/kg
C_{ip}	Insulin concentration in blood plasma	pmol/L
Insulin subsystem parameters		
V_i	Distribution volume of insulin in blood plasma	L/kg
a_{p1}	Rate of insulin transport from first subcutaneous compartment to blood plasma	1/min
a_{p2}	Rate of insulin transport from second subcutaneous compartment to blood plasma	1/min
d_i	Rate of insulin transport from first to second subcutaneous compartment	1/min
m	Clearance rate of insulin from blood plasma	1/min
m_{sc}	Clearance rate of insulin from the first subcutaneous compartment	1/min
τ_{Isc}	Transport delay in transfer of injected insulin to first subcutaneous compartment	min

3.3.2 Glucagon subsystem

The glucagon model in the Inreda Model [5] was based on the Dalla Man S2013 simulator [36]. It consists of submodels for subcutaneous glucagon absorption, alpha cell secretion and glucagon kinetics. Alpha cell secretion in the subjects that participated in the crossover study of Blauw et al. [13] is expected to be severely compromised [37, 6], since the diabetes duration was well over 10 years in most of the subjects: median duration was 18.0 years with an interquartile range of 18.0 (14.8-29.5) years [16]. Estimation of the parameters of the alpha cell model in the Inreda model has been attempted [48], but proved to be difficult due to limited data availability and model complexity. For both of these reasons, the assumption was made here that glucagon secretion by the alpha cells was negligible in the studied subjects. Although diabetes duration of the subjects participating in the glucagon study of Blauw et al. [16] is unknown, the same assumption was made for the identification of the glucagon subsystem. Initial glucagon concentrations at the start of each measurements were subtracted from the complete glucagon measurement. Parameters and variables with their meaning and unit are presented in Table 3.3.

Glucagon pharmacokinetics were left to be modelled. In the Inreda model [5], a three-compartmental model is applied to model subcutaneous absorption and kinetics of glucagon. However, since it has been suggested that glucagon concentrations can be modelled by a two-compartmental model as well [33, 35], it was attempted to fit de glucagon data to a two-compartmental to begin with, as shown in Figure 3.5 and Equation 3.2. This way, the parameters would be uniquely identifiable and parameter variations between the various dosages, initial glucose levels and subjects could be determined. The distribution parameter V_h (L/kg) was fixed at 0.25 L/kg, which was found by the manufacturer for the distribution volume of glucagon [88] applied in both the glucagon and crossover study. If parameter estimations showed this 2nd order model was not able to provide a fit to the data, the model structure would be extended to a model versions similar to what was proposed for the insulin subsystem.

$$\begin{cases} \dot{q}_{Hsc}(t) &= H_{IR}(t) - b_p \cdot q_{Hsc}(t) \\ \dot{q}_{hp}(t) &= b_p \cdot q_{Hsc}(t) - n_h \cdot q_{hp}(t) \\ C_{hp}(t) &= \frac{q_{hp}(t)}{V_h} \end{cases} \tag{3.2}$$

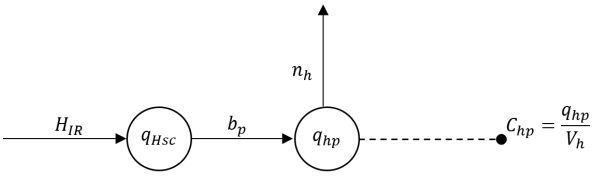

Figure 3.5: Model structure of glucagon model similar to what was done by Haidar et al. [33]. Flow of subcutaneously infused glucagon to the blood plasma is through a subcutaneous compartment (b_p).

Table 3.3: Overview of variables and parameters in glucagon subsystem model

Parameter	Description	Unit
Glucagon subsystem variables		
H_{IR}	Rate of glucagon infusion	pmol/kg/min
q_{Hsc}	Amount of glucagon in subcutaneous glucagon compartment	pmol/kg
q_{hp}	Amount of glucagon in blood plasma	pmol/kg
C_{hp}	Glucagon concentration in blood plasma	pmol/L
Glucagon subsystem parameters		
V_h	Distribution volume of glucagon in blood plasma	L/kg
b_p	Rate of insulin transport from subcutaneous compartment to blood plasma	1/min
n_h	Clearance rate of glucagon from blood plasma	1/min

3.3.3 Glucose subsystem

Various models were proposed in order to describe the glucose metabolism. The CL and OL datasets from the cross-over study [13] were applied to perform parameter estimations for the proposed models. Since the assumption was made that alpha cell glucagon secretion could be neglected in the participating subjects, it was possible to start with identification of a glucose model with the only input being the amount of insulin per kg of body weight. Identification and validation of four types of proposed glucose models with varying complexity was compared: a linear MM, a nonlinear MM, a model that applies the Michaelis-Menten relationship, and a two-compartmental linear model. Knowledge of physiology and existing glucose models (section 2.2) was applied to propose certain model structures, but assessment of the proposed models was largely data-driven. Modelling the glucagon action was attempted afterwards on CL data sections in which infusions of both glucagon and insulin were applied. In all models, the ratio between the glucose mass and glucose concentration was fixed. This ratio depended on the molar mass of glucose M_g, which was fixed at 180.156 g/mol, and on the distribution volume of glucose in the plasma V_g, which was fixed at 0.17683 L/kg [22]. This is the same as in the Inreda model [5].

Linear minimal model

For the first proposed model, the change of glucose mass in the blood plasma depends linearly on the various variables. The model equations are shown in Equation 3.3 and variables and parameters are explained in Table 3.4. It is a simplification of the Bergman minimal model [49]. The nonlinearity in the equations is removed and the effect of insulin is not delayed through an additional compartment but simply by the delay τ_I. There is a basal rate of appearance of glucose in the blood G_b, that is a the difference between a basal production and utilization rate of glucose. Glucose is cleared from the blood proportionally to the parameter k_g as its mass in the blood increases. Moreover, glucose is removed from the blood at an increasing rate, proportional to the rate parameter k_i, as the insulin concentration increases.

$$\begin{cases} \dot{q}_{gp}(t) & = G_b - k_g \cdot q_{gp}(t) - k_i \cdot q_{ip}(t - \tau_I) \\ C_{gp}(t) & = \dfrac{q_{gp}(t)}{M_g \cdot V_g} \end{cases} \tag{3.3}$$

Table 3.4: Variables and parameters in the linear MM with description of meaning and unit.

Parameter	Description	Unit
Linear MM glucose subsystem variables		
q_{gp}	Glucose mass in blood plasma	mg/kg
C_{gp}	Glucose concentration in blood plasma	mmol/L
Linear MM glucose subsystem parameters		
V_g	Distribution volume of glucose in blood plasma	L/kg
M_g	Molar mass of glucose	mg/mmol
G_b	Basal rate of appearance of glucose in blood plasma	mg/kg/min
k_g	Glucose clearance rate from blood plasma	1/min
k_i	Glucose mass disappearance rate from blood plasma per unit of insulin	mg/pmol/min
τ_I	Delay in effect of insulin on glucose mass in blood plasma	min

Nonlinear minimal model

A nonlinear model was also proposed. The model equations are shown in Equation 3.4 and variables and parameters are explained in Table 3.5. This model is similar to the linear MM, with the difference that the effect of insulin on the glucose concentration is nonlinear. This is closer to the model that was implemented by Bergman [49]: the nonlinearity in the effect of insulin was not removed. The effect of insulin is stronger when the glucose mass in the blood is higher, which is represented by a multiplication of the insulin concentration with the glucose concentration in the differential equation. The parameter k_i still determines the sensitivity to insulin.

$$\begin{cases} \dot{q}_{gp}(t) & = G_b - k_g \cdot q_{gp}(t) - k_i \cdot q_{gp}(t) \cdot q_{ip}(t - \tau_I) \\ C_{gp}(t) & = \dfrac{q_{gp}(t)}{M_g \cdot V_g} \end{cases} \tag{3.4}$$

Table 3.5: Variables and parameters in the nonlinear MM with description of meaning and unit.

Parameter	Description	Unit
Nonlinear MM glucose subsystem variables		
q_{gp}	Glucose mass in blood plasma	mg/kg
C_{gp}	Glucose concentration in blood plasma	mmol/L
Nonlinear MM glucose subsystem parameters		
V_g	Distribution volume of glucose in blood plasma	L/kg
M_g	Molar mass of glucose	mg/mmol
G_b	Basal rate of appearance of glucose in blood plasma	mg/kg/min
k_g	Glucose clearance rate from blood plasma	1/min
k_i	Glucose disappearance rate from blood plasma per unit of insulin	$(\text{pmol/kg})^{-1}/\text{min}$
τ_I	Delay in effect of insulin on glucose mass in blood plasma	min

Michaelis-Menten model

The third glucose submodel that was proposed is based on what was found by Wong et al. [4]. Two versions of this model were applied. For version 1, there were three main differences to the nonlinear MM: (1) the effect of insulin on the glucose concentration is considered through a Michaelis-Menten relationship (see section 2.2.4), (2) the variable q_{gd} describes the deviation of the glucose mass from the equilibrium value ($q_{gp,eq}$), instead of the glucose mass itself, and (3) a threshold q_{ipb} was applied to the insulin variable in the numerator of the relationship. This threshold was added to in order to increase the effect of low levels of insulin. The parameter a_g represents the saturation of the effect of insulin in the Michaelis-Menten relationship. No delay was added to the effect of insulin. The differential equation is shown in Equation 3.5 and explanation on the variables and the parameters can be found in Table 3.6.

$$\begin{cases} \dot{q}_{gd}(t) & = G_b - k_g \cdot q_{gd}(t) - k_i (q_{gd}(t) + q_{gp,eq}) \dfrac{q_{ip}(t) - q_{ipb}}{1 + a_g \cdot q_{ip}(t)} \\ C_{gp}(t) & = \dfrac{q_{gd}(t) + q_{gp,eq}}{M_g \cdot V_g} \end{cases} \tag{3.5}$$

Another version (version 2) of this model was also considered (Equation 3.6, Table 3.6). This version was similar to the linear MM, with the difference that the effect of insulin was considered through the Michaelis-Menten relationship. Similarly as for the version 1 Michaelis-Menten model, a threshold was added to the effect of insulin. This version 2 model was considered, because for version 1 parameter estimations were difficult and often not unique, which is discussed further in chapter 5. In contrast to version 1, the effect of the Michaelis-Menten parameter k_i was independent of the glucose concentration in the version 2 Michaelis-Menten model.

$$\begin{cases} \dot{q}_{gp}(t) & = G_b - k_g \cdot q_{gp}(t) - k_i \dfrac{q_{ip}(t) - q_{ipb}}{1 + a_g \cdot q_{ip}(t)} \\ C_{gp}(t) & = \dfrac{q_{gp}(t)}{M_g \cdot V_g} \end{cases} \tag{3.6}$$

Table 3.6: Variables and parameters in the Michaelis-Menten model with description of meaning and unit.

Parameter	Description	Unit
Michaelis-Menten glucose subsystem variables		
q_{gd}	Deviation of glucose mass from equilibrium value in blood plasma	mg/kg
q_{gp}	Glucose mass in blood plasma	mg/kg
C_{gp}	Glucose concentration in blood plasma	mmol/L
Michaelis-Menten subsystem parameters (version 1)		
V_g	Distribution volume of glucose in blood plasma	L/kg
M_g	Molar mass of glucose	mg/mmol
$q_{gp,eq}$	Equilibrium glucose mass in blood plasma	mg/kg
G_b	Basal rate of appearance of glucose in blood plasma	mg/kg/min
k_g	Glucose (dis)appearance rate from blood plasma	1/min
k_i	Glucose disappearance rate from blood plasma per unit of insulin	$(\text{pmol/kg})^{-1}/\text{min}$
a_g	Saturation parameter of insulin effect on glucose	kg/pmol
q_{ipb}	Threshold of insulin action	pmol/kg
Michaelis-Menten subsystem parameters (version 2)		
V_g	Distribution volume of glucose in blood plasma	L/kg
M_g	Molar mass of glucose	mg/mmol
G_b	Basal rate of appearance of glucose in blood plasma	mg/kg/min
k_g	Glucose clearance rate from blood plasma	1/min
k_i	Glucose mass disappearance rate from blood plasma per unit of insulin	mg/pmol/min
a_g	Saturation parameter of insulin effect on glucose	kg/pmol
q_{ipb}	Threshold of insulin action	pmol/kg

Two-compartmental model

A two-compartmental (2COM) model of the glucose concentration was also included. Parameters and variables are explained in Table 3.7. The first compartment q_{gp} represents the glucose mass in the blood plasma and quickly equilibrating tissues. The second compartment q_{gt} represents the glucose mass in other tissues. Parameter estimations were attempted for two versions of the model. The first version, presented in Equation 3.7, was the most extensive. This model contains many of the components of glucose kinetics and dynamics that occur physiologically: transfer of glucose between both quickly and slowly equilibrating tissues (k_1 and k_2), glucose utilization in both of these tissues types (k_{g1} and k_{g2}), a basal endogenous glucose production into the blood stream (G_b) and an insulin-dependent transfer of glucose (k_i) away from the quickly equilibrating tissues for stimulation of glucose utilization and glycogenesis in slowly equilibrating tissues [4]. This is similar to what was applied by one of the first two-compartmental versions of the Bergman minimal model (Vicini et al. [54]) with the difference that the influence of insulin is modelled to be an insulin-dependent transfer away from the first compartment. Initial mass in the tissue compartment was determined by estimation of i_g.

$$\begin{cases} \dot{q}_{gp}(t) & = -k_{g1} \cdot q_{gp}(t) - k_1 \cdot q_{gp}(t) + k_2 \cdot q_{gt}(t) - k_i \cdot q_{ip}(t) + G_b \\ \dot{q}_{gt}(t) & = -k_{g2} \cdot q_{gt}(t) + k_1 \cdot q_{gp}(t) - k_2 \cdot q_{gt}(t) + k_i \cdot q_{ip}(t) \\ C_{gp}(t) & = \dfrac{q_{gp}(t)}{M_g \cdot V_g} \\ q_{gt}(0) & = i_g \cdot q_{gp}(0) \end{cases} \tag{3.7}$$

The second version of the model is presented in Equation 3.8. Initial mass in the tissue compartment (q_{gt}) was calculated from the parameter values in the same way as in the Dalla Man model [3]. In contrast to Dalla Man et al. [3], there was no glucose-dependent clearance from the compartments included. Insulin-dependent clearance occurs in the remote tissue compartment, which is similar to what was done by Vicini et al. [54]. Physiological interpretation of this model version is slightly different from that of version 1. In this model, it was assumed that insulin-dependent uptake of glucose occurred directly in the slowly equilibrating compartment as opposed to indirectly through the transfer of glucose to the slowly equilibrating compartment in version 1. Moreover, removal of the glucose-dependent clearance from the compartments means that the model version 2 assumed that all glucose utilization and storage above the basal level was insulin-dependent.

$$\begin{cases} \dot{q}_{gp}(t) & = -k_1 \cdot q_{gp}(t) + k_2 \cdot q_{gt}(t) + G_b \\ \dot{q}_{gt}(t) & = k_1 \cdot q_{gp}(t) - k_2 \cdot q_{gt}(t) - k_i \cdot q_{ip}(t - \tau_I) \\ C_{gp}(t) & = \frac{q_{gp}(t)}{M_g \cdot V_g} \\ q_{gt}(0) & = \frac{k_1}{k_2} \cdot q_{gp}(0) \end{cases} \tag{3.8}$$

Table 3.7: Variables and parameters in version 1 of the 2COM model with description of meaning and unit.

Parameter	Description	Unit
Two-compartmental glucose subsystem variables		
q_{gp}	Glucose mass in blood plasma	mg/kg
q_{gt}	Glucose mass in other tissues	mg/kg
C_{gp}	Glucose concentration in blood plasma	mmol/L
Two-compartmental glucose subsystem parameters (version 1)		
V_g	Distribution volume of glucose in blood plasma	L/kg
M_g	Molar mass of glucose	mg/mmol
G_b	Basal rate of appearance of glucose in blood plasma	mg/kg/min
k_{g1}	Glucose clearance rate from blood plasma	1/min
k_{g2}	Glucose clearance rate from tissue compartment	1/min
k_1	Glucose transfer rate from blood plasma to tissue compartment	1/min
k_2	Glucose transfer rate from tissue compartment to blood plasma	1/min
k_i	Glucose mass disappearance rate from blood plasma to tissue compartment per unit of insulin	mg/pmol/min
i_g	Ratio parameter of initial mass in tissue compartment compared to initial mass in plasma compartment	-
Two-compartmental glucose subsystem parameters (version 2)		
V_g	Distribution volume of glucose in blood plasma	L/kg
M_g	Molar mass of glucose	mg/mmol
G_b	Basal rate of appearance of glucose in blood plasma	mg/kg/min
k_1	Glucose transfer rate from blood plasma to tissue compartment	1/min
k_2	Glucose transfer rate from tissue compartment to blood plasma	1/min
k_i	Glucose mass disappearance rate from tissue compartment per unit of insulin	mg/pmol/min

3.3.4 Addition of glucagon action

After identification of the parameters affecting the glucose concentration independently of glucagon concentrations, the glucose submodels were extended to modelling of the glucagon action. As described earlier, glucagon stimulates the EGP by the liver. In the current study, glucagon action was implemented similarly for all proposed glucose subsystem models. For the two-compartmental model, the glucagon action would only influence the glucose mass in the plasma compartment. This choice was made, because in existing models the EGP generally directly influences the glucose mass in this plasma compartment reflecting the release of glucose from the liver into the blood stream [36, 35]. Since the glucagon action would be modelled similarly for all proposed model structures, the identification was only performed on two of the proposed glucose models that could provide best model fit for parameter estimations for insulin input alone.

Two variations of glucagon action on glucose concentrations were proposed. The first option is that the rate of change of the glucose mass is linearly dependent on the amount of glucagon in the blood, depending on the rate of glucose mass appearance parameter k_h (mg/pmol/min). The second option is that the increase in the glucose mass is directly proportional to q_{hp} and the rate parameter k_{hp} (mg/pmol).

3.4 Parameter identification method

Parameter estimations were performed in order to be able to assess performance of the proposed models for the three different subsystems. Initial values of the insulin and glucagon concentration variables were

assumed to be zero for the insulin and glucagon submodel identification respectively. Initial values of the glucose concentration variable in the glucose model identification were based on the CGM measurements in the crossover study [13]. Initial values for the amounts of insulin per kg of bodyweight were based on simulations for the complete four-day period of the study. This could be done, since the insulin subsystem was identified before the glucose subsystem and the input I_{IR} was known. As explained earlier, it was assumed that basal levels amount of glucagon in the blood plasma could be neglected due to a lack of alpha cell secretion in T1DM patients. After the initial estimations, parameter estimations were grouped based on the outcomes of the estimations. Parameter estimations were repeated in conditions for which certain parameters were fixed or set to zero if the initial estimations indicated that this could improve model identifiability without loss of accuracy.

Parameter estimations were performed by Matlab [89]. The 'lsqnonlin' function [90] was applied to determine the parameter values that resulted in the best fit to the selected data. The function has the ability to solve nonlinear least-squares problems. The least-squares method relies on to assumptions: (1) there exists no error in the model input and (2) errors in the measured output are normally distributed with zero mean and constant variance. The input function of 'lsqnonlin' was set to be an anonymous function that loaded the Simulink model for which parameters were to be estimated. The algorithms that were available were a trust-region-reflective method and Levenberg-Marquardt. In general, the least squares method attempts to find parameter estimations (x) corresponding to the optimum in the function $f(x)$ that defines the residual error. An important factor in this method is determining the direction in which the solution is searched [91].

The trust-region-reflective method [92] functions by only considering the neighbourhood N around the point x, which contains the solution s. N is defined based on an approximate Gauss-Newton direction. The function $f(x)$ is approximated in this neighbourhood by the function $q(s)$. This function is minimized and the resulting solution s is applied to define a new point x. This procedure is repeated until one of the stopping criteria is met. The Levenberg-Marquardt method [92] tries to minimize the function $f(x)$ without simplifications. The Gauss-Newton method with an additional second order term is applied to determine the direction in which the solution is searched. This second order term is beneficial when the optimal function value is not equal to zero, which makes the function more robust.

Use of the trust-region-reflective method was advised in Matlab documentation [93]. In the current study, the Levenberg-Marquardt method was applied to find parameter estimations for the insulin and glucagon subsystems. This was done because the residual errors for this algorithm were smaller than those obtained when the trust-region-reflective algorithm was applied. For the glucose subsystem, the trust-region-reflective algorithm was used, since this method allowed for constraining the parameters within physiologically feasible ranges and as a result increased the efficiency of the estimation process. Both estimation methods attempt to find a local minimum in the residual error function, it is not certain that this local minimum is also a global minimum of the function.

3.5 Model validation & analysis

The measures that were used to assess model fit were root mean squared error (RMSe) and variance accounted for (VAF). RMSe is the root of the mean of all squared residuals, so it is a measure of the error between the output time-series concentrations and the measured concentrations. RMSe is measured in pmol/L for the insulin and glucagon subsystem models and in mmol/L for the glucose subsystem model. VAF is a percentage that measures the variance in the measured concentrations that is accounted for by the model, i.e. the variance in the measurement that is not seen in the residuals [94]. For the glucose subsystem, estimations were set to be successful if the model output could provide a reasonable fit for the glucose data. A reasonable fit was defined as a RMSe smaller than 0.35 mmol/L or a VAF larger than 75%. These boundaries were set based on visual inspection of the estimation results.

If neither with the Levenberg-Marquardt method nor with the trust-region-reflective algorithm successful parameter estimations for a certain model structure could be performed, the reason for this was determined. Adaptations to the parameter boundaries were made if this could solve the problem [95]. If necessary, it was attempted to solve the problem by relaxing the default solver tolerances [95]. The model structure was dropped when for several data sections consecutively, no parameter estimations could be performed. Results of parameter estimations were also not considered if the average of the VAF

value was below 50% in combination with outcome variables implying that results are physiologically impossible. Such parameter estimations would not have any value apart from showing that the model could not be fitted to the data or that the estimation method was unsuitable to find the solution for the considered model.

Precision of the parameter estimates was measured by the coefficient of variation (CV) over all estimated parameter values per subject, which shows the ratio between standard deviation and mean. The CVs are dimensionless and are valued >1 when the standard deviation is larger than the mean; it is a measure of the spread of a set of parameter values and a way of normalizing the standard deviation. For the glucagon subsystem, paired t-tests were applied to determine whether estimations for the experimental condition (initial BG and glucagon dosage) differed between subjects. Also, correlations of the initial BG levels and dosages with the parameter values, RMSe and VAF values and with the glucagon peak concentrations were determined. For the glucose subsystem, correlations between the identified parameters were determined. In addition, correlations of the identified parameters with the mean of the output variables, i.e. the glucose and insulin concentrations, were determined. This was done in order to determine whether relations existed that were not accounted for by the proposed models. Only moderate to strong correlations above 0.4 were considered for the glucose subsystem. Autocorrelations of the residuals were also determined. In case that the measurement errors are normally distributed with zero mean and constant variance, the model can be considered a good fit to the data if the autocorrelation between the residuals time series and all its time shifted copies is within the confidence interval [96]. This indicates that the residuals have the same white noise characteristics as the measurement errors.

For the glucose subsystem, the assumption of the least-squares method that the measurement errors of the output were normally distributed with zero mean and constant variance was tested. Accuracy of the CGM measurements from the open loop and closed loop study was determined by comparing the measurements to results of SMBG measurements that were performed during the study period. The mean and standard deviation of the error and absolute error between the CGM and SMBG measurements were calculated. In addition, correlations between the SMBG measurements and (absolute) errors was investigated. Mean absolute relative difference (MARD) values were also determined. This value represents the mean of the absolute errors between the SMBG and CGM measurements relative to the SMBG measurements themselves [97].

Proposed glucose subsystem model structures were also assessed by measuring how well these performed at predicting the blood glucose values. This was only done for the the glucose subsystem models for which glucagon input was not identified, since not enough data sections (only 24) were available to find valid estimates of glucagon action parameters. In order to determine prediction performance, a division was made between the 57 available data sections with insulin input only. The identification results were separated between the 10 subjects. When for a certain subject, three data sections were available, one data section was applied as a test interval and two sections as the estimations intervals. The total number of available data sections per subject was rounded to multiples of three to determine the number of test intervals. For each subject, parameter values were determined by taking the average of the parameter estimations resulting from identification of the estimation intervals of that subject. These parameter values were applied to determine prediction performance for the test intervals: it was measured by taking a simulation starting point at every 30 minutes after the interval start time for the duration of the interval. For each starting point, a simulation of 180 minute duration was performed. The difference with plasma glucose measurements were determined for 15, 30, 60, 90, 120, 150, and 180 minutes after the starting point. For each test interval, the residuals over time were determined by taking the average of each of these differences. Overall RMSe and VAF values were also determined for these test intervals and were defined as the average of the RMSe and VAF values over all 180-minute simulations performed for that test interval.

Transfer functions were determined to provide insight into the dynamics of the systems of differential equations that were applied. This was only done for the linear systems. Methods applied are discussed extensively by Franklin et al. [98]. Matlab [89] functions 'tf', 'fft', 'bode' and 'impulse' were applied to determine frequency content of the model inputs and outputs and study the Bode plot and impulse response of the identified models.

Chapter 4

Results

The aim of this research was to perform parameter identification and determine prediction performance for the identified glucose models of varying structures and complexity. This was accomplished by dividing the model of glucose metabolism into three subsystems that were identified separately. First, results of the parameter estimations of the three subsystems are presented (Section 4.1). Then, prediction performance for the various proposed glucose subsystem models is discussed (Section 4.2). The chapter concludes with the results of the model analysis (Section 4.3).

4.1 Parameter estimations

Parameter estimations were performed separately for the three subsystems in the model of glucose metabolism. As hormonal subsystems could not be identified based on the same data [13] as the glucose subsystem, the identification of the insulin and glucagon subsystems was aimed at obtaining parameter values for an average patient with T1DM. Next, these parameter values were applied to simulate insulin and glucagon concentrations that were used as input for the identification of various proposed structures for the glucose subsystem.

4.1.1 Insulin subsystem

As mentioned in Section 3.1, the parameters of the insulin subsystem were identified on three averaged plasma insulin concentration responses to subcutaneous bolus injections. In Table 4.1, the results of the identification of the insulin subsystem are presented. The parameter values in this table are the mean of the estimation results as performed for each of the three available averaged responses. RMSe and VAF values, the measures of model fit compared to the measured data, are also presented in this table. On the bottom of the table, averages of the parameter estimates for individual T1DM patients found by Schiavon et al. [26] are presented. Model fit of the four identified model versions to measurements of the three datasets is shown in Figure 4.1.

From Table 4.1, it can be seen that the RMSe value for the 2nd order model versions was higher than for the 3rd order model versions. For the VAF values the reverse was true. Addition of the subcutaneous insulin clearance term in model version 2 did result in better model fit compared to model version 1, which is reflected by lower RMSe and higher VAF values for version 2. Furthermore, it stands out that the value estimated for the parameter a_{p1} in model version 4 was low compared to the other rate parameters. The estimated values for the other parameters of model versions 3 and 4 were similar, as well as the RMSe and VAF values that were found. RMSe and VAF values were better for the 3rd order models (versions 3 and 4) than for the 2nd order models (version 1 and 2).

Table 4.1: Parameter estimations of proposed model versions of subcutaneous insulin kinetics

Model version	m (1/min)	d_i (1/min)	a_{p1} (1/min)	a_{p2} (1/min)	m_{sc} (1/min)	τ_{Isc} (min)	RMSe (pmol/L)	VAF (%)
1: 2nd order	0.0661	-	0.0041	-	-	-	93.4429	76.45
2: 2nd order (additional clearance)	0.0159	-	0.0026	-	0.0133	-	49.9044	93.05
3: 3rd order (indirect flow)	0.1061	0.0260	-	0.0155	-	-	18.7008	98.95
4: 3rd order (flow both directions)	0.1061	0.0223	$1.61 \cdot 10^{-11}$	0.0192	-	-	18.7008	98.95
Literature: Schiavon et al.	0.124	0.028	0.0034	0.014	-	7.6	-	-

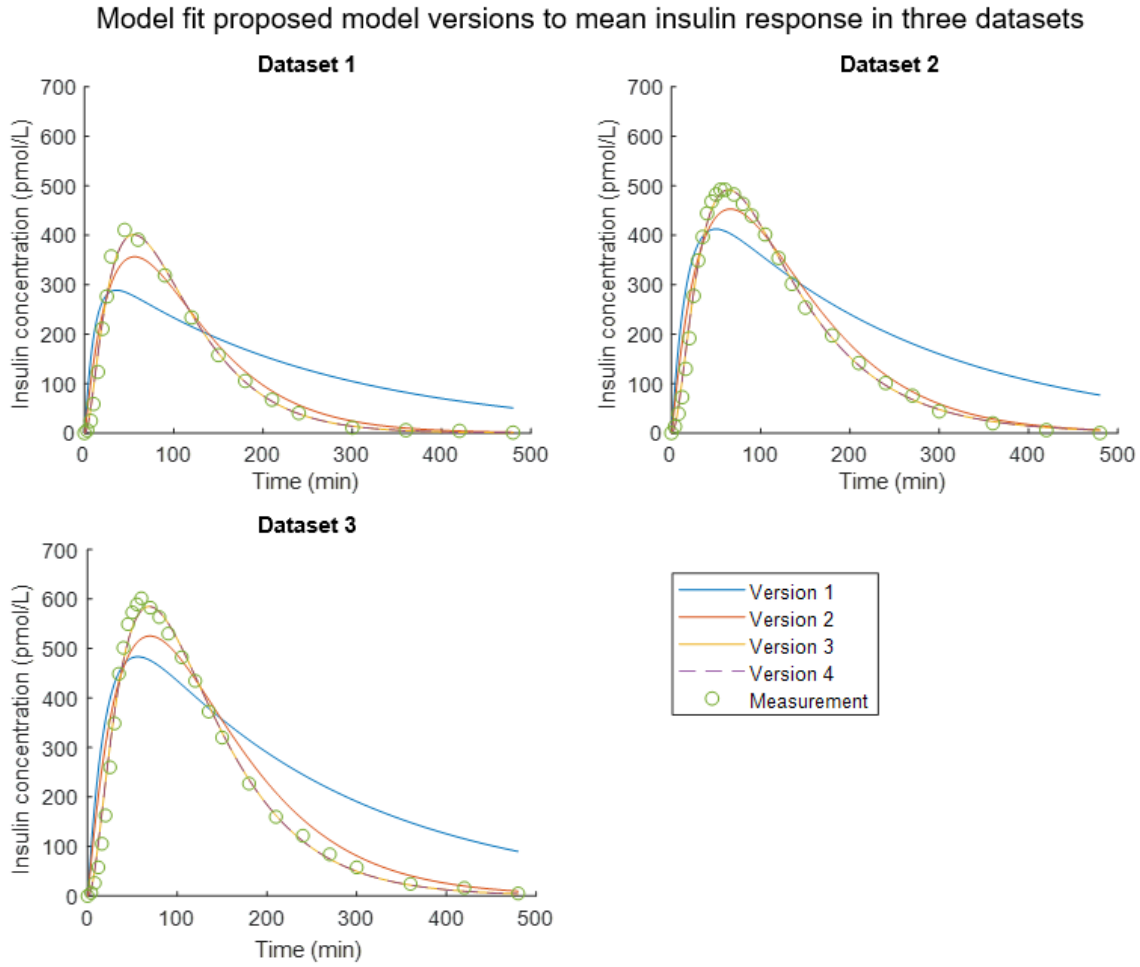

Figure 4.1: Model fit for dataset 2 [26] as accomplished by the four proposed models: the 2nd order model (version 1), the 2nd order model with additional clearance from the first compartment (version 2), the 3rd order model that discards direct flow from first subcutaneous compartment to plasma compartment (version 3) and the 3rd order model with estimations of all parameters (version 4).

These results are in line with what can be observed in Figure 4.1. Although the model version 1 resulted in a shape similar to that of the measured response to the insulin bolus injection, the peak height was lower and the decay was slower than in the measurements. For model version 2, the decay was more similar to what was measured on average, but the peak height was still slightly lower. Model fit of versions 3 and 4 seem similar and account for both the peak height and decay of the averaged insulin concentration responses.

In summary, the results indicate that model version 3 is the best model choice for modelling the insulin concentration response to a subcutaneous insulin bolus injection in an average T1DM patient. This model version with the average parameter estimates was applied for the identification and validation of the glucose subsystem models. This choice will be discussed further in Chapter 5.

4.1.2 Glucagon subsystem

For the glucagon subsystem, parameter estimations were performed on measurements of plasma glucagon concentrations in twelve different conditions for each of the six T1DM subjects. In Table 4.2, parameter estimations for the glucagon system are shown. The mean over all parameter estimations and the measured glucagon peak concentrations for the various conditions in all subjects are presented along with CV values. Mean and standard deviations (std.) of RMSe and VAF values of model fit are also shown. Correlations of these entities with the applied glucagon dosages and initial BG levels can also be found in this table. In Figure 4.2, the mean and range of parameter estimations for the various experimental conditions are shown. In Figure 4.3, model fit that was accomplished with the proposed model is shown. These graphs are typical of the fit that was accomplished in the identification.

Table 4.2: Parameter estimations of two-compartmental model of subcutaneous glucagon kinetics with RMSe and VAF as measures of model fit and glucagon peak concentrations.

	b_p (1/min)	n_h (1/min)	RMSe (pmol/L)	VAF (%)	Peak concentration (pmol/L)
Mean overall (N=65) with (CV) or ± std.	0.0291 (0.3336)	0.1678 (0.3402)	31.3635 ± 23.3412	97.60 ± 1.56	585 (0.6185)
Correlation with dosage	-0.9345	0.0965	0.8776	-0.5269	0.9712
Correlation with BG	0.5151	0.0351	-0.6902	0.5787	-0.6105

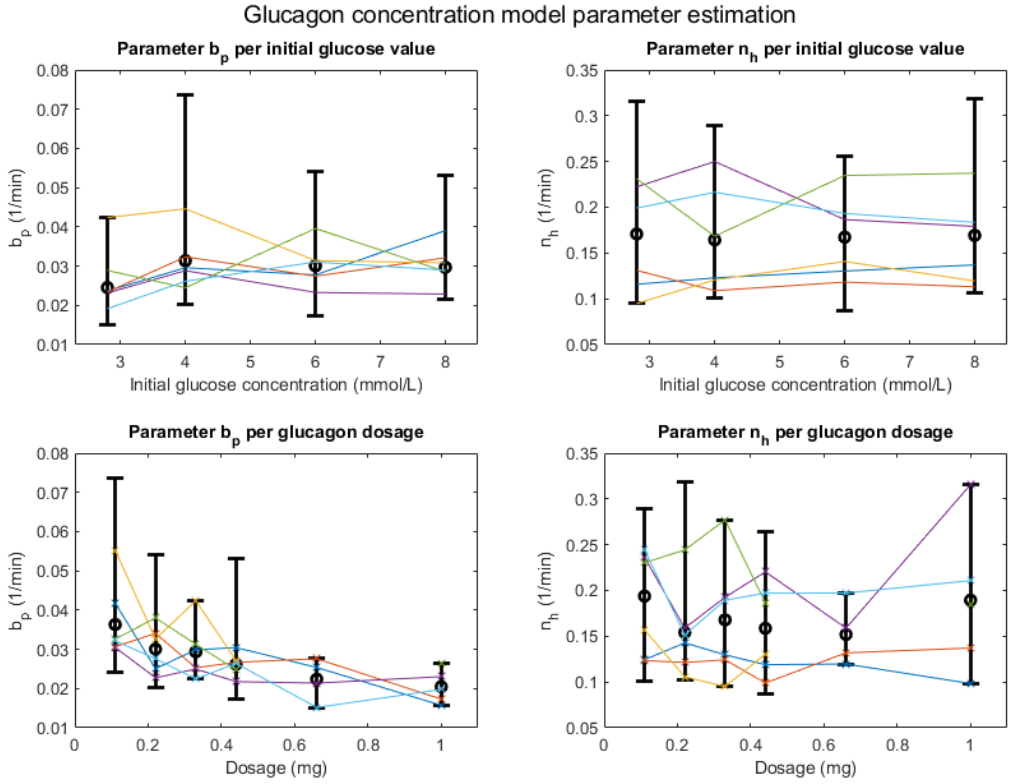

Figure 4.2: Result of parameter estimations of second order glucagon model in six patients. Minima and maxima of the parameter estimates are indicated by the bars, with the circle representing the mean. Coloured lines represent the estimations for each subject separately.

From Table 4.2, it is apparent that CV values for both parameters were similar. Glucagon transfer rate from the subcutaneous compartment (b_p) was found to be small compared to the clearance rate of glucagon from the blood plasma (n_h). It stands out that there was a strong negative correlation between the parameter b_p and the applied glucagon dosage. Since a strong correlation was found between the glucagon dosage and resulting glucagon peak concentration, it is suggested that the value for b_p is negatively correlated to the glucagon peak concentration and that there may be a relationship between the

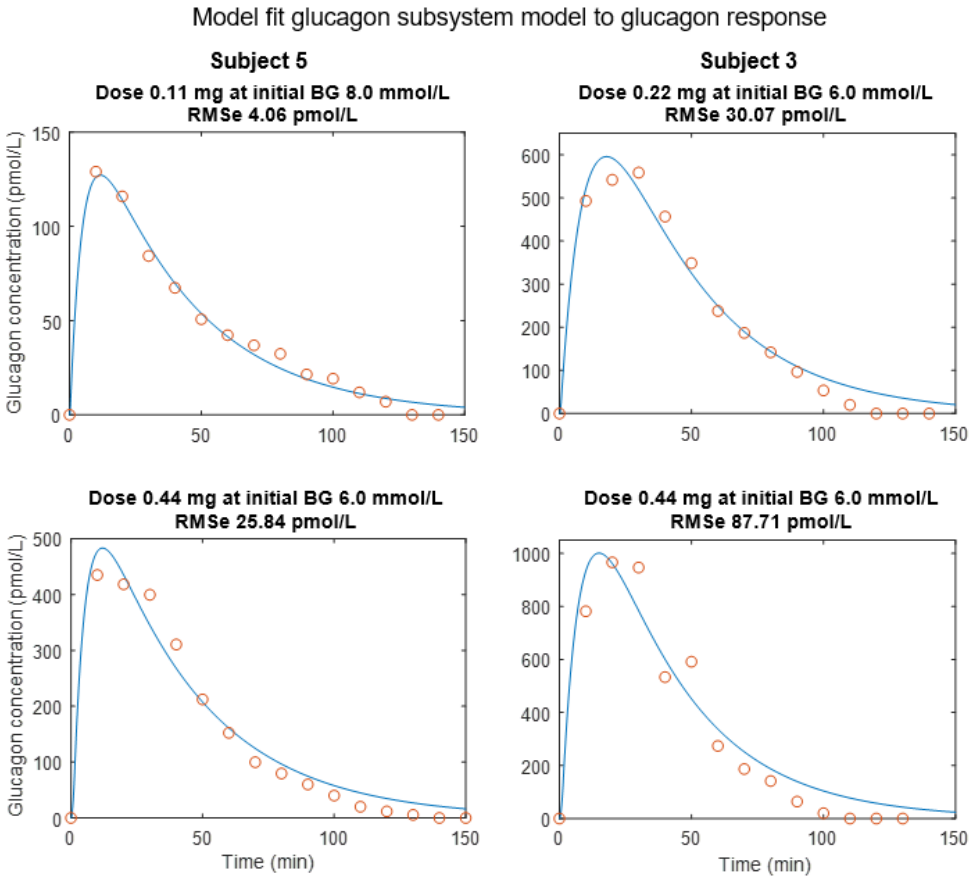

Figure 4.3: Model fit as accomplished with the two-compartmental glucose model for various dosages and initial BG levels in subject 5 on the left and subject 3 on the right. Smallest and largest RMSe values accomplished over all estimations were 4.06 pmol/L and 87.71 pmol/L. Corresponding fit is shown in the upper left and lower right sides of the figure respectively.

glucagon concentration and the parameter b_p that is not accounted for by the model. For the parameter n_h, no indicators for this were found. RMSe values were relatively small compared to the measured peak concentrations (5.3% on average). Correlations indicate that RMSe values increased with the applied glucagon dosage and decreased with the initial glucose level before application of a glucagon dosage. It appears that VAF values were high for all estimations.

In Figure 4.2, it can be seen that estimated parameter values varied between the six subjects. The parameter b_p appears to decrease as the glucagon dosage increases, which is in line with the result that there exists a negative correlation between these entities. It seems that mainly the parameter n_h was subject-dependent, which is suggested by the spread between the coloured lines in the graphs on the right side of the figure. From Figure 4.3, it can be observed that the model can be fit to a variety of glucagon concentration responses measured in various conditions and subjects. The experiments with the best and worst RMSe values obtained after identification are shown in the upper left en lower right corners of the figure respectively. Although the simulated glucagon concentrations deviate somewhat from the measurements, glucagon peak concentrations were approached and the decay of the response was also simulated with reasonable accuracy. Paired t-tests showed that n_h was subject-specific in 9 out of 15 cases en that b_p was subject-specific in 1 out of 15 cases.

To summarize, it appears that the 2nd order model that was proposed for modelling of subcutaneous glucagon kinetics provided a model fit to the data with relatively low RMSe en high VAF values. Also, estimated glucagon concentrations have a shape similar to the measured glucagon concentrations in response to the subcutaneous glucagon bolus injection. Averages of the parameter estimates for b_p and n_h as shown in Table 4.2 were applied for modelling of the plasma glucagon concentrations for the identification and validation of the glucose subsystem.

4.1.3 Glucose subsystem

For the glucose subsystem, four models were proposed. For the available data, input infusion rates of insulin and glucagon during the selected intervals were known. Glucose subsystem inputs, the insulin and glucagon plasma concentrations, were determined with the identified models from Sections 4.1.1 and 4.1.2. First part of the identification results were based on data sections for which glucagon input could be neglected. Then, models were extended to describe the effect of glucagon on the glucose concentrations.

Insulin input only

Parameters were estimated for the linear MM, nonlinear MM and the version 1 and 2 Michaelis-Menten models. For the 2COM model, parameter estimations are not considered here. For 2COM version 1, no solutions were found. For 2COM version 2, resulting model fit had an average VAF value smaller than 50% and q_{gt} was often very large compared to q_{gp} or even got negative and was therefore not considered to be physiologically possible. In Tables 4.3-4.6, results of the parameter estimations can be found. Correlations between these parameter estimates and also with the mean of the modelled glucose and insulin levels during the estimation intervals were calculated and are presented in Table 4.7.

When looking at the parameter estimations in Tables 4.3-4.6, it can be seen that the rate of glucose clearance k_g was often estimated to be virtually zero (Group 1A), indicating that the glucose dependent decay of the glucose concentration was negligible. For the linear and nonlinear MMs (Tables 4.3 and 4.4), this result became more frequent when the delay τ_I was removed from the models (Group 2A). In cases that estimation of k_g resulted in values well above zero (Group 1B and 2B), repeating the estimations for $k_g = 0$ resulted in a major decrease in the value found for the basal net glucose production G_b in all models.

Model fit after identification was determined by comparing CGM measurements to the simulation for the estimation interval. Measures of model fit are shown on the right side of the Tables 4.3-4.6. Precision of the parameter estimates was measured by the CVs which are in between brackets in these tables. The fit of the model to the data was better for the linear than for the nonlinear MM, which can be concluded from the lower RMSe, higher VAF and a higher succes rates (✓) for the linear MM compared to the nonlinear MM. Likewise, both versions of the Michaelis-Menten models performed worse than the linear and nonlinear MMs. Closer inspection of the CVs of the overall parameter estimates shows that CVs of parameters k_g and G_b of the linear MM were smaller than those of the nonlinear MM. In contrast, for the CVs of the insulin sensitivity k_i the reverse was true. For the Michaelis-Menten model versions, CVs were relatively large in all cases, except CVs for the estimations of G_b and $q_{gp,eq}$.

Now consider quantitative comparison of the parameter estimates, it is important to recognize which parameters have the same effect on model behaviour. We know that the parameters k_g and G_b had the same effect on the plasma glucose mass in all proposed models and therefore can be compared directly for all models. In addition, τ_I and a_g also play the same role in all model structures for which these are considered. The parameter k_g in the Michaelis-Menten version 1 model was the only exception since k_g influences the glucose mass relative to the basal level instead of the absolute glucose mass in the blood plasma. When comparing the parameter estimation results for the linear MM, nonlinear MM and Michaelis-Menten version 2 model in Tables 4.3, 4.4 and 4.6, it can be seen that the average estimated value for k_g was highest for the linear MM and lowest for the Michaelis-Menten version 2 model without an insulin threshold. Estimations of k_g were virtually zero for the Michaelis-Menten version 2 model more often than for the linear MM. This occurred even less for the nonlinear MM. Values found for G_b on average were lowest for the nonlinear MM, and highest for the Michaelis-Menten version 2 model. τ_I was found to be similar for both MMs. This delay was often estimated to be equal to zero or 90 min, which was the maximum allowed delay. This suggests that with the method that was applied, the estimation of this delay was not valid under all conditions.

The insulin sensitivity parameter k_i did not have the same effect on the plasma glucose mass in all proposed models. When the nonlinear MM k_i is multiplied with a certain glucose mass, its effect corresponds to k_i in the linear MM. At a basal plasma glucose concentration of 8.2 mmol/L [22], overall average of $k_i \cdot q_{gp}$ was valued 0.0521 mg/pmol/min for the nonlinear MM, which is lower than the value 0.1237 mg/pmol/min found for k_i in the linear MM. For the Michaelis-Menten models, model structure was such that k_i in the version 1 and 2 Michaelis-Menten models had similar effects as k_i in the non-

linear and linear MMs respectively. Results showed that the estimated values for k_i in the version 1 and 2 Michaelis-Menten models were over a factor 10 larger than k_i in the nonlinear and linear MMs respectively.

As explained in Section 3.3.3, the Michaelis-Menten version 1 model was most similar to a model as developed by Wong et al. [64]. The parameter a_g determines the saturation on the effect of insulin. From Table 4.5, it becomes clear that the parameter a_g received a very high value in all estimations. As a result, the effect of insulin on the clearance of glucose became negligible. Values well below 1 kg/pmol were expected from searching for the value of a_g in literature [64]. Another effect of the high values found for a_g, was that the value of k_i divided by a_g determined the glucose clearance rate dependent on the absolute level of glucose in the blood. As explained earlier in this section, this was different from the parameter k_g in this model version, which was a glucose clearance rate affecting the plasma glucose mass relative to the equilibrium level $q_{gp,eq}$. In an attempt to recover the effect of insulin on the glucose dynamics in the version 1 Michaelis-Menten model, a threshold q_{ipb} was added to the effect of insulin in the numerator of the fraction in the model equation. This resulted in a major improvement of the model fit to the data in the estimation intervals, which can be seen from the RMSe and VAF values in Table 4.5. It stands out that the values found for G_b decreased a lot after addition of this threshold.

Version 2 of the Michaelis-Menten model was set up with the goal of obtaining a model more similar to the linear MM, without losing the saturation of the insulin dependent glucose clearance. For $a_g = 0$, structure of this model was equivalent to that of the linear MM. From Table 4.6, it can be seen that estimated values for a_g were again higher than expected, but less excessively than for the Michaelis-Menten version 1 model. The high CV for the estimated values of a_g suggests that the effect of insulin was not negligible in all estimations. Addition of a threshold to the effect of insulin in the version 2 Michaelis-Menten model was not beneficial for the model fit, as can be concluded from the measures of model fit in the lower half of Table 4.6. The main difference between the version 2 model with and without the insulin threshold was that dropping the parameter k_g was less problematic when the threshold was included in the model structure and parameter estimations.

In the correlation analysis (Table 4.7) of the linear MM and nonlinear MM parameters, strong correlations were found between the insulin sensitivity k_i and the net basal glucose production G_b. This correlation became stronger when the parameter k_g was removed from the model structure. Strong correlations were also found between the estimated parameters k_g and G_b in the linear and nonlinear MMs. For both versions of the Michaelis-Menten model, mostly moderate correlations were found between parameters and of parameters with average glucose or insulin concentrations. These varied quite a lot depending on the inclusion or exclusion of an insulin threshold q_{ipb} and the parameter k_g. Strong correlations that stand out were between the parameters k_g and G_b and between a_g and q_{ipb}, for Michaelis-Menten version 2 with inclusion of k_g and q_{ipb}. A strong negative correlation was found between G_b and a_g for the version 2 model with exclusion of k_g and q_{ipb}. These results suggest that the more complex Michaelis-Menten models still show relations between the parameters that are unaccounted for by the model. Moreover, for the linear and nonlinear MMs, it is indicated that the negative and positive contributors to the rate of change of the glucose concentrations were related to each other.

Table 4.3: Linear model of glucose dynamics: parameter estimations. Parameter values presented as mean (CV). RMSe and VAF values presented as mean ± std. For group 1, τ_I was estimated. For group 2, $\tau_I = 0$ was applied. ✓ column contains percentage of successful estimations with RMSe < 0.35 mmol/L or VAF > 75%.

Condition	Group	k_g (1/min)	k_i (mg/pmol/min)	G_b (mg/kg/min)	τ_I (min)	RMSe (mmol/L)	VAF (%)	✓(%)
All parameters estimated	1: overall (N=57)	0.0049 (1.50)	0.1237 (1.41)	2.5339 (1.11)	28.88 (1.19)	0.2784 ± 0.1746	84.88 ± 17.98	85.96
	1A: k_g negligible (N=23)	-	0.1005 (0.95)	1.5843 (1.02)	27.83 (1.14)	0.3167 ± 0.1808	83.46 ± 19.53	86.96
	1B: k_g not negligible (N=34)	0.0082 (0.97)	0.1394 (1.52)	3.1762 (1.03)	29.59 (1.23)	0.2525 ± 0.1680	85.84 ± 17.09	85.29
Estimation with $k_g = 0$	1B: k_g set to zero (N=34)	-	0.1075 (1.32)	0.8543 (0.94)	24.10 (1.33)	0.2849 ± 0.1827	81.84 ± 23.28	85.29
All parameters estimated but τ_I	2: overall (N=57)	0.0039 (1.65)	0.1412 (1.84)	2.3320 (1.28)	-	0.3249 ± 0.2362	80.58 ± 21.21	80.70
	2A: k_g negligible (N=28)	-	0.1268 (1.88)	1.3264 (1.57)	-	0.4050 ± 0.2641	81.51 ± 17.16	78.57
	2B: k_g not negligible (N=29)	0.0076 (0.95)	0.1552 (1.82)	3.3029 (1.03)	-	0.2475 ± 0.1780	79.68 ± 24.78	82.76
Estimation with $k_g = 0$	2B: k_g set to zero (N=29)	-	0.1310 (1.50)	1.3315 (1.48)	-	0.2928 ± 0.1995	73.70 ± 30.93	79.31

Table 4.4: Nonlinear model of glucose dynamics: parameter estimations. Parameter values presented as mean (CV). RMS and VAF values presented as mean ± std. For group 1, τ_I was estimated. For group 2, $\tau_I = 0$ was applied. ✓ column contains percentage of successful estimations with RMSe < 0.35 mmol/L or VAF > 75%.

Condition	Group	k_g (1/min)	k_i (kg/pmol/min)	G_b (mg/kg/min)	τ_I (min)	RMSe (mmol/L)	VAF (%)	✓ (%)
All parameters estimated	1: overall (N=57)	0.0041 (1.65)	$2.96{\cdot}10^{-4}$ (1.09)	1.7224 (1.23)	28.06 (1.07)	0.3214 ± 0.1927	81.48 ± 19.09	78.9
	1A: k_g negligible (N=18)	-	$4.72{\cdot}10^{-4}$ (0.73)	1.3770 (1.21)	36.56 (0.87)	0.4001 ± 0.2378	82.94 ± 14.29	72.2
	1B: k_g not negligible (N=39)	0.0060 (1.25)	$2.15{\cdot}10^{-4}$ (1.30)	1.8819 (1.22)	24.13 (1.19)	0.2851 ± 0.1586	80.81 ± 21.07	82.1
Estimation with $k_g = 0$	1B: k_g set to zero (N=39)	-	$3.69{\cdot}10^{-4}$ (1.53)	0.8538 (1.48)	37.31 (1.03)	0.2777 ± 0.1746	80.02 ± 25.36	79.5
All parameters estimated but τ_I	2: overall (N=57)	0.0035 (1.78)	$2.00{\cdot}10^{-4}$ (1.26)	1.2309 (1.32)	-	0.3836 ± 0.2836	75.93 ± 22.99	71.9
	2A: k_g negligible (N=26)	-	$2.49{\cdot}10^{-4}$ (0.65)	0.7735 (0.89)	-	0.4805 ± 0.3490	75.10 ± 22.22	65.4
	2B: k_g not negligible (N=31)	0.0064 (1.13)	$1.58{\cdot}10^{-4}$ (1.93)	1.6145 (1.27)	-	0.3023 ± 0.1833	76.62 ± 23.96	77.4
Estimation with $k_g = 0$	2B: k_g set to zero (N=31)	-	$2.48{\cdot}10^{-4}$ (1.24)	0.4879 (1.36)	-	0.3164 ± 0.2047	74.26 ± 29.58	74.2

Table 4.5: Michaelis-Menten model (version 1) of glucose dynamics: parameter estimations. Parameter values presented as mean (CV). RMSe and VAF values presented as mean ± std. For group 1, τ_I was estimated. For group 2, $\tau_I = 0$ was applied. ✓ column contains percentage of successful estimations with RMSe < 0.35 mmol/L or VAF > 75%.

Condition	k_g (1/min)	k_i (kg/pmol/min)	a_g (kg/pmol)	G_b (mg/kg/min)	q_{ipb} (pmol/kg)	$q_{gp,eq}$ (mg/kg)	RMSe (mmol/L)	VAF (%)	✓ (%)
Without threshold (N=57)	0.0193 (6.13)	0.3515 (1.26)	130.86 (1.35)	10.7572 (3.70)	-	102.48 (0.14)	0.5144 ± 0.3505	56.93 ± 33.63	45.6
With threshold (N=57)	0.0018 (1.97)	0.5393 (2.04)	111.89 (1.52)	0.5260 (1.17)	8.5582 (1.16)	86.12 (0.43)	0.3554 ± 0.2263	76.22 ± 26.35	75.4

Table 4.6: Michaelis-Menten model (version 2) of glucose dynamics: parameter estimations. Parameter values presented as mean (CV). RMSe and VAF values presented as mean ± std. For group 1, τ_I was estimated. For group 2, $\tau_I = 0$ was applied. ✓ column contains percentage of successful estimations with RMSe < 0.35 mmol/L or VAF > 75%.

Condition	Group	k_g (1/min)	k_i (mg/pmol/min)	a_g (kg/pmol)	G_b (mg/kg/min)	q_{ipb} (pmol/kg)	RMSe (mmol/L)	VAF (%)	✓ (%)
All parameters estimated, no insulin threshold	1: overall (N=57)	0.0031 (1.69)	3.1254 (2.10)	5.71 (3.07)	3.9392 (0.96)	-	0.3397 ± 0.2322	79.23 ± 21.37	77.2
	1A: k_g negligible (N=32)	-	3.7457 (2.25)	7.61 (2.68)	3.6956 (1.12)	-	0.4105 ± 0.2500	75.59 ± 21.95	71.9
	1B: k_g not negligible (N=25)	0.0071 (0.85)	2.3314 (1.22)	3.28 (3.98)	4.2510 (0.78)	-	0.2492 ± 0.1727	83.88 ± 20.07	84.0
Estimation with $k_g = 0$	1B: k_g set to zero (N=25)	-	31.4778 (0.88)	59.99 (0.42)	1.4778 (2.47)	-	0.5996 ± 0.4700	24.96 ± 85.64	44.0
All parameters estimated, insulin threshold included	2: overall (N=57)	0.0047 (3.49)	2.3664 (2.49)	6.71 (3.17)	3.1309 (1.37)	4.9594 (2.18)	0.3691 ± 0.2580	74.87 ± 26.88	70.2
	2A: k_g negligible (N=30)	-	1.6387 (0.37)	6.39 (3.39)	2.4073 (0.48)	3.7233 (2.53)	0.4862 ± 0.2582	67.33 ± 27.08	56.7
	2B: k_g not negligible (N=27)	0.0099 (2.32)	3.1750 (2.69)	7.07 (3.00)	3.9350 (1.54)	6.3329 (1.92)	0.2391 ± 0.1888	83.24 ± 24.49	85.2
Estimation with $k_g = 0$	2B: k_g set to zero (N=27)	-	11.7468 (2.36)	8.29 (2.35)	2.4490 (0.96)	3.0137 (1.19)	0.2620 ± 0.1864	79.92 ± 29.67	85.2

Table 4.7: Correlations found between parameter estimates for the linear, nonlinear and Michaelis-Menten version 1 and 2 glucose subsystems. Correlations of parameter estimates with mean glucose concentrations (C_{gp}) and mean insulin concentrations (C_{ip}) during the estimation interval are also presented. Only correlations for which at least one absolute value higher than 0.4 was found are shown. Areas not relevant to the considered model type are marked grey.

Correlated parameters and variables	k_g,G_b	k_i,G_b	k_i,a_g	G_b,a_g	G_b,q_{ipb}	a_g,q_{ipb}	G_b,$q_{gp,eq}$	q_{ipb},$q_{gp,eq}$	k_i,$C_{gp}(t)$	q_{ipb},$C_{gp}(t)$	k_g,$C_{ip}(t)$	k_i,$C_{ip}(t)$
Linear model												
All parameters estimated	0.7542	0.7469										
All parameters estimated but k_g	-	0.7928										
All parameters estimated but τ_I	0.4910	0.7347										
All parameters estimated but k_g and τ_I	-	0.8455										
Nonlinear model												
All parameters estimated	0.7935	0.4115										
All parameters estimated but k_g	-	0.7249										
All parameters estimated but τ_I	0.8146	0.2784										
All parameters estimated but k_g and τ_I	-	0.6307										
Michaelis-Menten model version 1												
Threshold included	0.2825	-0.0417			-0.4300	0.4101	0.4288	-0.5972			-0.1327	
Threshold excluded	0.5222	0.5171			-	-	0.1239	-			0.4759	
Michaelis-Menten model version 2												
All parameters estimated, threshold included	0.9215		-0.0746	-0.2080		0.8617			0.1733	-0.4056		0.2283
All parameters estimated but k_g, threshold included	-		0.5280	-0.3629		0.6839			-0.4197	-0.1229		0.2247
All parameters estimated, threshold excluded	0.3496		0.5031	-0.3047		-			-0.3097	-		0.1467
All parameters estimated but k_g, threshold excluded	-		0.1445	-0.8484		-			-0.3601	-		0.4854

Table 4.8: Results of parameter estimations for the linear and nonlinear models of glucose dynamics including glucagon action. Estimations correspond to 'Group 2' results for insulin input only in Tables 4.3 and 4.4. Parameter values presented as mean (CV). RMSe and VAF values presented as mean ± std. Unit x of k_i is mg/pmol/min or kg/pmol/min for the linear and nonlinear models respectively. ✓ column contains percentage of successful estimations with RMSe < 0.35 mmol/L or VAF > 75%.

Condition	Glucagon action	k_g (1/min)	k_i (x)	G_b (mg/kg/min)	k_h (mg/pmol/min)	k_{hp} (mg/pmol)	RMSe (mmol/L)	VAF (%)	✓(%)
Linear model: all parameters estimated but τ_I	Linear	0.0022 (1.93)	0.0699 (0.67)	0.8798 (1.22)	0.0360 (1.40)	-	0.4588 ± 0.2030	81.72 ± 15.01	79.2
	Proportional	0.0068 (1.71)	0.0631 (0.83)	2.3468 (1.04)	-	0.1959 (3.51)	0.5385 ± 0.2500	71.34 ± 27.71	62.5
Nonlinear model: all parameters estimated but τ_I	Linear	0.0033 (2.24)	$2.58{\cdot}10^{-4}$ (0.84)	0.5810 (1.09)	0.0323 (1.29)	-	0.5288 ± 0.2336	76.89 ± 17.41	66.7
	Proportional	0.0052 (2.12)	$2.37{\cdot}10^{-4}$ (0.72)	1.6135 (1.20)	-	0.2556 (3.88)	0.6015 ± 0.2674	67.41 ± 27.18	50.0

Insulin and glucagon input

Modelling of the glucagon action on glucose concentrations was only considered in the linear and nonlinear glucose MMs. This choice was made because the estimations of the Michaelis-Menten model were relatively time consuming and the models did not perform better in the estimations than the linear and nonlinear MMs. Furthermore, methodically it was not planned to model glucagon action differently in the various proposed glucose models. As explained in Section 3.3.3, a first order transfer of the amount of glucagon in the plasma to the plasma glucose rate of change, as well as a direct proportional transfer of the amount of glucagon in the plasma to the plasma glucose mass were considered. The parameter k_g was not set to zero and delay τ_I was dropped, similar to the Group 2 estimations for the linear and nonlinear MMs. Results of these estimations are presented in Table 4.8. No correlation coefficients with absolute values higher than 0.4 were found of k_h or k_{hp} with the other model parameters or with average modelled glucose, insulin or glucose concentrations in the estimation intervals were found.

From Table 4.8, it is evident that both for the linear and nonlinear MMs, both k_g and G_b were assigned larger values for the proportional glucagon action than for the linear glucagon action. Average parameter values were not very similar to the averages found when insulin was considered the only input as in the Group 2 estimations in Tables 4.3 and 4.4. CV values of the proportional parameter of glucagon action, k_{hp} were relatively high. Model fit was clearly better for the linear glucagon action than for the proportional glucagon action, judging from the lower RMSe and higher VAF values. Model fit was worse than for the situation that glucagon infusions were negligible.

4.2 Prediction performance

As explained in Section 3.5, prediction performance was determined for the various proposed model structures for the glucose subsystem with insulin input only. Modelling of the glucagon kinetics and action was not considered. Parameters of the insulin subsystem were fixed to the same average values as in the identification of the glucose subsystem models with insulin input only. For each subject, parameter values were based on estimation intervals and prediction performance was determined for the selected test intervals.

An overview RMSe and VAF values of predictions performed with the linear MM, nonlinear MM and Michaelis-Menten models is presented in Table 4.9. The residual errors of these 3-hour predictions compared to the measured glucose concentrations are pictured in Figure 4.4. From Table 4.9, it is apparent that for the linear model the RMSe increased and the VAF decreased when the same parameters were removed from the model. This means that prediction performance became worse. In contrast, for the nonlinear model, the performance became better when these parameters were removed. The table also shows that the Michaelis-Menten models perform worse than de linear and nonlinear models.

The same observations can be made from Figure 4.4. For the linear MM (Figure 4.4a), the model version that performed best included all four model parameters. For this model version, median of the residuals was below 1 mmol/L for over 80 minutes and below 1.5 mmol/L for the entire 180 minutes. Prediction errors of over 1.5 mmol/L within the first 60 minutes of the prediction were found in less than 25% of the cases. The nonlinear MM (Figure 4.4b) showed even smaller residual errors. Overall, the best predictions were made with the model version that only included two model parameters: G_b and k_i. Median of the residuals was below 1 mmol/L for the entire 180 minutes of the prediction. This median was even smaller for the nonlinear MM version that included the delay τ_I. However, maximum prediction errors increased when this delay was included. A selection of the predictions with the Michaelis-Menten model versions are shown in Figure 4.4c. It is clear that the residual errors were much larger than for the linear and nonlinear MMs. Version 1 of the Michaelis-Menten model with inclusion of the threshold showed the smallest errors in this Figure, which is in line with what can be seen from the RMSe and VAF values in Table 4.9.

In order to directly compare the best performing models with those that were applied in literature, RMSe values were also determined over the first 30 minutes of the performed predictions for the linear MM with inclusion of τ_I and k_g and for the nonlinear MM with exclusion of these parameters. Resulting RMSe values were 0.3625 mmol/L and 0.1747 mmol/L respectively.

Table 4.9: Prediction performance of proposed models measured by RMSe and VAF values. Predictions were performed with the parameter values being the mean of the parameters estimated on the estimation intervals taken from the same subject. Each RMSe and VAF value was the mean of the RMSe and VAF values found for all 3-hour predictions during 1 test interval. Mean ± standard deviation (std.) values are shown.

Prediction performance	RMSe ± std. (mmol/L)	VAF ± std. (%)
Linear model		
All parameters estimated	1.2362 ± 0.7623	-228.81 ± 305.42
All parameters estimated but k_g	1.2654 ± 0.9412	-300.13 ± 592.04
All parameters estimated but τ_I	1.3230 ± 0.9866	-332.62 ± 512.51
All parameters estimated but k_g and τ_I	1.3728 ± 1.0326	-394.82 ± 674.90
Nonlinear model		
All parameters estimated	0.9642 ± 0.6055	-142.81 ± 225.80
All parameters estimated but k_g	0.9274 ± 0.8131	-131.17 ± 269.33
All parameters estimated but τ_I	0.8454 ± 0.4841	-114.21 ± 287.14
All parameters estimated but k_g and τ_I	0.7525 ± 0.4602	-31.95 ± 115.13
Michaelis-Menten model version 1		
Threshold included	1.7124 ± 1.7001	$-4.28 \cdot 10^4 \pm 1.65 \cdot 10^4$
Threshold excluded	8.1820 ± 1.0847	$-1.19 \cdot 10^4 \pm 1.08 \cdot 10^4$
Michaelis-Menten model version 2		
All parameters estimated, threshold included	4.0392 ± 0.7632	$-3.63 \cdot 10^3 \pm 2.44 \cdot 10^3$
All parameters estimated but k_g, threshold included	4.0329 ± 2.0831	$-5.60 \cdot 10^3 \pm 7.71 \cdot 10^3$
All parameters estimated, threshold excluded	3.4430 ± 0.2322	$-3.78 \cdot 10^3 \pm 6.47 \cdot 10^3$
All parameters estimated but k_g, threshold excluded	2.5919 ± 3.2990	$-3.37 \cdot 10^3 \pm 8.22 \cdot 10^3$

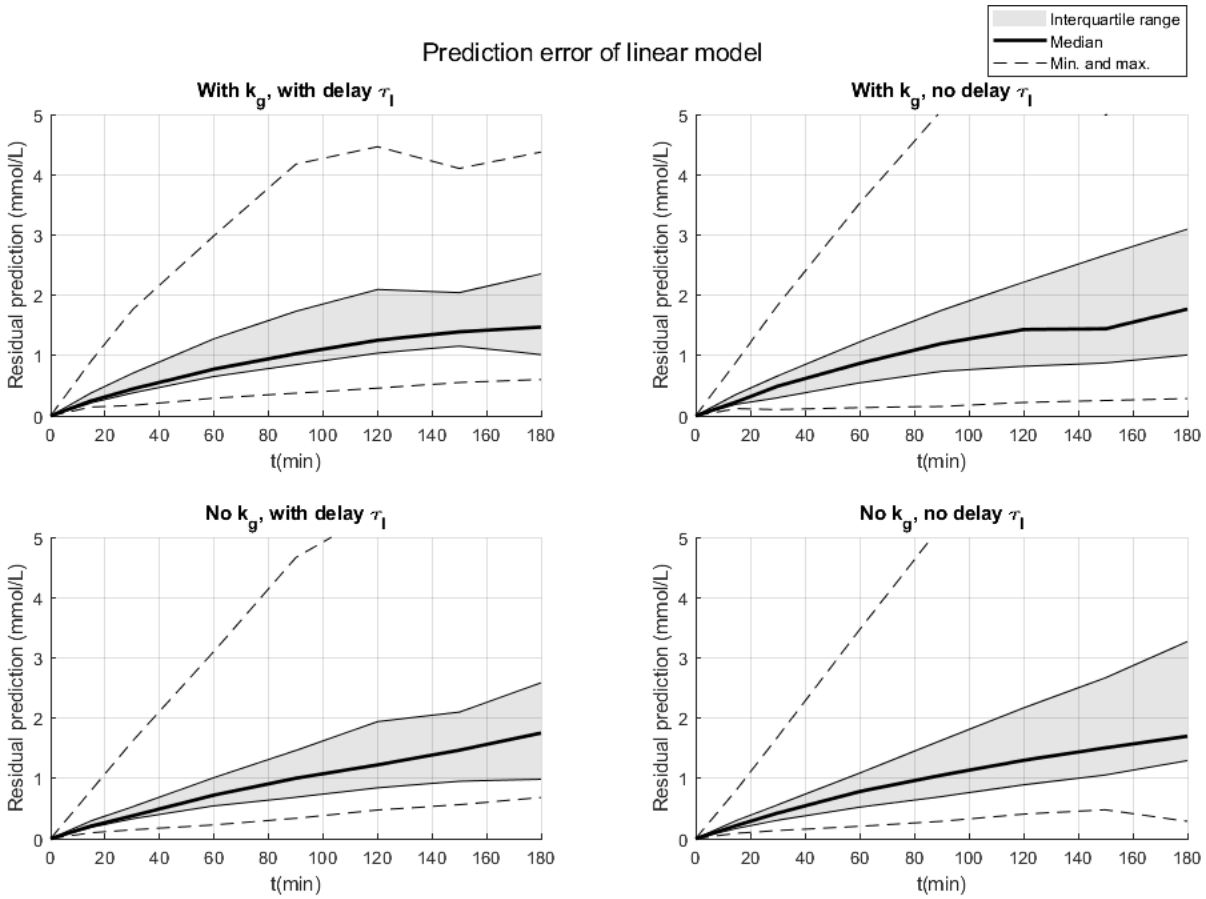
Prediction error of linear model
Interquartile range
Median
Min. and max.
With k_g, with delay τ_l
With k_g, no delay τ_l
No k_g, with delay τ_l
No k_g, no delay τ_l
Residual prediction (mmol/L)
t(min)

(a)

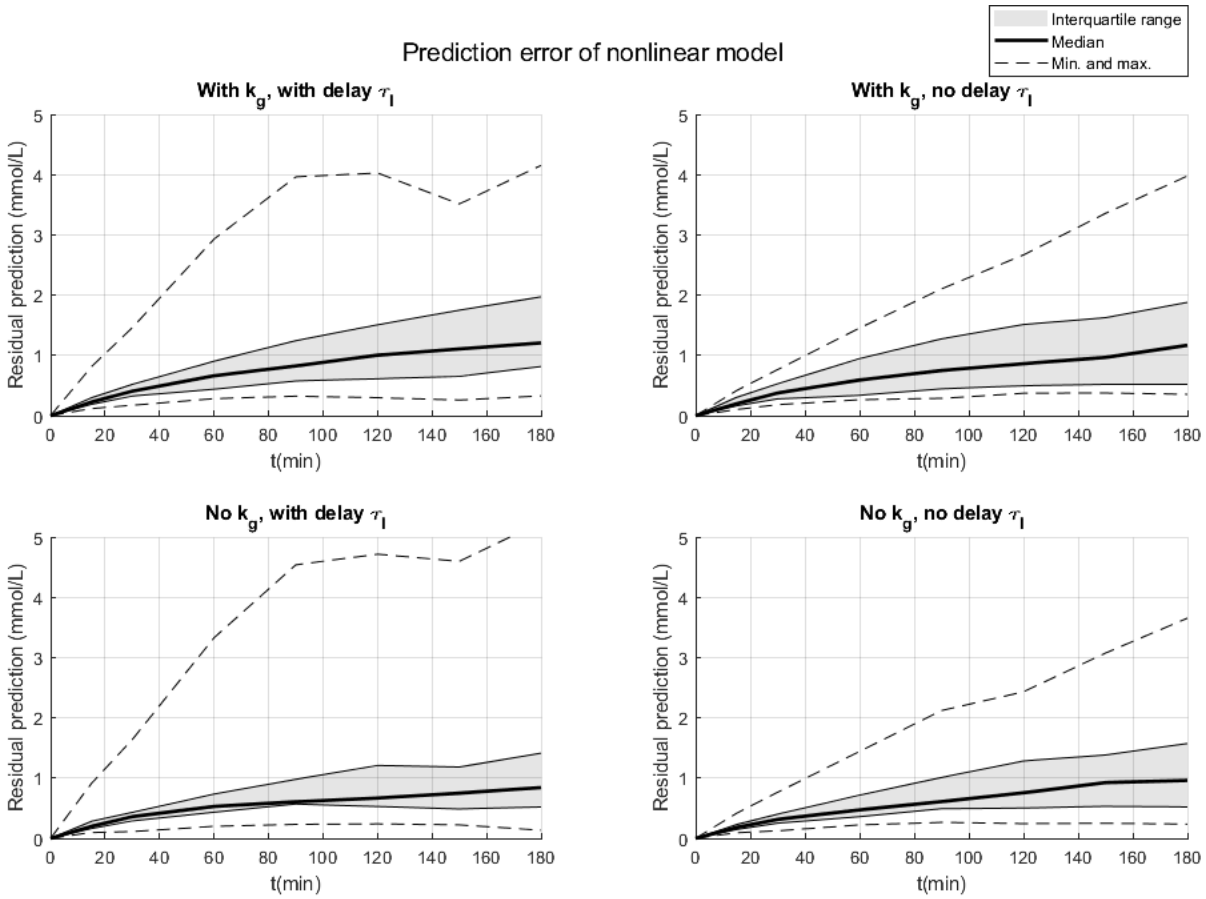
Prediction error of nonlinear model
Interquartile range
Median
Min. and max.
With k_g, with delay τ_l
With k_g, no delay τ_l
No k_g, with delay τ_l
No k_g, no delay τ_l
Residual prediction (mmol/L)
t(min)

(b)

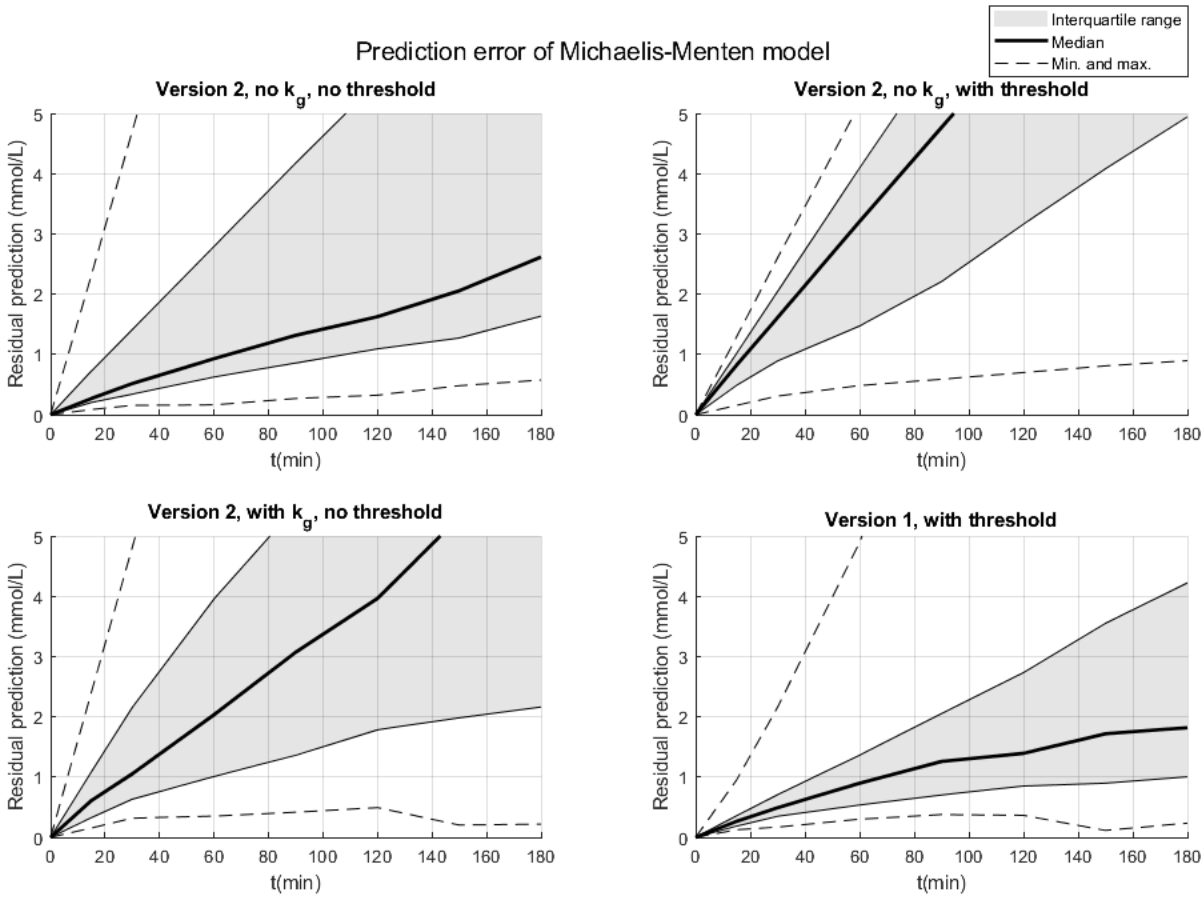

(c)

Figure 4.4: Prediction performance of (a) linear, (b) nonlinear and (c) Michaelis-Menten models. Predictions were performed with the parameter values being the mean of the parameters estimated on the estimation intervals taken from the same subject. One prediction error array was the mean error over all 3-hour predictions during 1 test interval. Median, interquartile range and spread of these prediction error arrays over all test intervals are shown.

4.3 Model analysis

As described in section 3.5, some additional analysis on the identified models was performed. Results of this analysis are discussed next.

4.3.1 Analysis of residuals

Autocorrelations were determined for the residuals of the estimations of all three subsystems. For the insulin subsystem, the autocorrelations were within the confidence bounds. For the glucagon subsystem, autocorrelations were within the confidence bounds most of the time. The one-sample phase shift (10 minutes) autocorrelation was outside the confidence bounds in 23 out of 65 cases. The autocorrelation for a two-sample phase shift (20 minutes) was outside the confidence bounds in only 3 out of 65 cases. This suggests that for both the insulin and glucagon subsystems, the models were an accurate representation of the data at the end of the identification process.

For the glucose subsystem, residuals analysis indicated that this was not the case. Autocorrelations of the residuals were mostly outside of the confidence bounds. Differences between the CGM measurements and SMBG measurements were analysed in order to determine whether the assumption that the CGM measurement error was normally distributed with zero mean and constant variance was met. The results of the CGM error analysis are presented in Table 4.10. First of all, it is apparent that the absolute errors and MARD values of the CGM errors were relatively large. For the OL experiments, the average absolute sensor error and MARD value was larger than for the CL experiments. It also stands out that the CGM error in both experiments did not have a zero mean. Moreover, moderate correlations were found between the errors and the SMBG measurements.

Table 4.10: Results analysis errors of CGM measurements compared to SMBG measurements in the crossover study [13] for the closed loop and open loop experiments. Mean and standard deviations (std.) of the actual error and absolute (abs.) errors are presented. Correlations of these errors with the SMBG measurements were determined. MARD values are presented.

	Error mean ± std. (mmol/L)	Correlation error with SMBG (-)	Abs. error mean ± std. (mmol/L)	Correlation abs. error with SMBG (-)	MARD (%)
CL	0.3056 ± 1.3484	0.5330	1.0162 ± 0.9356	0.3993	13.88
OL	0.2309 ± 2.6029	0.4852	1.7339 ± 1.9529	0.2037	26.40

4.3.2 Analysis of model dynamics

Laplace transforms were applied to find the transfer functions for the linear systems of differential equations that were considered in this study. Furthermore, frequency content of insulin and glucagon input, the modelled insulin and glucagon output and the measured glucose output were determined. Elaborate description of this analysis and the results can be found in Appendix A. Analysis showed that both the glucagon and insulin subsystems have stable outputs. Both have a low-frequent output, with the insulin subsystem showing an even lower cut-off frequency than the glucagon subsystem. Phase shift of these low frequencies is zero and they are amplified depending on the gain of the transfer functions. The linear MM glucose subsystem shifts low-frequent insulin signals with 180 degrees if k_g is well above zero and the shift is only 90 degrees for k_g close to zero. The input delay τ_I introduces a phase delay. The magnitude of the output frequencies of the linear glucose MM is also affected by k_g. For $k_g = 0$, the amplification of low-frequent signals does not level off but becomes stronger as frequency decreases with 20 dB/decade. Exact meaning of these findings for the behaviour of the system is discussed further in the next chapter.

Chapter 5

Discussion

In the current study, models of the insulin and glucagon subsystems were identified with the aim of modelling the plasma insulin and glucagon concentrations in response to subcutaneous hormonal infusions in an average patient with T1DM. Parameter estimations were performed for both subsystems. Results of these parameter estimations were applied to simulate the insulin and glucagon plasma concentrations as input for the glucose subsystem. For the glucose subsystem, linear and nonlinear models of varying complexity were proposed. These models were identified and validated.

5.1 Insulin subsystem

For the insulin subsystem, the only data available were averages of three datasets that contained measurements of insulin concentration responses to subcutaneous bolus injections. Model parameters correspond to what is shown in Figure 3.4 in section 3.3.1. Results of the parameter estimations showed that model version 3 was able to provide best model fit to the three average insulin responses. This 3rd order model with estimation of three parameters was able to provide a fit both to the peak insulin concentration and the decay afterwards. Results indicated that, compared to Schiavon et al. [26] that applied individual subject data, a less complex model can be fitted to averaged insulin responses. In model version 3, the input delay τ_{Isc} was not considered and addition of the parameter a_{p1} as in model version 4 resulted in it being estimated virtually zero. This was not surprising, since results of the study by Schiavon et al. [26] estimated a_{p1} in the same model structure to be valued above zero in only 23% of the cases. Model versions 1 and 2 as proposed in the current study were dropped because model fit was worse than for model version 3, which was concluded from the higher RMSe and lower VAF values. Note that the transfer rate parameters d_i and a_{p2} in the version 3 insulin subsystem model are exchangeable without resulting in a change in model behaviour. This can be seen clearly when looking at the corresponding transfer function in Equation A.3 in the Appendix. The selected model is also less complex than the Inreda model of insulin kinetics [5], which was a 4th order model with 8 parameters.

This study indicated that insulin kinetics can be modelled with a third order system, which is in agreement with what was found by Hovorka et al. [74], Lv et al. [30] and Schiavon et al. [26]. The study of Schiavon et al. and the current study were in contradiction with the study by Lv et al. [30], in which it was indicated that there is a need for inclusion of a delayed first order transfer from the first subcutaneous compartment in order to accurately model insulin concentrations in the first 30 minutes after injection. In contrast, other studies have also applied less complex models with either two or three compartments. For the two-compartmental model structure, only parameters corresponding to V_I, a_{p1} and m were estimated with the condition $a_{p1} = m$. In addition, a basal insulin concentration I_b was identified [33, 99]. A basal insulin concentration parameter was not included in the current study since this implies that there is still a background beta cell secretion of insulin [33], which is normally negligible in T1DM patients [22]. It is possible that the addition of estimation of V_I compared to the current study's model in the identification may compensate for the assumption that $a_{p1} = m$. However, it is in line with expectations [26] and results presented here that, when both estimation of the parameters V_I and I_b are discarded, a two-compartmental model cannot account for the dynamics involved in subcutaneous insulin absorption.

Less complex three-compartmental model structures involved estimation of parameters corresponding to V_I, a_{p2}, d_i and m with the condition $a_{p2} = d_i$ [74, 28]. This last condition was met in the study of Schiavon et al. in only 25% of the cases [26]. Although it was not attempted in the current study, assuming equality of these parameters may be a simplification that can be applied without major decrease in the model fit to the average insulin response data. This would be advantageous in the interpretation of these parameters since they can be exchanged in the selected model without resulting in changes of model behaviour, as was explained earlier.

Unlike the study by Schiavon et al. [26], no transport delay of the insulin input was considered in the current study, since applied methods could not provide reproducible estimations. Addition of the delay parameter would have definitely resulted in a better model fit for the lower order insulin subsystems, but the early effect of insulin on the glucose concentration can then not be modelled and it is therefore not desirable to apply this delay. Moreover, this delay is a worse reflection of the physiology than the addition of a compartment representing an additional delay in the insulin response.

It is not certain that the insulin submodel is capable of accurately describing insulin concentrations after subcutaneous infusions through the application of a bi-hormonal CL or insulin delivery system. The model was identified on insulin responses to bolus injections, which is in contrast to multiple smaller bolus injections or continuous infusion that were applied in the CL and OL parts of the crossover study respectively [13]. Although it is expected that identification based on such data is still possible [33, 28], it is possible that parameter estimations are affected by the type of dosage pattern that is applied.

Another major limitation to this study is that the identified model of insulin kinetics only gives a representation of the average response to a bolus injection. Inter- and intra-subject variations in these kinetics were not considered. It depends on the response of the glucose subsystem and degree of the variations whether it is important to take these into consideration. In addition, the influence of insulin and glucagon kinetics on each other is unknown. Haidar et al. [33] already suggested that subcutaneous absorption rates of both hormones are related. It could also be worthwhile to determine whether parameters are correlated to each other or to patient characteristics. Schiavon et al. [26] indicated that the value for a_{p2} could be related to the body weight of the patient.

It is advisable to perform a clinical study in which the effect of administration of both hormones by the Inreda AP is studied by taking regular blood samples during a treatment protocol. Insulin, glucagon and glucose concentrations can be determined from these samples. Such a study can provide data to determine influences of the factors mentioned above: the CL control situation, inter- and intra-subject variations, as well as correlations between parameters and with patient characteristics. It can then be determined whether the simplified model version of Schiavon et al. [26] that was applied here for an average patient, can also describe insulin levels with sufficient accuracy in these conditions.

5.2 Glucagon subsystem

For the glucagon subsystem, responses to various glucagon dosages at various initial glucose concentrations were available for six different subjects. Model parameters correspond to what is shown in Figure 3.5 in section 3.3.2. Results of the parameter estimations indicated that the proposed 2nd order model with two parameters was able to provide a good model fit. This was concluded from the RMSe values being small compared to the glucagon peak concentrations and the VAF values approaching 100%. This glucagon kinetics model is a simplification of that applied in the Inreda model [5], that used a 3rd order model with 5 parameters. Alpha cell glucagon production was also considered in this Inreda model, but it was neglected in the current study. Results of the glucagon subsystem confirm earlier findings [33, 99] that a two-compartmental model with estimation of two parameters can be applied to model glucagon concentrations. More complex models like proposed by Lv et al. [34] and Dalla Man et al. [36] do not seem to be required to obtain a model fit as reported in the results section.

N. Middelhuis [100] performed parameter identification for the glucagon kinetics submodel of Inreda [5]. The same assumption of absence of glucagon secretion was made and the same glucagon study [16] data was applied as in the current study. In this study [100], no RMSe or VAF values of the model fit were determined; autocorrelations of the residuals were found to be within the confidence bounds in 59 out of 65 estimations. Similar fit to the data was accomplished in the current study. Analysis indicated that

parameter sets as a whole were dependent on patient characteristics and glucagon dosage, but not on the initial BG level [100]. Results of paired t-tests and correlation analysis in the current study strongly suggest existence of similar dependencies. These seem to exist in the transfer rate parameter b_p for the dosage-dependency and in the clearance rate parameter n_h for the subject-dependency. Dependency of glucagon kinetics on the initial BG level could not be ruled out. It is advantageous that each of these dependencies turned out to exist in only one of the parameters. This might simplify the process of implementation of these dependencies into the model. It is advisable to perform further studies in order to confirm existence and quantify these relationships on a larger subject group.

Behaviour of the developed glucagon pharmacokinetics model was compared to the 2nd order glucagon models applied by Haidar et al. [33] and Wendt et al. [99] that were identified on T1DM patients. Main difference between these studies were that Haidar et al. applied one parameter for the transfer rate b_p and clearance rate n_h, while Wendt et al. kept these parameters separated as in the current study. Both models added a basal glucagon level to the output glucagon concentration, but as this was neglected in the current study this was set to zero. Average parameter estimates were applied. The input was a glucagon infusion rate pattern as applied in the CL part of the crossover study [13]. Output glucagon concentrations turned out to be shaped similarly for all three models, but with proportional differences between the outcomes. It is probable that conversion of dosed glucagon units was not performed in the same way. The current model and that of Wendt et al. [99] reached peak glucagon concentrations more quickly than that of Haidar et al. [33]. This confirms the finding in the current study that the transfer rate and clearance rate parameters are clearly different, with the transfer rate being much smaller than the clearance rate. Since these two-compartmental models [33, 99] were applied in a CL control situation, the outcome of the comparison supports the assumption that the model found in the current study is not only applicable to isolated glucagon dosage inputs but also to repeated dosages as applied in a CL system. Moreover, it indicates that the model structure applied can also account for inter-subject variations that occur in such a CL control situation.

In the glucagon model, alpha cell secretion was neglected and absence of basal glucagon concentrations was assumed. Studies have already indicated that this is not true, in people with T1DM there is still a basal glucagon concentration [43, 16]. For the methods applied, this has multiple effects: firstly, initial concentrations of glucagon being assumed zero cannot be true; secondly, glucose dynamics may always be influenced by the basal glucagon concentrations, which was not considered in the identification of the glucose model. The second effect may be negligible. The study performed by Dalla Man [36] has indicated that there is a threshold glucagon concentration for glucagon action to occur. Extension of the glucagon subsystem model simulate basal alpha cell secretion could be performed simply by addition of a constant to the simulated plasma glucagon concentration. This strategy was also applied to model basal glucagon concentrations in the two-compartmental models of Haidar et al. [33] and Wendt et al. [99] that were mentioned above. Value for this basal glucagon concentration constant might be dependent on the diabetes duration [101, 6, 37]. It may be required to study whether decay of plasma glucose concentrations and hypoglycaemia [36, 37] have a major influence on the glucagon concentration in people with T1DM.

To summarize, a two-compartmental model of glucagon kinetics is able to describe glucagon concentrations in T1DM patients. It is advisable to further study dependency of model parameters on the patient characteristics, glucagon dosage size and BG levels. More research on alpha cell secretion may also be necessary. As mentioned as well in the discussion of the insulin subsystem, a clinical study in which regular blood samples are taken for a bi-hormonal CL control situation could gain insight into these uncertainties. Inter- and intrasubject variations of the model parameters and influence of insulin and glucagon on each other's kinetics can also be studied from these measurements. Part of the data may be applied to validate the models of insulin and glucagon kinetics for predicting plasma glucose levels in a variety of conditions. It is questionable whether insulin and glucagon kinetics need to be simulated to a high degree of accuracy, since the effects on the simulation of glucose levels may be limited. Therefore, it is advisable to start with a sensitivity analysis to determine sensitivity of the glucose concentrations to known variations in the insulin kinetics [26] and glucagon kinetics [16]. Methods for such a sensitivity analysis are described in Appendix C.

5.3 Glucose subsystem

The glucose subsystem was identified and validated based on data acquired in a crossover study on T1DM patients with an OL period with regular insulin pump treatment and a CL period in which treatment with the Inreda AP was applied [13]. Results of the parameter estimations indicated that the proposed glucose subsystem models of varying complexity could be identified on CGM data. All of the proposed model structures were much simpler than what was applied in the Inreda model [5] that was based on the physiology of the glucose metabolism [3, 36]. For modelling of the glucose part of the metabolism without submodels of meal intake or hormonal concentrations, the model already consisted of six differential equations with over 16 model parameters. Glucose subsystem models proposed in the current study only had one or two compartments with at most 8 model parameters. The glucose concentration was modelled to be affected by plasma glucose, insulin and glucagon concentrations through the parameters k_g, k_i and $k_{h(p)}$ respectively. There was also a parameter accounting for the basal net glucose production G_b. Other parameters determined the delay on insulin action τ_I, the saturation on insulin action a_g and the rates of transfer between two compartments: k_1 and k_2. In addition, basal plasma glucose mass $q_{gp,eq}$ and amount of insulin q_{ipb} were considered. The glucose distribution volume V_g and molar mass M_g were fixed.

5.3.1 Parameter estimations

Overall, results showed that when all parameters were considered, model fit in terms of RMSe and VAF values was best for the linear MM, followed by the nonlinear MM, the Michaelis-Menten version 2 model and the Michaelis-Menten version 1 model. All parameters showed relatively large variability between the estimation intervals, which can be concluded from the CV values exceeding 1 in most cases. The two-compartmental models were the only proposed glucose subsystem models that could be identified on the data. This may be caused by a faulty model structure or by the estimation methods applied not being suitable for finding the right parameter values. It is probable that the estimation method was at least some part of the problem for both model versions. For the Michaelis-Menten models, the algorithm did not find the right optimum in the residuals function either. For 2COM version 1, the model structure may also have caused some problem, since there was no insulin-dependent clearance of glucose included.

Parameter estimations were performed for a linear MM, nonlinear MM and two versions of a Michaelis-Menten model. As explained earlier, the linear and nonlinear MMs as well as the Michaelis-Menten version 2 model in the current study are simplifications of the glucose minimal model that was developed by Bergman et al. [49]. Many studies have performed parameter estimations for this Bergman MM. As becomes clear from section 2.2.1, the parameter k_g corresponds to the glucose effectiveness S_G in the Bergman MM. The Bergman MM also contains a parameter that corresponds to the basal net glucose production G_b in the proposed models. The insulin sensitivity S_I in the Bergman MM does not correspond directly to the parameter k_i in the linear and nonlinear MMs or the Michaelis-Menten models. However, both parameters express the rate at which a certain amount of insulin affects the plasma glucose concentration and therefore the values can be compared.

According to literature [61], there is little variability in the parameter k_g. Therefore, its value was fixed in several studies [28, 102]. The estimates found in these studies are slightly larger than the estimations for k_g that were found in the current study. CVs corresponding to the estimation results indicate that there was a relatively large variability of the parameter k_g, which is not in agreement with earlier studies [61]. Results also showed that in the proposed models, k_g was often estimated to be virtually zero. For the linear MM and Michaelis-Menten version 2 models, this results in the glucose concentration not being affected by its own value in any way. For the other proposed models it means that the glucose dynamics become completely nonlinear. No reports of k_g being estimated or valued virtually zero were found in other Bergman MM studies. It is logical that estimations of k_g are higher for the linear MM than for the nonlinear MM, since the nonlinear MM includes part of glucose dynamics in the nonlinear term of the differential equation.

The basal net glucose production called G_b in the current study, is often defined as the glucose effectiveness S_G multiplied by a constant basal glucose level in other studies [28, 102]. The parameter values found here for G_b were in the same range as applied in other studies [22, 103, 28]. Coefficients of variation were smaller than those found for the parameter k_g. However, variations were still large compared to other studies [22]. Values for G_b were relatively large in the Michaelis-Menten version 2, which is probably caused by the strong effect that insulin has for the identified parameter values. The basal net glucose production being lower in the nonlinear MM than in the linear MM suggests that the effect of k_g and k_i together is stronger for the linear MM.

The nonlinear MM k_i can be compared by unit conversion to S_I in the Bergman MM. Values found in literature [28, 102] were approximately a factor 10 larger than what was found in the current study. For the linear MM and Michaelis-Menten version 2 model, k_i needs to be divided by a certain glucose mass q_{gp} before a similar comparison can be performed. Dividing by a relatively low glucose mass corresponding to 5 mmol/L will result in overestimation of the insulin sensitivity that is comparable to S_I in the Bergman MM. Even then, similar as for the nonlinear MM, the Bergman MM study's insulin sensitivity [28, 102] was found to be about five times stronger than the overestimated S_I calculated here. These differences may be explained by the higher complexity model applied in the MMs in literature (section 2.2.1) that considered insulin action through an additional compartment that accounts for the delayed effect of insulin. The effect of this delayed action may be smaller than when the actual plasma insulin level is considered directly in the differential equation. Earlier studies [28, 104] and the current study were in agreement on the large inter-subject and diurnal variations for the insulin sensitivity.

Results of the estimations of τ_I suggest that insulin action is delayed compared to the excursion of plasma insulin concentrations resulting from subcutaneous infusion, since the delay was often estimated to be larger than zero. Large spread of the estimations of this delay with estimates often being at the allowed boundaries, indicates that this delay was not estimated correctly in all cases. In order for valid estimation of this delay, a certain variation in the plasma insulin concentration is required within the considered time period. If there is not enough variation, value assigned to τ_I becomes random because its value does not influence model output. In the original Bergman MM, the delayed effect of the insulin concentration was modelled by addition of transfer to a remote insulin compartment. For the current study, it may be determined whether such a structure improves model fit. It is however expected that such a delay is more complex than required for modelling of the insulin action.

As explained in the results section 4.1.3, the parameter a_g in the Michaelis-Menten models was expected to be valued very small. This way, the effect of a higher amount of insulin would not be linear but it would level off depending on the value of a_g. When $a_g \gg 0$, the effect of insulin becomes negligible already for low levels of insulin in the blood plasma. Since the approach taken was data-driven, it was attempted whether addition of a threshold to the effect of insulin in the numerator of the Michaelis-Menten relation could improve model fit. This threshold has the effect of allowing small excursions of the insulin concentration away from the threshold to have a larger effect on the eventual glucose concentration. For model version 1, this had the desired effect of improving the model fit for the estimations. For model version 2, this was not the case. It is unknown why the parameter a_g was given such high values. It is clear that for $a_g = 0$, the fit of the Michaelis-Menten version 2 model could be improved simply by conversion to the linear MM. It is possible that the nonlinear least-squares method converged to optimal error for very large values of a_g and did not search for solutions in the values near zero.

Then, turning back to the results of the estimations of the insulin threshold in the Michaelis-Menten models, it was found that this threshold was estimated to be valued in the lower range of insulin concentrations that were found in the model. This was expected, since larger values would have resulted in insulin action having the effect of increasing glucose concentrations instead of decreasing them, which of course is not expected behaviour. Correlation analysis showed that a_g was strongly correlated to q_{ipb} for the version 2 Michaelis-Menten model, which confirms the statement made above about q_{ipb} functioning as a counteracting factor for the overestimation of a_g. For $q_{gp,eq}$ in the version 1 Michaelis-Menten model, estimations were valued in the lower range of glucose masses that were measured. This means that q_{gd} describes the glucose concentration above hypoglycaemic values.

It is interesting that for the linear and nonlinear MMs, strong correlations were found to exist between G_b and k_g as well as between G_b and k_i. This means that the parameter that contributes positively to the glucose rate of change is related to the parameters contributing negatively to the glucose rate of change. It is not surprising that when k_g is set to zero, the relation between the remaining parameters, G_b and k_i became stronger. It is apparent that for the nonlinear MM, the relation of G_b with k_g was dominant over that with k_i. This implies that allowing values above zero for k_g, increases independency of the estimate found for k_i. In contrast, for the linear MM, the relation between G_b and k_i seemed to depend less on the value for k_g. This was not surprising as well, since in the linear MM the glucose mass affected only the role of k_g and not of k_i in the glucose rate of change. For the nonlinear MM, the relation of G_b with k_i became less strong when the delay τ_I was set to zero. Linear MM correlations were also affected by inclusion of the delay τ_I. If further studies confirm existence of these parameter correlations, knowledge of these correlations may be applied to improve identifiability of the parameters such that parameter estimations can be performed quicker and more accurate.

System analysis indicated that the parameter k_g in the linear MM has a stabilizing influence for the system output, since it constrains the system gain for lower frequencies. As a result, for basal insulin and glucagon levels, there will be an equilibrium value that the output glucose level converges to. If $k_g = 0$, glucose levels will start to increase linearly unless the insulin levels start to rise. It is more critical that the parameter values applied for G_b and k_i are balanced. The Michaelis-Menten model version 2 is expected to show similar behaviour, since it is equivalent to the linear MM, except from the saturation on the effect of insulin. It is advisable to fix the value of a_g to a value close to 0 [64], in case that parameter estimations are performed again for the Michaelis-Menten version 2 model. Then, the system will have the effect of damping the model sensitivity to high insulin concentrations, which may be desirable but was not tested in this study. For the nonlinear MM, removing the parameter k_g still leaves a glucose-dependent term in the differential equation. As a result, there will still be an equilibrium value of the output glucose level when the insulin concentration is basal. This may explain why setting $k_g = 0$ worsens prediction performance for the linear MM, while prediction performance for the nonlinear MM improves for this condition.

Glucagon action was estimated for the linear and nonlinear MM with estimation of the parameter k_g, but without the delay τ_I. Glucagon action modelled as a linear component of the differential equation performed better than adding the glucagon level directly onto the modelled glucose mass. This means that apparently, there is some delay to the effect of glucagon on the plasma glucose concentration. System analysis showed that, as could be expected from the lower cut-off frequency of the glucagon subsystem, the response of the plasma glucose concentration to glucagon is slightly quicker than the response to insulin. Model fit as measured by the RMSe and VAF values was worse than what was accomplished for the linear MM and nonlinear MM with insulin input only. Furthermore, precision of the estimation of the parameter $k_{h(p)}$ was relatively low. Inaccuracy of estimations of the glucagon action may be caused by a lack of sufficient glucagon infusion input.

From what was found in EGP submodel studies [59, 71], it can be seen that including a term that makes glucose concentration dependent on the rate of change of the amount of plasma glucagon instead of only on the amount of plasma glucagon itself, the model fit may be improved. Estimation of glucagon action may also be improved by adding either a (transport) delay to the effect of glucagon or by adding a compartment accounting for the delayed effect of glucagon [28], similarly as was done for insulin action in the Bergman MM [49]. It is expected that addition of a simple transport delay should be sufficient, since glucagon kinetics and dynamics are quicker than that of insulin [16]. Estimation of this delay could not be performed accurately for the available crossover study data in the current study, since little data sections were available and measurement error was often large compared to the effect of infused glucagon. Absence of correlation between $k_{h(p)}$ and other parameters or output variables suggests that the effect of glucagon is not linearly related to the glucose, insulin or the glucagon concentration itself.

5.3.2 Prediction performance

Results showed that models that obtained the best model fit after parameter estimations, did not necessarily perform best at predicting the plasma glucose concentrations in the different subjects. When seeing the large CV values for the parameter estimates, it may be concluded that setting parameter values for each subject individually was a good choice, since this at least allows for accounting for inter-subject variability of the dynamics for the predictions. The disadvantage of this choice is that parameter values are based on very little estimations intervals and therefore do not have high validity and accuracy. Intra-subject or diurnal variations of the parameter values were also not accounted for. Although results showed that the nonlinear model without the parameters k_g and τ_I had best overall prediction performance, it may be true that addition of the right variability of the model parameters results in better predictions for other proposed model versions.

There are two types of models that can be found in literature for predicting of glucose levels. The first type applies compartmental modelling of plasma glucose concentrations that is some sort of simplification of what occurs in physiology. These models have been developed with varying complexity, as is explained in Chapter 2. For multiple of these compartmental models, a population of virtual subjects has been set up for which certain parameters vary between subjects. One study that has quantified the performance of such a compartmental model was performed by Wendt et al. [99]. A similar approach for identification and validation was taken as in the current study: three datasets were applied for training and one for testing the model for an individual patient. Data sets were acquired in a more controlled setting than in the current study. After a fasting period, an insulin dosage was given. This was followed by subcutaneous injection of a glucagon dosage as soon as glucose concentrations became hypoglycaemic. For the duration of this controlled 7-hour experiment, mean absolute prediction errors (MAPEs) were found to vary from 4.5 to 174.1% with a mean of 26.84%. For fairly low glucose levels of 4 mmol/L, these percentages correspond to mean glucose errors of 0.18 mmol/L to 6.96 mmol/L with a mean of 1.07 mmol/L. The mean absolute error of 1.07 mmol/L was larger than mean RMSe of 0.7525 mmol/L, but they were calculated of measurements during a 7-hour and 3-hour period respectively. Comparing the results, it may be concluded that the nonlinear MM with exclusion of k_g and τ_I performs relatively good at predicting the glucose concentrations. Especially when considering that predictions were performed for uncontrolled experimental conditions.

A study by Wilinksa et al. [75] validated a similar compartmental simulation model based on measures like 'time in euglycaemia', but no actual errors were determined. For this reason, comparison to prediction performance in the current study could not be performed. The Dalla Man model [36] is another compartmental model that was validated for its prediction performance [79]. The FIT was applied to measure the prediction error relative to the variation in the measurement. Outcome was good, but testing data was applied to find the optimal combination of parameter estimations in the population of virtual subjects. Therefore, results can not be compared with the current study, in which the parameter estimates for predictions were identified and fixed before the actual validation.

The second type of glucose prediction model is completely data-driven and attempts to predict glucose levels (test data) by taking into account earlier glucose measurements (training data) [94]. These prediction models can be a linear time series model, a type of regression model, or another model that is based on more complex nonlinear algorithms. Now, recall from the results that the nonlinear model with exclusion of k_g and τ_I had the best overall prediction performance. RMSe for this model was on average 0.7525 mmol/L for a 180-minute prediction period and 0.1747 mmol/L for a 30 minute prediction period. This prediction was performed without any time delay with the initial BG concentration based on the CGM measured at that time. When comparing this to the literature overview of this type of prediction model by Georga et al. [94], it is found that known linear time series prediction models have similar performance for a 30-minute period (RMSe of 0.1 - 0.21 mmol/L). 90-minute predictions have and error of 1.6 mmol/L on average for these types of models and thus performs much worse than the model applied in the current study for long-term glucose predictions. Predictions of these data-driven models was improved by addition of extra inputs, but was not better than for the predictions in the current study. Applying more complex nonlinear models did result in better results for the 30 minute prediction, but for over 120 minutes forward the current study's nonlinear MM was more accurate [94]. To conclude, the approach as applied in the second type of glucose prediction model can result in better short-term predictions of the glucose level but mostly result in worse long-term predictions when compared to the nonlinear MM identified in the current study.

Although the results discussed here may not seem conclusive, considering that parameter estimates were determined for only several data sections in each subject, no accurate predictions were expected. In addition, due to diurnal variations in the glucose dynamics and kinetics, there is a need for identification of the extend of these variations and how these can be represented by the parameters in the models that are proposed. The relatively good prediction performance that was measured shows the feasibility of a simple glucose model for performing short-term predictions of glucose levels. The nonlinear MM with two parameters seems the most feasible for such application based on the prediction errors. Moreover, in adaptive prediction models, a simple glucose model is beneficial, since finding optimal parameter estimations becomes less costly in terms of time and computational strength.

No similar studies were found in literature. Studies of simpler models were mostly developed with the goal of measuring physiological parameters instead of simulating glucose concentrations [49, 53, 54]. The model structures and study design applied in the current study were most similar to the minimal model extensions studied by Herrero et al. [28] and Wendt et al. [99]. Although direct comparison with these models was not possible, performance seemed similar. The main difference of these models with the developed glucose model was that these models also contained models of meal absorption and could be applied to perform predictions during the day as a result. This is not yet possible with the models proposed in the current study.

5.3.3 Limitations & recommendations

There are several limitations to the results of the current study. First of all, the lack of variation in the insulin concentrations during many of the periods taken from the crossover study made identification of the glucose subsystem difficult. Validity and accuracy of the values estimates is limited as a result. Especially for the estimation of the delay in the insulin signal, sufficient variation in the insulin signal is required. This is the main reason why identification was repeated without this delay. Higher perturbed signals could show whether this delay is actually required. Another disadvantage of using data from the crossover study [13] was that data was acquired during daily life and that perturbations to the process were not completely known as a result. Moreover, it is unknown whether the treatment type (OL and CL) influences the glucose dynamics and kinetics in the patients. The limited availability of participants and stable CGM data was also a problem.

Results showed that CGM errors did not have zero mean with a fixed standard deviation. Errors were large compared to the measured signals. It was shown that there was a moderate correlation between the CGM errors and the SMBG measurements. This suggests that CGM measurements are an overestimation of the true value at low glucose levels. Also, it suggests that at high glucose levels, the CGM measurements were an underestimation of the true value. These results indicate that the assumption made by the estimation algorithm on the CGM errors being white and Gaussian was not met. This is important, since a direct method of parameter estimations is susceptible to noise, which is explained in Appendix B. Violation of this assumption may be an explanation for the autocorrelations of the residuals in the glucose subsystem identification not being within the confidence bounds. It is advisable to include a model of the CGM error for the sensors applied in the crossover study [13]. Such models do not yet exist for the applied sensors, but they have been developed for other sensor types in the past [105, 106].

Furthermore, the estimation method did not perform very well when model complexity increased in terms of number of compartments and number of parameters to be estimated. This became clear in the parameter estimation of the two-compartmental model. The algorithm was not able to find convergence of the parameter values. This could be caused by a faulty model structure, but it is expected that especially for 2COM version 2 the estimation method is the limiting factor, since similar models have been successfully identified in the past [54, 3]. Although parameter estimations of the Michaelis-Menten models could be performed, these were very time-consuming (over three hours for the 57 data sections). Moreover, as mentioned earlier, solutions found for the Michaelis-Menten model parameters were clearly not optimal. Using shorter intervals and applying a lower sampling frequency may improve these issues. It is also possible to fix certain parameters before the estimation. Problems may have occurred because the assumption on the CGM error being white and Gaussian made by the algorithm was not met. The algorithm also assumed absence of an error on the model input, which was not verified in this study.

Another limitation to the value of the identified models is that the meal intake and intestinal glucose absorption were not yet considered. A problem for identifying such a model is that the effect of various types of meals in a situation with unknown perturbations as in the crossover study data [13] varies a lot. For in silico testing of CL control systems as the Inreda AP, meal intake is an important factor tot consider. If the glucose can be modelled accurately for unperturbed situations, it becomes possible to determine what the effect is of a meal. This may need to be combined with the effect of the increased insulin dosages that will be applied in the period influenced by meal absorption. Earlier studies applied tracers in different kinds of experiments to model EGP and utilization. This was used to determine what part of the glucose level increase was caused by a labelled meal and this was applied to model rate of appearance of meal glucose into the blood plasma. Such a model or a simplification of such a model may be applied to identify the influence of meal intake during bi-hormonal CL control by the Inreda AP in daily life.

The last limitation to this study is that parameter identification was applied without taking into account that the control algorithm imposes a relation between the noise in the measured output and the I_{IR} and H_{IR} input signals. As explained in Appendix B, application of closed loop identification in which the influence of external perturbations on the output can be determined, may improve the identifiability of the parameters. A possibility to implement such perturbations would be to make slight changes in the applied insulin and glucagon dosages compared to what is determined by the control system. Other perturbations that may be applied without harming the patient are meal intake or a combination of meal intake with an additional subcutaneous bolus injection. Meal intake in the crossover study [13] can already be applied for closed loop identification if the transfer of the control system is known. Application of a model of the CGM error would improve this identification. It needs to be taken into consideration that glucose dynamics were shown to be very slow, meaning that the effect of perturbations may last for many hours. The effect of perturbations can already be tested on short term in silico with the glucose model proposed in the current study. The nonlinear minimal model with the parameters k_i and G_b is probably the best choice for this.

A final recommendation follows from the advise given on closed loop identification in combination with the finding that variability of the parameter estimates between estimation intervals showed to be quite large. When closed loop identification is applied, for example by simply measuring the effect of ingestion of three meals during the day, parameter estimations may be performed separately for each of these meals. This way, diurnal variations in the parameters can be identified. Ideally, this would be performed multiple times for a patient during treatment with a system such as the Inreda AP. Changes in glucose dynamics and kinetics for a patient over a longer period of time can then be identified. When such data is used to determine parameter variability for individual patients over time, this knowledge can be applied to set up a database of virtual patients. These virtual patients can be used for in silico testing of a control system in a variety of virtual patients with variability in the glucose metabolism that could also occur in a clinical situation. The regulation by the control system could even be adapted based on the results of continuous closed loop identification.

5.4 Conclusion

It was shown that the combination of models of subcutaneous glucagon and insulin kinetics in an average T1DM patient with a patient-specific model of glucose dynamics and kinetics, can describe glucose levels in different patients. A nonlinear glucose model with only two parameters and one compartment was promising for short-term (<180 min) predictions of glucose levels, since the prediction error was less than 1 mmol/L for over 80 minutes in advance for 75% of the predictions. This work shows the potential of one-compartmental linear and nonlinear models of glucose dynamics and kinetics to be applied for in silico testing of bi-hormonal glucose control systems and to the development of adaptive control systems.

Bibliography

[1] RIVM. Diabetes mellitus. `https://www.volksgezondheidenzorg.info/onderwerp/diabetes-mellitus`, 2017.

[2] American Diabetes Association. Standards of medical care in diabetes (2010). *Diabetes care*, 33(Suppl 1):S11–S61, 2010.

[3] C. Dalla Man, R. A. Rizza, and C. Cobelli. Meal simulation model of the glucose-insulin system. *IEEE Trans Biomed Eng*, 54(10):1740–9, 2007.

[4] E. Carson and C. Cobelli. *Modelling Methodology for Physiology and Medicine*. Elsevier, 2nd edition, 2014.

[5] A.J. Onvlee. *In silico modeling of patients with type 1 diabetes mellitus*. Master, University of Twente, 2016.

[6] M. Lorenzi, N. Bohannon, E. Tsalikian, and J. H. Karam. Duration of type i diabetes affects glucagon and glucose responses to insulin-induced hypoglycemia. *The Western Journal of Medicine*, 141(4):467–471, 1984.

[7] J.E. Sprague and A.M. Arbeláez. Glucose counterregulatory responses to hypoglycemia. *Pediatric endocrinology reviews : PER*, 9(1):463–475, 2011.

[8] American Diabetes Association. Hyperglycemia (high blood glucose).

[9] V. Pathak, N.M. Pathak, C.L. O'Neill, J. Guduric-Fuchs, and R.J. Medina. Therapies for type 1 diabetes: Current scenario and future perspectives. *Clinical Medicine Insights: Endocrinology and Diabetes*, 2019.

[10] D. Elleri, D.B. Dunger, and R. Hovorka. Closed-loop insulin delivery for treatment of type 1 diabetes. *BMC Medicine*, 9(1):120, 2011.

[11] L. Bally, H. Thabit, S. Hartnell, E. Andereggen, Y. Ruan, M.E. Wilinska, M.L. Evans, M.M. Wertli, A.P. Coll, C. Stettler, and R. Hovorka. Closed-loop insulin delivery for glycemic control in noncritical care. *The New England journal of medicine*, 379(6):547–556, 2018.

[12] F.H. El-Khatib, S.J. Russell, D.M. Nathan, R.G. Sutherlin, and E.R. Damiano. A bihormonal closed-loop artificial pancreas for type 1 diabetes. *Science translational medicine*, 2(27):27ra27–27ra27, 2010.

[13] H. Blauw, A.C. van Bon, R. Koops, J.H. DeVries, and on behalf of the PCDIAB consortium. Performance and safety of an integrated bihormonal artificial pancreas for fully automated glucose control at home. *Diabetes, obesity & metabolism*, 18(7):671–677, 2016.

[14] B.M. Bergenstal, S. Garg, and S.A. Weinzimer. Notably, the US Food and Drug Administration has recently approved the first artificial pancreas system for use by people with type 1 diabetes over 14 years of age, based on a safety outpatient study. *JAMA*, 316:1407–1408, 2018.

[15] L. Wecker, D.A. Taylor, and R.J. Theobald Jr. *Brody's Human Pharmacology - Mechanism-Based Therapeutics*. Elsievier, 6th edition, 2018.

[16] H. Blauw, I. Wendl, J.H. DeVries, T. Heise, T. Jax, and on behalf of the PCDIAB consortium. Pharmacokinetics and pharmacodynamics of various glucagon dosages at different blood glucose levels. *Diabetes, Obesity and Metabolism*, 18(1):34–39, 2015.

[17] D. Boiroux, V. Bátora, M. Hagdrup, S.L. Wendt, N.K. Poulsen, H. Madsen, and J.B. Jørgensen. Adaptive model predictive control for a dual-hormone artificial pancreas. *Journal of Process Control*, 68:105–117, 2018.

[18] R. Hovorka, J. K. Powrie, G. D. Smith, P. H. Sonksen, E. R. Carson, and R. H. Jones. Five-compartment model of insulin kinetics and its use to investigate action of chloroquine in niddm. *American Journal of Physiology-Endocrinology and Metabolism*, 265(1):E162–E175, 1993.

[19] M. Koschorreck and E.D. Gilles. Mathematical modeling and analysis of insulin clearance in vivo. *BMC Systems Biology*, 2(1):43, 2008.

[20] K. Ohashi, M. Fujii, S. Uda, H. Kubota, H. Komada, K. Sakaguchi, W. Ogawa, and S. Kuroda. Increase in hepatic and decrease in peripheral insulin clearance characterize abnormal temporal patterns of serum insulin in diabetic subjects. *Systems Biology and Applications*, 4(1):14, 2018.

[21] E. Ferrannini and C. Cobelli. The kinetics of insulin in man. I. general aspects. *Diabetes/Metabolism Reviews*, 3(2):335–363, 1987.

[22] M.D. Breton, B.P. Kovatchev, C. Dalla Man, C. Cobelli, and F. Micheletto. Method and system for simulation of endogenous and exogenous glucose/insulin/glucagon interplay in the type 1 diabetic patient, 2010.

[23] G. Nucci and C. Cobelli. Models of subcutaneous insulin kinetics. a critical review. *Computer Methods and Programs in Biomedicine*, 62(3):249–257, 2000.

[24] M. E. Wilinska, L. J. Chassin, H. C. Schaller, L. Schaupp, T. R. Pieber, and R. Hovorka. Insulin kinetics in type-1 diabetes: continuous and bolus delivery of rapid acting insulin. *IEEE Transactions on Biomedical Engineering*, 52(1):3–12, 2005.

[25] E.W. Kraegen and D.J. Chisholm. Insulin responses to varying profiles of subcutaneous insulin infusion: kinetic modelling studies. *Diabetologia*, 26(3):208–213, 1984.

[26] M. Schiavon, C. Dalla Man, and C. Cobelli. Modeling subcutaneous absorption of fast-acting insulin in type 1 diabetes. *IEEE Transactions on Biomedical Engineering*, 65(9):2079–2086, 2018.

[27] S. Shimoda, K. Nishida, M. Sakakida, Y. Konno, K. Ichinose, M. Uehara, T. Nowak, and M. Shichiri. Closed-loop subcutaneous insulin infusion algorithm with a short-acting insulin analog for long-term clinical application of a wearable artificial endocrine pancreas. *Frontiers of Medical and Biological Engineering*, 8(3):197–211, 1997.

[28] P. Herrero, P. Georgiou, N. Oliver, M. Reddy, D. Johnston, and C. Toumazou. A composite model of glucagon-glucose dynamics for in silico testing of bihormonal glucose controllers. *Journal of Diabetes Science and Technology*, 7(4):941–951, 2013.

[29] C. Dalla Man, D.M. Raimondo, R.A. Rizza, and C. Cobelli. Gim, simulation software of meal glucose—insulin model. *Journal of Diabetes Science and Technology*, 1(3):323–330, 2007.

[30] D. Lv, S.D. Kulkarni, A. Chan, S. Keith, R. Pettis, B.P. Kovatchev, L.S. Farhi, and M.D. Breton. Pharmacokinetic model of the transport of fast-acting insulin from the subcutaneous and intradermal spaces to blood. *Journal of Diabetes Science and Technology*, 9(4):831–840, 2015.

[31] P. Li, L. Yu, Q. Fang, and S. Lee. A simplification of cobelli's glucose–insulin model for type 1 diabetes mellitus and its fpga implementation. *Medical & Biological Engineering & Computing*, 54(10):1563–1577, 2016.

[32] R.L. Dobbins, S.N. Davis, D.W. Neal, C. Cobelli, J. Jaspan, and A.D. Cherrington. Compartmental modeling of glucagon kinetics in the conscious dog. *Metabolism - Clinical and Experimental*, 44(4):452–459, 1995.

[33] A. Haidar, C. Duval, L. Legault, and R. Rabasa-Lhoret. Pharmacokinetics of insulin aspart and glucagon in type 1 diabetes during closed-loop operation. *Journal of diabetes science and technology*, 7(6):1507–12, 2013.

[34] D. Lv, M.D. Breton, and L.S. Farhy. Pharmacokinetics modeling of exogenous glucagon in type 1 diabetes mellitus patients. *Diabetes technology & therapeutics*, 15(11):935–941, 2013.

[35] S.L. Wendt, J. Møller, C. Knudsen, H. Madsen, A. Haidar, and J. Jørgensen. PK/PD modelling of glucose-insulin-glucagon dynamics in healthy dogs after a subcutaneous bolus administration of native glucagon or a novel glucagon analogue. Technical report, Kgs. Lyngby: Technical University of Denmark (DTU), 2016.

[36] C. Dalla Man, F. Micheletto, D. Lv, M. Breton, B. Kovatchev, and C. Cobelli. The UVA/PADOVA type 1 diabetes simulator: New features. *Journal of Diabetes Science and Technology*, 8(1):26–34, 2014.

[37] A. Siafarikas, R.J. Johnston, M.K. Bulsara, P. O'Leary, T.W. Jones, and E.A. Davis. Early loss of the glucagon response to hypoglycemia in adolescents with type 1 diabetes. *Diabetes Care*, 35(8):1757, 2012.

[38] N.J. Wewer Albrechtsen, R.E. Kuhre, J. Pedersen, F.K. Knop, and J.J. Holst. The biology of glucagon and the consequences of hyperglucagonemia. *Biomarkers in Medicine*, 10(11):1141–1151, 2016.

[39] R.H. Unger and L. Orci. Paracrinology of islets and the paracrinopathy of diabetes. *Proceedings of the National Academy of Sciences*, 107(37):16009, 2010.

[40] R.H. Unger and D. Cherrington, A. Glucagonocentric restructuring of diabetes: a pathophysiologic and therapeutic makeover. *The Journal of Clinical Investigation*, 122(1):4–12, 2012.

[41] S.J. Le Marchand and D.W. Piston. Glucose suppression of glucagon secretion - metabolic and calcium responses from alpha-cells in intact mouse pancreatic islets*. *J Biol Chem*, 285(19):14389–14398, 2010.

[42] V.J. Briscoe and S.N. Davis. Hypoglycemia in type 1 and type 2 diabetes: Physiology, pathophysiology, and management. *Clinical Diabetes*, 24(3):115, 2006.

[43] L. Hinshaw, C. Dalla Man, D.K. Nandy, A. Saad, A.E. Bharucha, J.A. Levine, R.A. Rizza, R. Basu, R.E. Carter, C. Cobelli, Y.C. Kudva, and A. Basu. Diurnal pattern of insulin action in type 1 diabetes: implications for a closed-loop system. *Diabetes*, 62(7):2223–2229, 2013.

[44] L.S. Farhy and A.L. McCall. Models of glucagon secretion, their application to the analysis of the defects in glucagon counterregulation and potential extension to approximate glucagon action. *Journal of Diabetes Science and Technology*, 4(6):1345–1356, 2010.

[45] M. Watts and A. Sherman. Modeling the pancreatic alpha-cell: dual mechanisms of glucose suppression of glucagon secretion. *Biophysical journal*, 106(3):741–751, 2014.

[46] M. Watts, J. Ha, O. Kimchi, and A. Sherman. Paracrine regulation of glucagon secretion: the β-α-δ model. *American journal of physiology. Endocrinology and metabolism*, 310(8):E597–E611, 2016.

[47] F Micheletto, C Dalla Man, A Vella, and C Cobelli. A model of glucagon secretion and action in healthy subjects [abstract a106]. *Book of Abstracts. 10th Diabetes Technology Meeting. Bethesda, MD: Diabetes Technology Society*, 2010.

[48] C. Braem. Parameter estimation of the glucagon dynamics in type 1 diabetes mellitus patients. Technical report, University of Twente; Inreda Diabetic - Goor; Rijsntate Ziekenhuis - Arnhem, 2017.

[49] R.N. Bergman, Y.Z. Ider, C.R. Bowden, and C. Cobelli. Quantitative estimation of insulin sensitivity. *American Journal of Physiology-Endocrinology and Metabolism*, 236(6):E667, 1979.

[50] C. Cobelli, A. Caumo, and M. Omenetto. Minimal model S_g overestimation and S_i underestimation: improved accuracy by a Bayesian two-compartment model. *American Journal of Physiology-Endocrinology and Metabolism*, 277(3):E481–E488, 1999.

[51] C. Cobelli, G. Pacini, G. Toffolo, and L. Sacca. Estimation of insulin sensitivity and glucose clearance from minimal model: new insights from labeled IVGTT. *American Journal of Physiology-Endocrinology and Metabolism*, 250(5):E591–E598, 1986.

[52] A. Caumo, A. Giacca, M. Morgese, G. Pozza, P. Micossi, and C. Cobelli. Minimal models of glucose disappearance: Lessons from the labelled IVGTT. *Diabetic Medicine*, 8(9):822–832, 1991.

[53] A. Caumo and C. Cobelli. Hepatic glucose production during the labeled IVGTT: estimation by deconvolution with a new minimal model. *American Journal of Physiology-Endocrinology and Metabolism*, 264(5):E829–E841, 1993.

[54] P. Vicini, A. Caumo, and C. Cobelli. The hot IVGTT two-compartment minimal model: Indexes of glucose effectiveness and insulin sensitivity. *American Journal of Physiology - Endocrinology and Metabolism*, 273(5 36-5):E1024–E1032, 1997.

[55] E. Ferrannini, J. D. Smith, C. Cobelli, G. Toffolo, A. Pilo, and R. A. DeFronzo. Effect of insulin on the distribution and disposition of glucose in man. *The Journal of clinical investigation*, 76(1):357–364, 1985.

[56] A. Avogaro, J.D. Bristow, D.M. Bier, C. Cobelli, and G. Toffolo. Stable-label intravenous glucose tolerance test minimal model. *Diabetes*, 38(8):1048, 1989.

[57] R. Hovorka, F. Shojaee-Moradie, P.V. Carroll, L.J. Chassin, I.J. Gowrie, N.C. Jackson, R.S. Tudor, A.M. Umpleby, and R.H. Jones. Partitioning glucose distribution/transport, disposal, and endogenous production during IVGTT. *American Journal of Physiology-Endocrinology and Metabolism*, 282(5):E992–E1007, 2002.

[58] R. Basu, B. Di Camillo, G. Toffolo, A. Basu, P. Shah, A. Vella, R. Rizza, and C. Cobelli. Use of a novel triple-tracer approach to assess postprandial glucose metabolism. *American Journal of Physiology-Endocrinology and Metabolism*, 284(1):E55–E69, 2003.

[59] C. Dalla Man, G. Toffolo, R. Basu, R. A. Rizza, and C. Cobelli. A model of glucose production during a meal. In *2006 International Conference of the IEEE Engineering in Medicine and Biology Society*, pages 5647–5650, 2006.

[60] C. Dalla Man, A. Caumo, and C. Cobelli. The oral glucose minimal model: Estimation of insulin sensitivity from a meal test. *IEEE Transactions on Biomedical Engineering*, 49(5):419–429, 2002.

[61] C. Dalla Man, K.E. Yarasheski, A. Caumo, H. Robertson, G. Toffolo, K.S. Polonsky, and Claudio Cobelli. Insulin sensitivity by oral glucose minimal models: validation against clamp. *American Journal of Physiology-Endocrinology and Metabolism*, 289(6):E954–E959, 2005.

[62] C. Dalla Man, M. Camilleri, and C. Cobelli. A system model of oral glucose absorption: Validation on gold standard data. *IEEE Transactions on Biomedical Engineering*, 53(12):2472–2478, 2006.

[63] H. Yki-Järvinen, A. A. Young, C. Lamkin, and J. E. Foley. Kinetics of glucose disposal in whole body and across the forearm in man. *The Journal of clinical investigation*, 79(6):1713–1719, 1987.

[64] X. W. Wong, I. Singh-Levett, L. J. Hollingsworth, G. M. Shaw, C. E. Hann, T. Lotz, J. Lin, O. S. W. Wong, and J. G. Chase. A novel, model-based insulin and nutrition delivery controller for glycemic regulation in critically ill patients. *Diabetes Technology & Therapeutics*, 8(2):174–190, 2006.

[65] R. A. DeFronzo, J. D. Tobin, and R. Andres. Glucose clamp technique: a method for quantifying insulin secretion and resistance. *American Journal of Physiology-Endocrinology and Metabolism*, 237(3):E214, 1979.

[66] J. Proietto, A. Nankervis, P. Aitken, G. Caruso, and F. Alford. Glucose utilization in type 1 (insulin-dependent) diabetes: Evidence for a defect not reversible by acute elevations of insulin. *Diabetologia*, 25:331–5, 1983.

[67] H.N. Ginsberg. Investigation of insulin sensitivity in treated subjects with ketosis-prone diabetes mellitus. *Diabetes*, 26(4):278, 1977.

[68] B.P. Kovatchev, L.S. Farhy, D.J. Cox, M. Straume, V.I. Yankov, L.A. Gonder-Frederick, and W.L. Clarke. Modeling insulin-glucose dynamics during insulin induced hypoglycemia. evaluation of glucose counterregulation. *Journal of Theoretical Medicine*, 1(4), 1999.

[69] B.P. Kovatchev, M. Straume, L.S. Farhy, and D.J. Cox. Dynamic network model of glucose counterregulation in subjects with insulin-requiring diabetes. In *Methods in Enzymology*, volume 321, pages 396–410. Academic Press, 2000.

[70] L. Hinshaw, A. Mallad, C. Dalla Man, R. Basu, C. Cobelli, R.E. Carter, Y.C. Kudva, and A. Basu. Glucagon sensitivity and clearance in type 1 diabetes: insights from in vivo and in silico experiments. *American journal of physiology. Endocrinology and metabolism*, 309(5):E474–E486, 2015.

[71] A. Emami, Joseph El Youssef, Remi Rabasa-Lhoret, Joelle Pineau, Jessica R. Castle, and Ahmad Haidar. Modeling glucagon action in patients with type 1 diabetes. *IEEE Journal of Biomedical and Health Informatics*, 21(4), 2017.

[72] J.T. Sorensen. *A Physiologic Model of Glucose Metabolism in Man and Its Use to Design and Assess Improved Insulin Therapies for Diabetes*. PhD thesis, Massachussets Institute of Technology, 1978.

[73] P. Colmegna and R. S. Sánchez Peña. Analysis of three T1DM simulation models for evaluating robust closed-loop controllers. *Computer Methods and Programs in Biomedicine*, 113(1):371–382, 2014.

[74] R. Hovorka, V. Canonico, L.J. Chassin, U. Haueter, M. Massi-Benedetti, M.O. Federici, T.R. Pieber, H.C. Schaller, L. Schaupp, T. Vering, and M.E. Wilinska. Nonlinear model predictive control of glucose concentration in subjects with type 1 diabetes. *Physiological Measurement*, 25(4):905–920, 2004.

[75] M. E. Wilinska, L. J. Chassin, C. L. Acerini, J. M. Allen, D. B. Dunger, and R. Hovorka. Simulation environment to evaluate closed-loop insulin delivery systems in type 1 diabetes. *Journal of diabetes science and technology*, 4(1):132–44, 2010.

[76] P.G. Fabietti, V. Canonico, M.O. Federici, M.M. Benedetti, and E. Sarti. Control oriented model of insulin and glucose dynamics in type 1 diabetics. *Medical and Biological Engineering and Computing*, 44(1):69–78, 2006.

[77] S.S. Kanderian, S. Weinzimer, G. Voskanyan, and G.M. Steil. Identification of intraday metabolic profiles during closed-loop glucose control in individuals with type 1 diabetes. *Journal of diabetes science and technology*, 3(5):1047–1057, 2009.

[78] R. Visentin, E. Campos-Náñez, M. Schiavon, D. Lv, M. Vettoretti, M. Breton, B.P. Kovatchev, C. Dalla Man, and C. Cobelli. The UVA/Padova type 1 diabetes simulator goes from single meal to single day. *Journal of Diabetes Science and Technology*, 12(2):273–281, 2018.

[79] R. Visentin, C. Dalla Man, B. Kovatchev, and C. Cobelli. The university of Virginia/Padova type 1 diabetes simulator matches the glucose traces of a clinical trial. *Diabetes technology & therapeutics*, 16(7):428–434, 2014.

[80] R.S. Parker, F.J. Doyle, and N.A. Peppas. A model-based algorithm for blood glucose control in type I diabetic patients. *IEEE Transactions on Biomedical Engineering*, 46(2):148–157, 1999.

[81] E.D. Lehmann and T. Deutsch. A physiological model of glucose-insulin interaction in type 1 diabetes mellitus. *Journal of Biomedical Engineering*, 14(3):235–242, 1992.

[82] M. Wilinska and R. Hovorka. Simulation models for in-silico evaluation of closed-loop insulin delivery systems in type 1 diabetes. In *Data-driven Modeling for Diabetes*, pages 131–149. 2008.

[83] S.S. Kanderian, S.A. Weinzimer, and G.M. Steil. The identifiable virtual patient model: comparison of simulation and clinical closed-loop study results. *Journal of diabetes science and technology*, 6(2):371–379, 2012.

[84] P. Li, L. Yu, L. Guo, J. Dong, J. Hu, and Q. Fang. Pid control of glucose concentration in subjects with type 1 diabetes based on a simplified model: An in silico trial. In *Proceedings of the 10th World Congress on Intelligent Control and Automation*, pages 5051–5055, 2012.

[85] Q. Fang, L. Yu, and P. Li. A new insulin-glucose metabolic model of type 1 diabetes mellitus: An in silico study. *Computer Methods and Programs in Biomedicine*, 120(1):16–26, 2015.

[86] C. Dalla Man, A. Caumo, R. Basu, R. Rizza, G. Toffolo, and C. Cobelli. Minimal model estimation of glucose absorption and insulin sensitivity from oral test: validation with a tracer method. *American Journal of Physiology-Endocrinology and Metabolism*, 287(4):E637–E643, 2004.

[87] A. Gradel, T. Porsgaard, J. Lykkesfeldt, T. Seested, S. Gram-Nielsen, N.R. Kristensen, and H. Refsgaard. Factors affecting the absorption of subcutaneously administered insulin: Effect on variability. *Journal of diabetes research*, 2018(1205121), 2018.

[88] Eli Lilly and Company. Glucagon for injection, 2018.

[89] Mathworks, Inc. *MATLAB 2018b*. Natick, Massachusetts, United States.

[90] Mathworks. lsqnonlin. `https://nl.mathworks.com/help/optim/ug/lsqnonlin.html`.

[91] Mathworks. Least-squares fitting. `https://nl.mathworks.com/help/curvefit/least-squares-fitting.html`.

[92] Mathworks. Least-squares (model fitting) algorithms. `https://nl.mathworks.com/help/optim/ug/least-squares-model-fitting-algorithms.html`.

[93] Mathworks. Choosing the algorithm. `https://nl.mathworks.com/help/optim/ug/choosing-the-algorithm.html`.

[94] E.I. Georga, D.I. Fotiadis, and S.K. Tigas. *Personalized predictive modeling in Type 1 diabetes*. Academic Press, an imprint of Elsevier, 2018.

[95] Mathworks. When the solver fails. `https://nl.mathworks.com/help/optim/ug/when-the-solver-fails.html`.

[96] Mathworks. Residual analysis with autocorrelation. `https://nl.mathworks.com/help/signal/ug/residual-analysis-with-autocorrelation.html`.

[97] S. Pardo and D.A. Simmons. The quantitative relationship between ISO 15197 accuracy criteria and mean absolute relative difference (MARD) in the evaluation of analytical performance of self-monitoring of blood glucose (SMBG) systems. *Journal of Diabetes Science and Technology*, 10(5):1182–1187, 2016.

[98] G.F. Franklin, J.D. Powell, and Amami-Naeini A. *Feedback Control of Dynamic Systems*. Pearson, 8th edition, 2019.

[99] S.L. Wendt, A. Ranjan, J.K. Møller, S. Schmidt, C.B. Knudsen, J.J. Holst, S. Madsbad, H. Madsen, K. Nørgaard, and J.B. Jørgensen. Cross-validation of a glucose-insulin-glucagon pharmacodynamics model for simulation using data from patients with type 1 diabetes. *Journal of diabetes science and technology*, 11(6):1101–1111, 2017.

[100] N. Middelhuis. Estimation of the parameters in the glucagon dynamics with use of available data, 2016.

[101] A. Haidar, D. Elleri, K. Kumareswaran, L. Leelarathna, J.M. Allen, K. Caldwell, H.R. Murphy, M.E. Wilinska, C.L. Acerini, M.L. Evans, D.B. Dunger, M. Nodale, and R. Hovorka.

[102] M. Schiavon, C. Dalla Man, Y.C. Kudva, A. Basu, and C. Cobelli. Quantitative estimation of insulin sensitivity in type 1 diabetic subjects wearing a sensor augmented insulin pump. *Diabetes Care*, 37(5):1216–1223, 2014.

[103] P. Denti, A. Bertoldo, P. Vicini, and C. Cobelli. Ivgtt glucose minimal model covariate selection by nonlinear mixed-effects approach. american journal of physiology. *Endocrinology and metabolism*, 298:E950–E960.

[104] C. McDonald, A. Dunaif, and D.T. Finegood. Minimal-model estimates of insulin sensitivity are insensitive to errors in glucose effectiveness, the journal of clinical endocrinology & metabolism. *The Journal of Clinical Endocrinology & Metabolism*, 85:2504–2508, 2000.

[105] M.D. Breton and B. Kovatchev. Analysis, modeling, and simulation of the accuracy of continuous glucose sensors. *Journal of Diabetes Science and Technology*, 2(5):853–862, 2008.

[106] A. Facchinetti, S. Del Favero, G. Sparacino, J. R. Castle, W. K. Ward, and C. Cobelli. Modeling the glucose sensor error. *IEEE Trans Biomed Eng*, 61(3):620–9, 2014.

[107] A. Facchinetti, S. Del Favero, G. Sparacino, and C. Cobelli. Model of glucose sensor error components: identification and assessment for new dexcom g4 generation devices. *Medical & Biological Engineering & Computing*, 53(12):1259–1269, 2015.

[108] R. Isermann. On-line identification in closed loop. In Rolf Isermann, editor, *Digital Control Systems: Volume 2: Stochastic Control, Multivariable Control, Adaptive Control, Applications*, pages 158–169. Springer Berlin Heidelberg, Berlin, Heidelberg, 1991.

[109] M. Ye and M.C. Hill. Global sensitivity analysis for uncertain parameters, models, and scenarios. In *Sensitivity Analysis in Earth Observation Modelling*, pages 177–210. Florida State University, Tallahassee, FL, United States; University of Kansas, Lawrence, KS, United States, 2017.

[110] L. Vuilleumier, R.A. Harley, and N.J. Brown. First- and second-order sensitivity analysis of a photochemically reactive system (a green's function approach). *Environmental Science & Technology*, 31(4):1206–1217, 1997.

[111] R.P. Dickinson and R.J. Gelinas. Sensitivity analysis of ordinary differential equation systems-a direct method*. *Journal of Computational Physics*, 21:123–143, 1976.

[112] A.M. Dunker. The decoupled direct method for calculating sensitivity coefficients in chemical kinetics. *The Journal of Chemical Physics*, 81(5):2385–2393, 1984.

Appendices

Appendix A

System analysis

In this appendix, analysis are performed to gain insight into the behaviour of the identified model structures. All three subsystems of the model of glucose metabolism are considered. These model subsystems describe the concentrations of insulin, glucagon and glucose in the blood plasma in people with T1DM. The system analysis includes applying Laplace transforms to linear systems to find the system transfer functions. Bode plots were determined to study the frequency response. Frequency content of the input and output signals were determined to verify the interpretation of the Bode plots. Impulse responses were determined in order to study the effect of the system characteristics from the response to a signal containing all frequencies. Methods applied were described in [98] and Matlab functions 'tf', 'fft', 'bode' and 'impulse' were used [89].

For the insulin subsystem, the transfer function determines the frequency transfer of the insulin infusion rate I_{IR} to the output amount of insulin in the blood plasma q_{ip} that is proportional to the insulin plasma concentration C_{ip}. Equations A.1-A.4 are the transfer functions for model versions 1-4 respectively. The Bode plot of the frequency response of these identified model versions are shown on the left side of Figure A.1. Similarly, for the glucagon subsystem, the transfer function determines transfer from H_{IR} to the output amount of glucagon q_{hp} proportional to the glucagon plasma concentration C_{hp}. Equation A.5 is the transfer function for the glucagon subsystem model. The Bode plot of the frequency response of the identified glucagon subsystem model is shown on the right side of Figure A.1. Then, considering the identified model version 3 insulin subsystem and glucagon subsystem models, frequency contents of input signals and corresponding output signals for these systems are shown in Figure A.2. Also, the impulse responses are shown in Figure A.3.

$$H_{I1}(s) = \frac{q_{ip}(s)}{I_{IR}(s)} = \frac{a_{p1}}{(s+m)(s+a_{p1})} \tag{A.1}$$

$$H_{I2}(s) = \frac{q_{ip}(s)}{I_{IR}(s)} = \frac{a_{p1}}{(s+m)(s+a_{p1}+m_{sc})} \tag{A.2}$$

$$H_{I3}(s) = \frac{q_{ip}(s)}{I_{IR}(s)} = \frac{a_{p2} \cdot d_i}{(s+m)(s+a_{p2})(s+d_i)} \tag{A.3}$$

$$H_{I4}(s) = \frac{q_{ip}(s)}{I_{IR}(s)} = \frac{a_{p1} \cdot s + a_{p2}(d_i + a_{p1})}{(s+m)(s+a_{p2})(s+d_i)} \tag{A.4}$$

$$H_H(s) = \frac{q_{hp}(s)}{H_{IR}(s)} = \frac{b_p}{(s+n_h)(s+b_p)} \tag{A.5}$$

From the insulin transfer functions in Equations A.1-A.4, it can be seen that the poles are real and have negative values for positive parameter values [98]. This means that all these systems are stable. Model versions 1 and 2 are second order transfer functions with slightly different characteristics. Both have a natural frequency that is rounded to 0.00025 min^{-1}. However, damping ratio of model version 1 is high

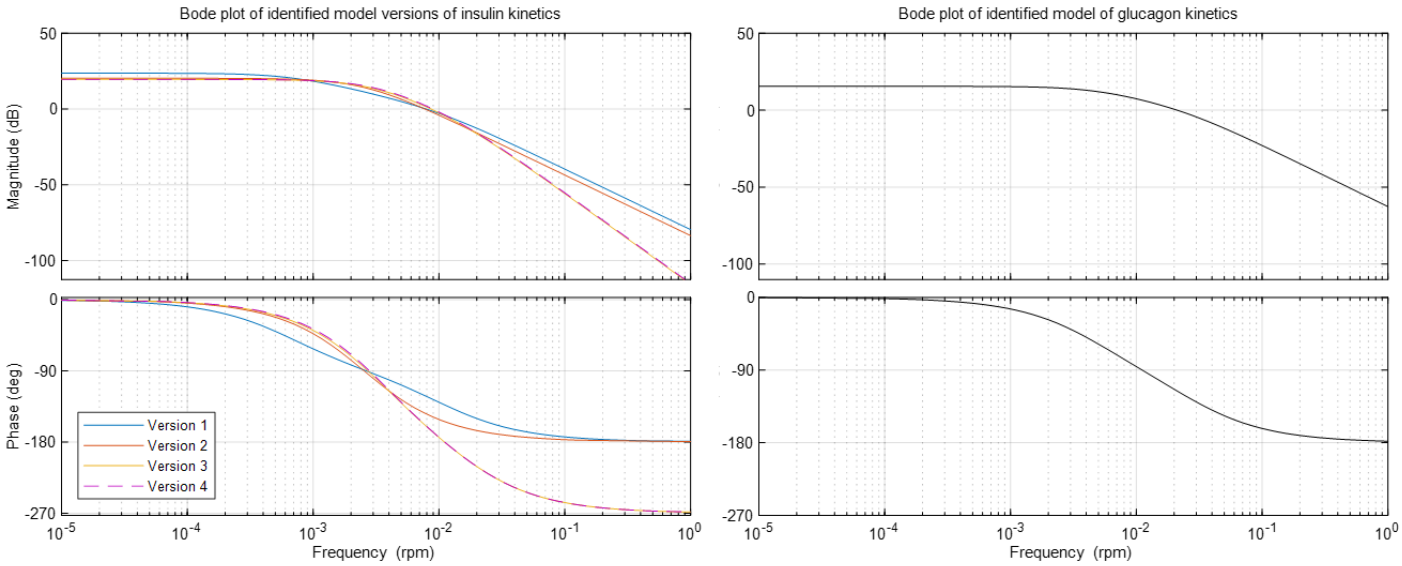

Figure A.1: Bode plot for the four identified model versions of insulin kinetics on the left side and for the glucagon subsystem model on the right side. Note that lines for insulin subsystem models version 3 and 4 overlap the left Bode plot.

with a value of 2.13 and is overdamped, while model version 2 has a damping ratio of 1.00 and is therefore critically damped. This difference can be seen as well from the Bode plot (Figure A.1) of the transfer of both model functions, that shows a clear difference in the phase delay between both model versions. Typical for the 2nd order transfer are the effect of a lowpass filter in which for higher frequencies, the decay in the magnitude plot is 40 dB/decade and the phase delay is -180 degrees. Model versions 3 and 4 are of third order and do not have a clear natural frequency as the 2nd order systems. Characteristics of a 3rd order system can be recognized in the Bode plot, since the phase delay for higher frequencies is -270 degrees and the magnitude decay is 60 dB/decade. Cut-off frequency of the model version 3 and 4 transfer is determined by the poles. From the Bode plot, it can be seen that decay in the magnitude plot occurs near the same frequency range as for the 2nd order systems. If for model version 4, a_{p1} would be valued well above zero, the effect of the zero in the transfer function would visible in the Bode plot: phase delay and signal attenuation become less strong for higher frequencies. The value of the zero of this system determines the frequency range for which this occurs.

From Equation A.5, it can be seen that poles of the glucagon subsystem are equal to $-b_p$ and $-n_h$, which means that the poles are real and have negative values for positive parameter values. Therefore, the system is always stable. The damping ratio of the system is 1.41, indicating that the 2nd order system is overdamped. Natural frequency of the 2nd order transfer is 0.011 min^{-1}. From the Bode plot of the transfer function of the identified glucagon model, it can be seen the model acts as a lowpass filter on the input with a cut-off frequency equal to the natural frequency of the system. For higher frequencies, a 180-degree phase delay is present and decay of the magnitude is 40 dB/decade.

From Figure A.2, the same low-pass filter characteristics as in the Bode plots can be seen for both the insulin subsystem model version 3 and the glucagon subsystem. The input infusion rates of both insulin and glucagon have a strong power for frequencies below 5 min^{-1}, both for a single bolus input as well as repeated bolus infusions. The outputs however, consists of much lower frequencies with most power being below 0.04 min^{-1}. Frequency content of the q_{ip} output is even lower than of the q_{hp} output. This was expected, since Bode plots showed that higher frequencies were passed for the glucagon subsystem. The impulse responses in Figure A.3 confirm that the glucagon subsystem passes through higher frequencies by showing that the impulse response of this system is much quicker than for the insulin subsystem. The impulse responses of both systems do have similar shapes, which is due to the low-pass filter characteristics and negative real poles that both systems have.

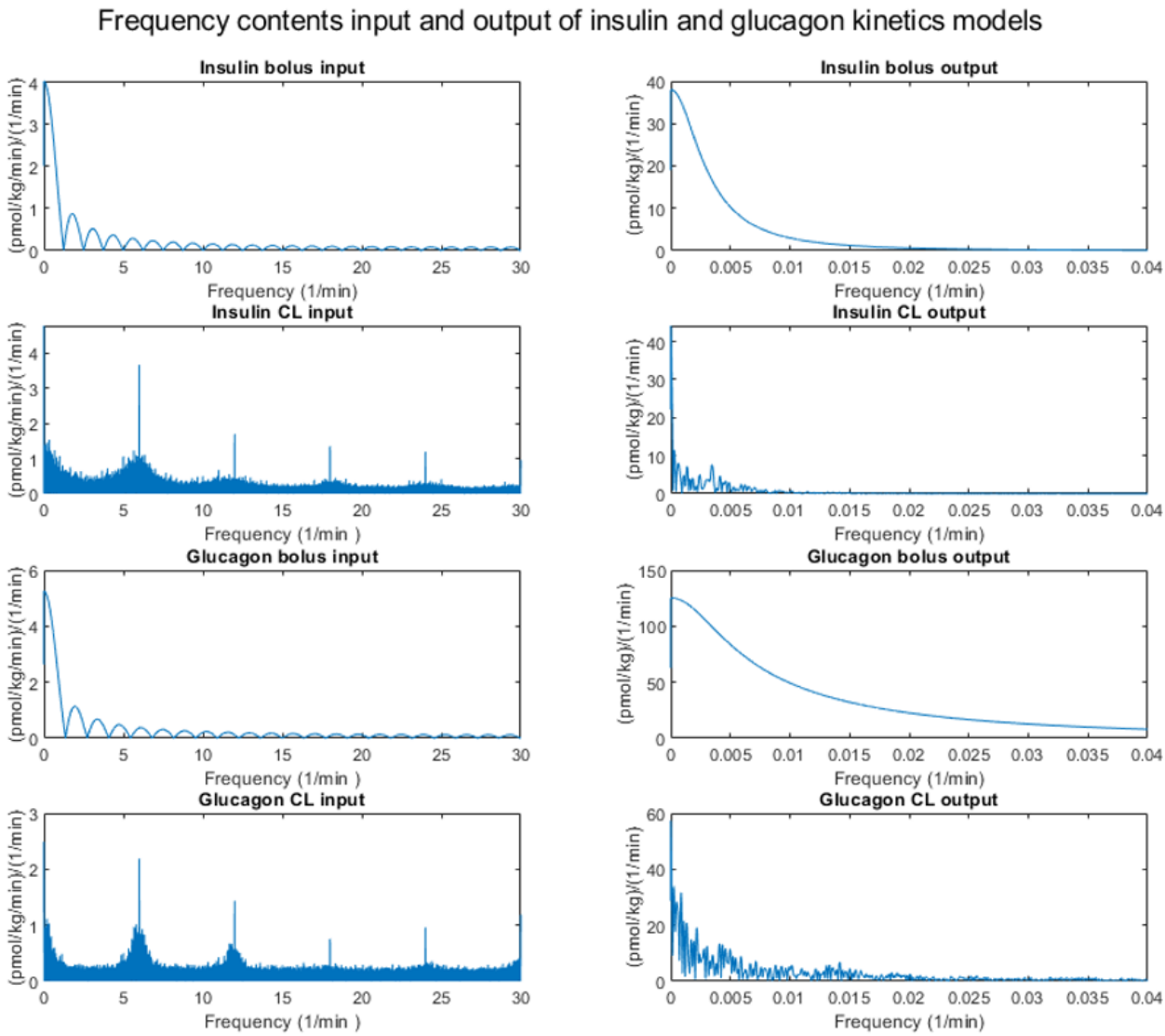

Figure A.2: Frequency contents determined with 'fft' of infusion rate inputs on the left side and the 'fft' of the corresponding output amount of hormone in the plasma on the right side. Output was determined for average parameter estimates. Upper four plots are input-output plots of the insulin model version 3 subsystem. Lower four plots are input-output plots of the glucagon subsystem. Bolus input consists of a single subcutaneous bolus injection and CL input consists of repeated subcutaneous infusion as in a CL control situation [13].

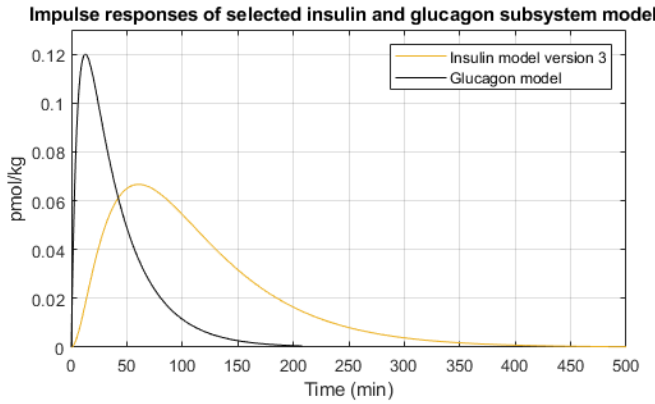

Figure A.3: Impulse response of insulin model version 3 subsystem and glucagon subsystem for averages of the parameter estimates.

The transfer function of the various proposed glucose subsystems in this study cannot be determined as a whole, since the differential equation for q_{gp} depends on multiple variables and contains nonlinearities in all proposed models except from the linear minimal model (MM). For this model, transfer functions can then be determined by setting all model inputs to zero, except the input considered. The transfer function of the amount of insulin q_{ip} to the glucose mass q_{gp} is shown in Equation A.6. In addition, the transfer function of the amount of glucagon q_{hp} to the glucose mass q_{gp} is shown in Equation A.7. Since glucagon action was estimated with most accuracy by adding a linear component to the differential equation, this is considered in the analysis.

$$H_{G,I}(s) = \frac{q_{gp}(s)}{q_{ip}(s)} = \frac{-k_i \cdot \exp(-\tau_I \cdot s)}{s + k_g} \tag{A.6}$$

$$H_{G,H}(s) = \frac{q_{gp}(s)}{q_{hp}(s)} = \frac{k_h}{s + k_g} \tag{A.7}$$

In Figure A.4, the frequency content of CGM measurements is shown. In Figure A.5, transfer $H_{G,I}$ is considered for $k_g = 0$ and also $\tau_I = 0$. The Bode plot is shown on the left side and the impulse response on the right side. The same is shown in Figure A.6, but now for the transfer $H_{G,I}$ with $k_g > 0$ and $\tau_I = 0$. In Figure A.7, transfer $H_{G,H}$ is considered, this case combined with the glucagon subsystem model.

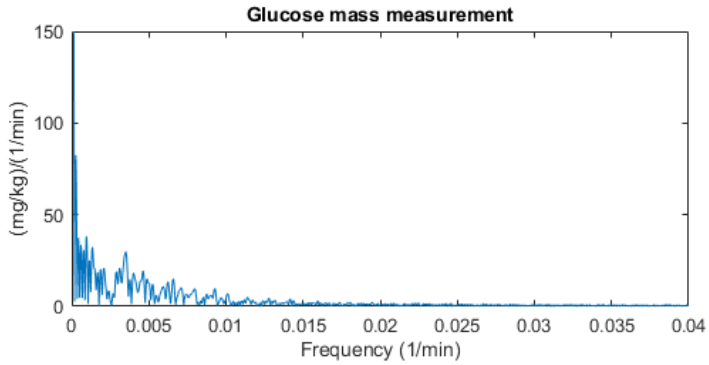

Figure A.4: Frequency content of glucose mass levels derived from CGM measurements. Content was determined with fft.

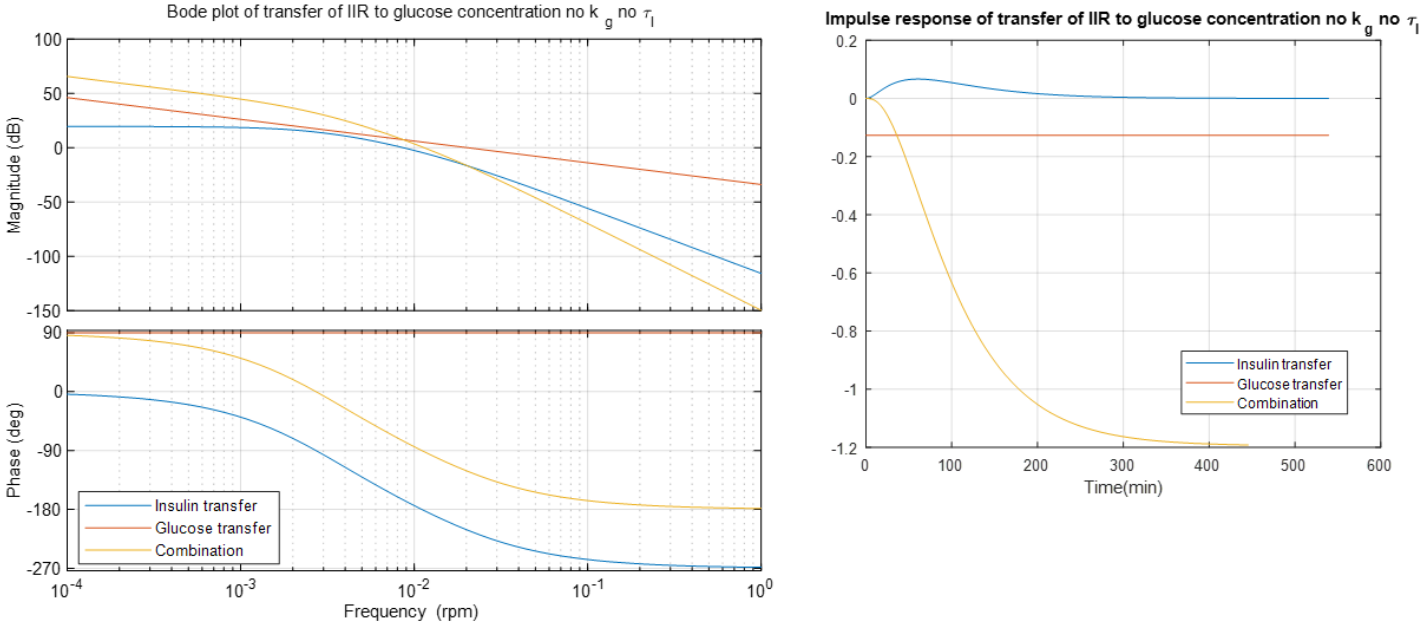

Figure A.5: Bode plot (left) and impulse responses (right) of insulin subsystem (blue), glucose linear MM with $k_g = 0$ and $\tau_I = 0$. (red) and that of both systems combined (yellow).

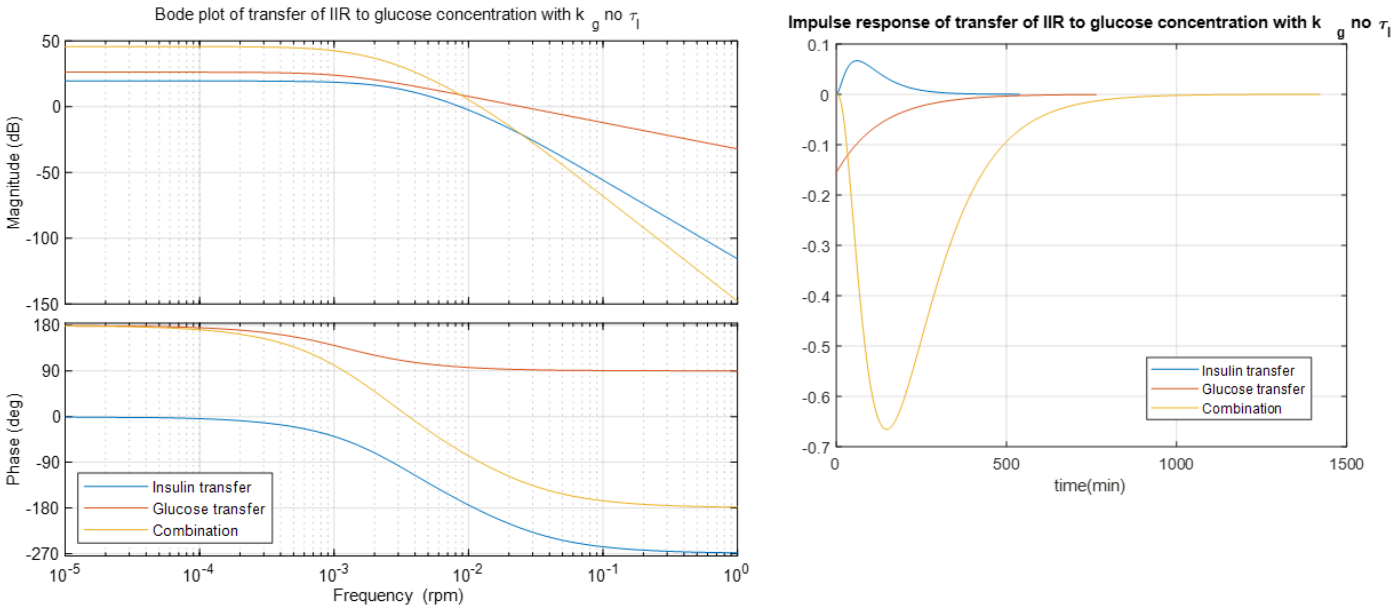

Figure A.6: Bode plot (left) and impulse responses (right) of insulin subsystem (blue), glucose linear MM with $k_g > 0$ and $\tau_I = 0$. (red) and that of both systems combined (yellow).

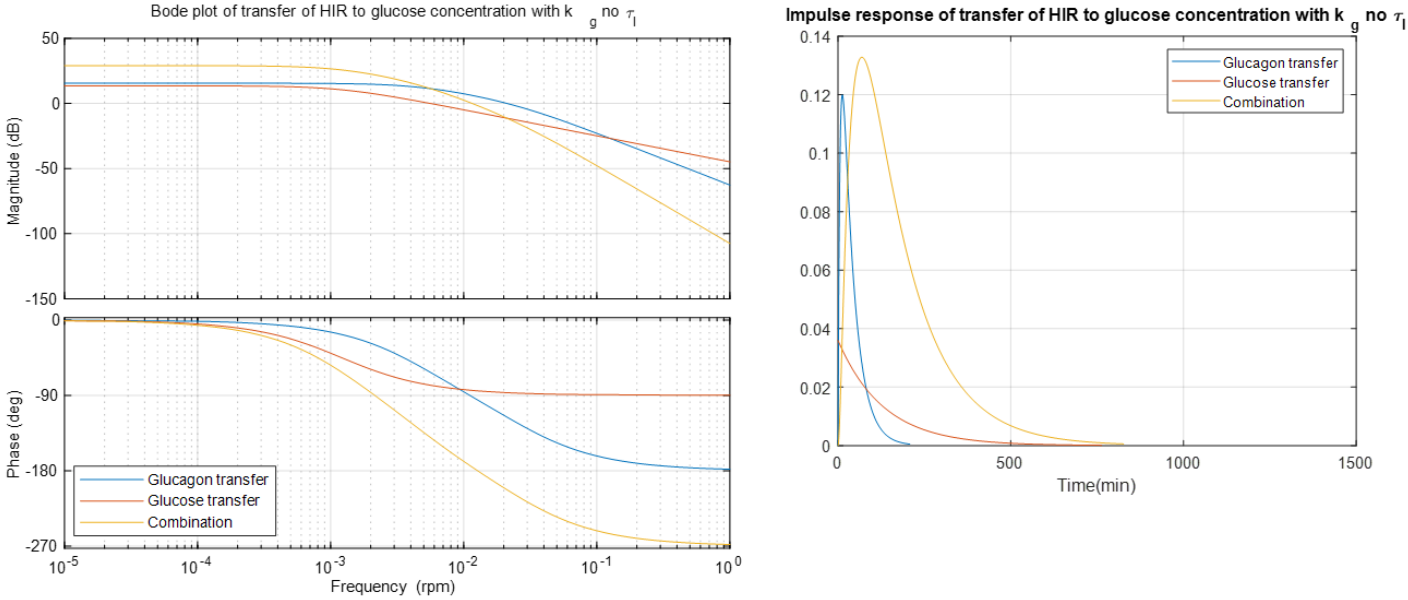

Figure A.7: Bode plot (left) and impulse responses (right) of glucagon subsystem (blue), glucose linear MM with $k_g > 0$ and $\tau_I = 0$. (red) and that of both systems combined (yellow).

Bode plot and impulse responses of the transfer of the amount of insulin to the glucose mass in the linear MM is represented by the red lines in Figures A.5 and A.6. Parameter values applied to these figures were taken to be the Group 2A and 2B estimations in Table 4.3 respectively. It can be seen that for $k_g > 0$ (Figure A.6), the transfer is of first order and acts as a lowpass filter with a cut-off frequency of 0.0012 min^{-1}. The pole $-k_g$ determines the filter cut-ff frequency. Lower frequency phase is shifted +180 degrees due to the system gain being negative. For higher frequencies, phase is shifted 90 degrees less than for the lower frequencies, so the phase shift becomes +90 degrees. For $k_g = 0$ (Figure A.5), the transfer acts as an integral instead of a first order transfer. As a result, the transfer $H_{G,I}$ does not have one pole with a negative real value, but a pole equal to zero. This means that for $k_g = 0$, frequencies are amplified more when they are lower and the phase shift is 90 degrees for all frequencies. It was found that addition of the delay τ_I to the input does not affect the magnitude plot. However, the plot

of the phase shift is massively influenced. This additional phase delay can be seen clearly in the impulse response of the $\tau_I > 0$ linear MM by a delayed appearance of the response, which is not shown here.

The combined effect of the insulin and glucose kinetics and dynamics in the linear MM is represented by the yellow lines in Figures A.5 and A.6. Magnitude and phase plots in the Bode plot are obtained by calculation of the complete system transfer function by multiplication of the individual insulin and glucose subsystem transfer functions. When looking at the frequency content of the measured glucose concentration in Figure A.4, it can be seen that power is largest for frequencies below 0.001 min^{-1} and that it is not completely lost for frequencies in between 0.01 and 0.001 min^{-1}. This is in agreement with the effect that the linear MM has on its input when looking at the frequency response. Therefore, frequency content analysis indicates that the insulin subsystem and linear MM are designed correctly in terms of passing through the right frequencies.

The effect of combining these systems on the impulse responses can be seen on the right side of Figures A.5 and A.6. For $k_g > 0$, the 180 degree phase shift is reflected by the negative deflection in the complete system's impulse response, while the insulin subsystem's impulse response has a similar shape but in positive direction. For $k_g = 0$, the 90 degree phase shift is reflected by the decrease in the complete system's impulse response that is steepest at the peak of the insulin subsystem's impulse response. Increase of the glucose mass in this system can still occur, but will result from the balance with other components in the transfer function.

Lastly, the effect of glucagon on the glucose mass in the linear MM with $k_g > 0$ and $\tau_I = 0$ is shown in Figure A.7. Only the value for k_h was taken from the results of glucagon action identification in Table 4.8. The other parameters were taken from the Group 2B parameter values found for the linear MM in order to allow for comparison of insulin action (Figure A.6) and glucagon action (Figure A.7) on the glucose level. Comparing these figures, it can be seen that due to the glucagon subsystem's natural frequency being higher than cut-off for the insulin subsystem, the combined effect with the glucose subsystem is that cut-off of higher frequencies occurs less abrupt for glucagon. This can also be seen from the impulse response on the right side of these figures: the impulse response reaches its peak slightly quicker for the transfer from H_{IR} than that of I_{IR}. Phase shift for the combined transfer of the glucagon and glucose subsystems is zero for lower frequencies, which results in glucagon resulting in an increase of the glucose level in the impulse response similar to the increase that occurs in the amount of plasma glucagon.

Appendix B

Perturbations in system identification

In the current study, parameter estimations have been performed by a direct method: inputs and outputs were known and have been generated in a closed-loop control system. Control by the artificial pancreas system that was developed by Inreda Diabetic BV [13] is based on the difference between the current and target glucose level and the rate of change of the glucose level. Additional mechanisms in the control system are included that are not discussed here. In Figure B.1, a scheme is shown with the components that are involved in a closed loop process such as in an artificial pancreas system. Variables s and u_s and transfer G_S can be ignored for now.

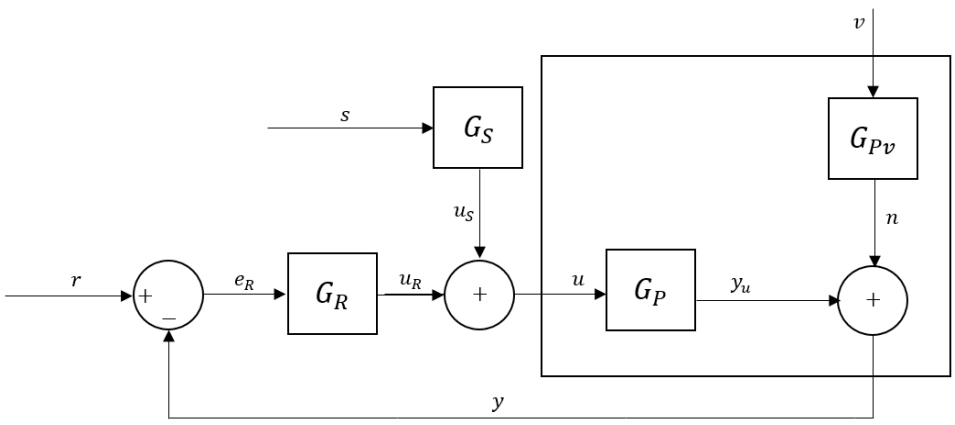

Figure B.1: Scheme of closed loop control with process G_P, process noise transfer G_{Pv}, controller G_R and disturbance transfer G_S. Procces input is u, process output is y, r is the reference.

The process to be estimated consists of two parts [108]: the process itself, that is represented by the transfer function G_P, and the noise that arises in the process, which is determined by the transfer function G_{Pv}. The controller transfer function is G_R. The input of the controller is the error between the output y and the reference r. If the controller is known, the input of the process can be determined from this error. The output y is the sum of y_u en n. y_u is the output of the plant in response to the input u given by the system. n represents the effect that the noise v has on the output. The total output y provides feedback to the controller.

The method of direct process identification, that was applied in the current study, requires that the noise transfer G_{Pv} needs to be known. This way, when both u and y are measured, the process output y_u can be determined. In contrast, for indirect process identification, the process can be identified based on knowledge of the output only, since the input can be determined by the controller G_R. For proper identification, it is required that the input u is not correlated with the noise n. However, the feedback loop imposes such a relation. A proper way of identifying a process which is part of a closed loop system is to apply closed loop identification. In closed loop identification, an independent disturbance signal

should be provided at a well-chosen point in the closed-loop and to analyse the responses to this independent disturbance at the input and output from cross-correlation of these signals with the independent external output. In Figure B.1, this disturbance u_s is added to the controller output u_R. An additional advantage may be that the independent disturbance input may excite the process more extensively than the closed loop system itself.

For a glucose model, perturbations can be additions to the insulin or glucagon input as provided by an artificial pancreas system. Other perturbations that can be applied are meal intake or physical activity [17]. These can be used to identify additional submodels for such perturbations as well. Furthermore, perturbed system inputs can be applied to study the effect of such perturbations in silico [5].

Appendix C

Sensitivity analysis

As pointed out in section '5 Discussion', sensitivity analysis is a useful tool to determine the sensitivity of the model to certain parameters. This can provide information about the influence of uncertainties or variability in parameter estimates on model output. Sensitivity analysis can be performed either locally or globally. Global sensitivity analysis focuses on the identification of important parameters, in case of a fully identified model structure and unknown parameter values [109]. Local sensitivity analysis shows how small perturbations of certain (known) parameters influence the value of the output [110].

In this study, parameter estimations were performed for an average T1DM patient for both the insulin and glucagon subsystems. Suppose that these are described by differential equations $\dot{\mathbf{y}}$, that vary with time t and depend on a certain parameter vector p, as is expressed in Equation C.1. When the sensitivity of the combination of all subsystems is of interest, the differential equations for the glucose subsystem should also be included in the vector $\mathbf{y}$. It is possible to perform local sensitivity analysis for the considered parameter values. One local sensitivity coefficient is the partial derivative of the output $\mathbf{y}$ with respect to a certain parameter. A sensitivity matrix is a matrix containing the sensitivity of each variable in the output vector with respect to each parameter value considered (Equation C.2). Sensitivity coefficients can be determined by finite difference approximation or more analytically by solving differential equations for the sensitivity coefficients [109]. The latter case will be described first.

Since the output y is not known before a solution to the system of differential equations is found, it is not possible to determine the sensitivities by directly calculating the partial derivatives in Equation C.2. It is however, possible to calculate them by solving Equation C.3. This can be done either by solving the partial derivatives by a coupled method [111], simultaneously with the model equations (Equation C.1), or by a decoupled method [112], separately from the model equations. The Green's function method [110] can also be applied.

$$\dot{\mathbf{y}} = \mathbf{f}(\mathbf{y}, t, \mathbf{p}) \tag{C.1}$$

$$\mathbf{S} = \frac{\partial \mathbf{y}}{\partial \mathbf{p}} \tag{C.2}$$

$$\dot{\mathbf{S}} = \frac{\partial \mathbf{y}}{\partial \mathbf{p} \partial t} = \left(\frac{\partial \mathbf{f}(\mathbf{y}, t, \mathbf{p})}{\partial \mathbf{y}} \right) \mathbf{S} + \left(\frac{\partial \mathbf{f}(\mathbf{y}, t, \mathbf{p})}{\partial \mathbf{p}} \right) \tag{C.3}$$

Next to this analytical approach, sensitivities can also calculated by a finite difference approach [110], by computing the blood glucose levels for two different parameter values. These parameter values are preferably chosen based on the known mean parameter value and the variance of this value: for example, mean - std. and mean + std. are applied. The sensitivity coefficient for a certain parameter (p_j) and output combination (y_i) is then calculated as follows shown in Equation C.4.

$$s_{ij} = \frac{y_i(p_j + \Delta p_j) - y_i(p_j - \Delta p_j)}{2\Delta p_j} \tag{C.4}$$